INVESTIGATING THE ROLE OF A GENETIC INCOMPATIBILITY INVOLVING MISMATCH REPAIR GENES IN ADAPTIVE EVOLUTION

A Dissertation

Presented to the Faculty of the Graduate School

of Cornell University

In Partial Fulfillment of the Requirements for the Degree of

Doctor of Philosophy

By Duyen Thanh Bui

May 2016

Investigating the Role of a Genetic Incompatibility involving Mismatch Repair Genes in Adaptive Evolution

Duyen Thanh Bui

Cornell University, 2016

In nature, bacterial populations tend to minimize their mutation rates to avoid accumulating harmful mutations that ultimately reduce their fitness. However, a mutator state may allow for a higher rate of appearance of beneficial mutations that provide an adaptive advantage to new environments. My work shows that eukaryotic cells can use an elevated mutation rate as a strategy to adapt to new environments. This mutator state is achieved by becoming defective in a DNA mismatch repair (MMR) pathway that acts to repair DNA replication errors. My model proposes that mating between two divergent baker's yeast strains, SK1 and S288c, can yield progeny that contain S288c *MLH1* and SK1 *PMS1* MMR genes. Such hybrids display elevated mutation rates and fitness advantages when adapting to a selective pressure, high salt. Strains bearing this combination are defined as incompatible because they are defective in MMR function and also display long-term fitness costs. Interestingly, I found that incompatible strains can transiently achieve a fitness advantage in a high salt stress environment without displaying a fitness cost. These observations support my model where defects in MMR provide an increase in genomic mutation rate that permits adaptation to changing environments. Moreover, genomic data from distinct yeast strains found around the world support the existence of such hybrids in nature and thus emphasize an important role for incompatibilities in adaptive evolution. When I analyzed *MLH1* and *PMS1* sequences from 1011 different yeast strains, I found three clinical strains that contain an incompatible *MLH1-PMS1* genotype, two of which

contain a polymorphism in MLH1 that acts as an intragenic suppressor of the mutator phenotype. In addition, all three strains show evidence of being non-mutators, suggesting that the incompatible strains developed extragenic suppression strategies to avoid long-term fitness costs. Based on these observations, I propose a model in which an incompatible mutator state is generated through mating between distant yeast strains, creating a mutator phenotype that allows strains to better adapt to environmental challenges. Once adaptation is achieved, strains can either mate to wild type strains to regenerate, after sporulation, an MMR compatibility, or acquire a suppressor of the mutator phenotype to become non-mutators. Both strategies would provide mechanisms to allow long-term survival in populations.

BIOGRAPHICAL SKETCH

Duyen Bui was born in Hagiang, Vietnam on a spring day in April, 1987. Most of her childhood was spent studying to be the top in all the subjects in her classes. Her mom was the source of motivation and determination for her to study and get through all grade schools. She graduated from Chuyen-Hagiang high school in 2005 and was accepted to the Honor Program of Vietnam National University- Hanoi University of Science, majoring in Biochemistry and Molecular Biology. The first time she met and talked to an American was also to Professor Harvey Lodish of MIT, which then motivated her to look into possibilities to further her graduate study in America.

In 2010, she found Dr. Eric Alani's laboratory a very interesting research group through online searching and thus chose Cornell University as her graduate school. She joined the research group one year later.

Cornell is also where she met and fell in love with her husband, Tuan Cao. After graduation, she plans to join Prof. Joachim Li's lab at University of California, San Francisco for Postdoctoral Research position.

ACKNOWLEDMENTS

I want to thank my mom for always supporting me and loving me unconditionally and my father for protecting me in life. I would like to thank Prof. Baer and his wife for being my second family in the US and all members of Alani lab as they have been cheering for me and being very encouraging to me during my time in the lab. Special thanks for Carol who advises me a lot throughout the years. I would also like to thank Prof. Aquadro for advising me throughout my PhD with a lot of constructive suggestions and critical thoughts.

I am greatly thankful to Prof. Alani, for everything that he has done during my PhD. He was a wonderful mentor; he made time for advising us and caring for us in great extent. It was very lucky for me to have a teacher like him as I have learned a lot, especially in doing research independently and also in mentoring others. He set a great example for me to my future dream of becoming a professor, mentoring and doing research with a great extent of passion, honesty and self-discipline. I would also like to thank Dr. Nishant. K.T and Elliot Dine for contributing to analyzing sequencing of evolved strains; Dr. James Anderson for ideas and feedbacks on the adaptive evolution experiment; Dr. Anne Friedrich for collaboration on the sequences of 1011 yeast strains.

Finally, I want to whole-heartedly thank my husband, Tuan Cao, who showed me a whole new world in Ithaca that I have enjoyed experiencing so far. He has been a wonderful husband, supporting me in every single step of my way.

TABLE OF CONTENTS

page

LIST OF FIGURES page

LIST OF TABLES page

CHAPTER 1

INTRODUCTION

Overview of DNA repair

DNA, the genetic information found in all living cells, is constantly subjected to damage through both exogenous (UV radiation, chemicals, and viruses) and endogenous (replication, recombination, and cellular stress) processes [1–5]. DNA damage, if unrepaired, can lead to severe consequences such as decreased cell survival. DNA repair mechanisms ensure genome stability and disrupting such mechanisms causes increased mutation rates. Primary DNA repair pathways in cells include base excision repair (BER), mismatch repair (MMR), nucleotide excision repair (NER), homologous recombination (HR) and non-homologous end joining (NHEJ) [6]. Organisms from the very simplest forms of bacteria to humans possess such repair machineries, indicating that they are indispensable.

DNA replication is a tightly regulated process that is essential to maintain cell ploidy following cell division. While DNA polymerases, which synthesize DNA, are highly accurate, errors can occur at rates of ~10^{-5} to 10^{-7} per base per cell division through polymerase misincorporation events. Errors include base substitutions, frame-shift mutations, and insertion/deletion due to DNA slippage [7–9]. Some of these errors are corrected by DNA polymerase proofreading activities [10]. However, many others escape the proofreading process and are corrected through the post-replicative MMR mechanisms to achieve mutation rates as low as 10^{-9} [7]. Therefore, MMR plays a crucial role to correct errors that occur during DNA replication [11].

Post-replicative MMR

In *Saccharomyces cerevisiae* MMR, Msh protein complexes detect and bind to DNA mismatches. The Msh2-Msh6 complex preferentially binds to base-base mismatches and small insertion/deletion loops while the Msh2-Msh3 complex binds to larger insertion/deletion loops [12,13]. The protein complex Mlh1-Pms1 is then recruited to sites marked by Msh complexes (Fig. 1.1). The Msh complex interacts with Mlh1-Pms1 to form an ATP – dependent ternary complex [14]. The resulting ternary complex recruits downstream excision factors such as Exo1 to remove the newly replicated DNA strand containing the mismatch. Subsequently, polymerase δ is recruited to resynthesize the resulting gap using the parental DNA strand as template. In order to achieve DNA mismatch repair, additional factors such as RPA (single strand binding protein) and PCNA (processivity clamp) are also required in both early and late steps [15,16]. How MMR machinery can distinguish newly synthesized daughter strand to repair from the parental DNA strand remains unclear. In bacteria, hemi-methylated dGATC sites play a role in strand discrimination during MMR by directing MutH incision [17], while in eukaryotes several mechanisms have been proposed to direct strand specific repair. Previous studies showed that Mlh1-Pms1 is an endonuclease that is activated by PCNA and RFC, and PCNA has been hypothesized to direct activity of MMR complexes to newly replicated DNA [18,19]. Other studies have proposed that the misincorporation of ribonucleotides on the newly replicated strand, primarily by the leading strand polymerase ε, could act as a signal for strand discrimination in MMR [20]. In addition to recognizing and correcting DNA mismatches that arise during DNA replication, MMR recognizes DNA mispairs that form in heteroduplex DNA during genetic recombination [21], and can act through anti-recombination mechanisms to prevent recombination between divergent DNA sequences [22].

Figure 1.1. Overview of eukaryotic DNA mismatch repair (MMR). (A) DNA polymerase errors can lead to mismatches, such as base-base (left) or insertion/deletion loops (right). (B) MSH proteins recognize and bind to mismatches. Msh2-Msh6 preferentially binds to base-base mismatches and small DNA insertion/deletion loops while Msh2-Msh3 binds to larger insertion/deletion loops. (C) In the major MMR pathway, MSH proteins interact with the Mlh1-Pms1 heterodimer. Mlh1-Pms1, directed by an existing nick on the newly replicated strand (dotted black arrow), will introduce a nick distal to the mismatch site (blue arrow). This triggers the recruitment of additional factors for resecting, resynthesizing, and ligating the new DNA strand so that the repair process can be completed.

A

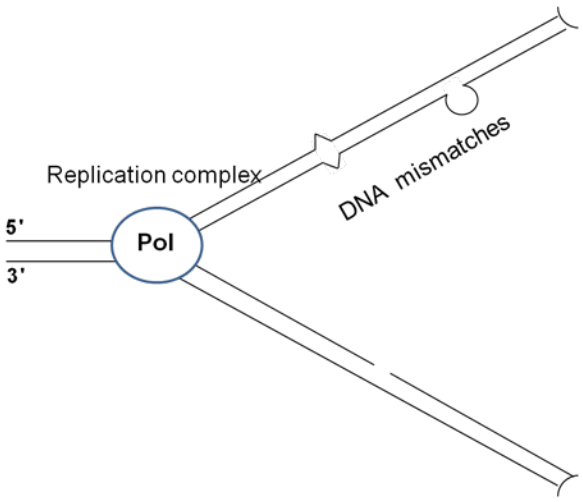

B

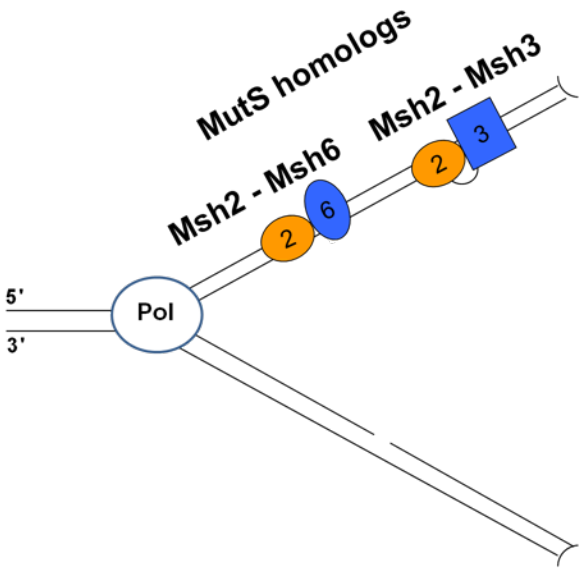

C

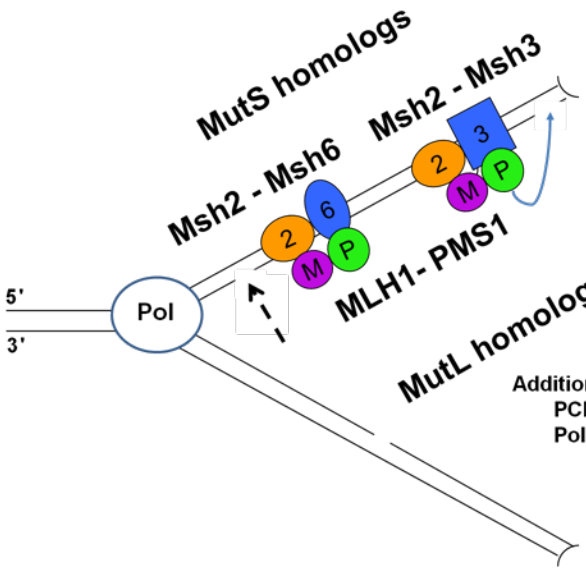

Additional MMR factors:
PCNA, RFC, EXO1, RPA
Polδ, Ligase

Strains that are *mlh1* and *pms1* null show severe defects in MMR [7]. In this thesis, I analyzed a hybrid of two yeast strains, S288c and SK1, which contains the *MLH1* gene from the S288c strain (S288c*MLH1*) and the *PMS1* gene from the SK1 strain (SK1*PMS1)*. This hybrid shows a mutator phenotype, likely due to defects in Mlh1-Pms1 subunit interactions or endonuclease activity. The *MLH1*-S288c and *PMS1*-SK1 combination contains unique polymorphisms, D761G in *MLH1*-S288c and K822R in *PMS1*-SK1; both polymorphisms map to interaction domains that are important to form the Mlh1-Pms1 heterodimer. The mechanism by which these amino acid polymorphisms causes the incompatibility remains unknown because the incompatible MLH combination does not dramatically disrupt Mlh1-Pms1 interactions [23].

Mutator populations with defects in MMR can play roles in adaptive evolution

Although defects in MMR result in the accumulation of deleterious mutations and an overall loss in fitness (e.g.[24]), some bacterial populations defective in MMR are found at a higher frequencies than expected [25], suggesting that these strains display an adaptive advantage to new environments [26]. In support of this idea, I show that an elevated mutation rate in yeast can promote adaptation to stress conditions (Chapter 2). Lenski *et al*., showed through evolution experiments that microorganisms with high mutation rates have initial fitness advantages when adapting to new environments [27], especially when under directional selection [28]. Thus, there are short-term advantages for organisms with high mutation rates. One supporting hypothesis is that high mutation rates allow for a faster acquisition of beneficial mutations under selection, giving an organism an increased likelihood of acquiring the first adaptive mutations within a population and thereby increasing their fitness. Another explanation for the short-term fitness advantage of individual microorganisms with mutator alleles is that having a high mutation rate generates a larger pool of genetic variation, thereby giving the entire population better choices to adapt. This is supported by the observation that weak mutators are

present at high frequency in a population for a long period of time, consistent with providing an advantage during adaptation [26]. Once a beneficial mutation occurs, many factors in the population and surrounding environment can affect the fate of the new mutation. These include population size and the availability and fitness effects of other mutations that accumulate in the population. Depending on a variety of factors including fitness effects, clonal interference and chance variations in a population, mutations that cause initial increased fitness can later lose an advantage while mutations that display lower fitness could eventually be dominant in a population [29]. In short, background genetic variation is important to obtain a fitness advantage and can strongly influence the dynamics of adaptation [30].

Bacteria with a mutator phenotype have a long-term fitness cost that can be overcome by regaining a functional MMR pathway

A defective MMR pathway is not sustainable in the long-term due to the accumulation of deleterious mutations that ultimately outweigh the advantages of beneficial mutations [28,31]. Bacteria can solve this problem through horizontal transfer in which they are able to obtain a functional MMR gene from other individuals in the same population. Studies in bacteria have shown that mismatch repair genes have been exchanged between genomes at a higher rate than other genes [31]. Denamur *et al.* showed that there was a high correlation between horizontal gene transfer and the hyper-recombination phenotypes of MMR-deficient mutators, especially for MMR genes [31]. They also suggested the idea that MMR genes are more flexible and can be replaced to avoid the ultimate demise of an organism through the accumulation of many deleterious mutations.

Studying mutator strains in yeast populations

Human cells isolated from several types of tumors have been shown to have high mutation rates; these tumors also evolve very rapidly [32]. An increase in mutation rate due to MMR deficiency has been widely shown to increase the number of mutations that provide selective advantage [33,34]. These mutations ultimately result in faster growth of cancer cells [33]. In yeast, defects in MMR also lead to elevated mutation rates and their growth dynamics resemble populations of MMR defective bacteria and cancer cells [8,9]. How high mutation rates exert influence in adaptation remains a question in evolution studies.

In Chapter 2, I show that MMR defective yeast strains evolve faster than MMR proficient strains due to a combination of selection and the generation of a greater pool of genetic variants that can serve as material for adaptive evolution [35]. As described earlier in this chapter, I used a mutator strain containing an incompatible combination *of MLH1* and *PMS1* variants to determine where this combination provides an adaptive advantage. I also hypothesize that this incompatible hybrid is not maintained in nature because of associated long-term fitness costs. Finally, I propose a model to explain how a genetic incompatibility could arise by mating to provide adaptive advantage and then disappear through re-mating to avoid long-term fitness costs.

Dobzhansky-Muller model and hybrid incompatibilities in yeast. Dobzhansky and Muller developed a model to explain how hybrid incompatibilities can be generated to produce a negative epistatic effect [36,37] (Fig. 1.2). In this model, mutations arise and reach fixation in two independent populations. Such mutations are neutral or beneficial because they fix in diverging lineages. However, hybrids generated between the two lines can create combinations

that have not been sampled in nature and can yield genotypes that are not beneficial and might cause severe defects [36]. In my work I define these as being “incompatible” (Fig. 1.3).

Consistent with a Dobzhansky-Muller model, a hybrid between two baker’s yeast strains, S288c and SK1, displayed an incompatibility phenotype [23]. DNA sequence analysis of the two genomes suggested that the two strains diverged from an ancestral population. In an assay in which *mlh1* and *pms1* null strains display a 10,000-fold higher mutation rate than wild type, the hybrid that bears the *MLH1* allele from S288c strains and the *PMS1* allele from SK1 strains shows a 100-fold higher mutation rate than the parental wild type, indicating a moderate defect in the MMR pathway [23]. Hence, the S288c *MLH1*-SK1 *PMS1* combination is inferred as “incompatible”, while the other three combinations, which do not display a mutator phenotype, are labeled “compatible.” A post-zygotic reproductive barrier also exists between SK1 and S288c strains which have roughly 0.7% nucleotide sequence divergence. This was demonstrated by reduced spore viability of SK1-S288c inter-strain crosses compared to S288c-S288c and SK1-SK1 crosses [23]. A single nucleotide polymorphism (SNP) in *PMS1* and a SNP in *MLH1* were later found to be primarily responsible for the incompatibility [23]. Together, this hybrid displayed a phenotype consistent with a Dobzhansky - Muller model for an incompatibility involving MMR genes [23].

The incompatible hybrid strain described above could be created through mating between S288c and SK1, thus leading to progeny with a specific combination of MMR genes that display a high mutation rate. In my thesis, I was interested in testing if higher mutation rates due to an MMR incompatibility would lead to an adaptive advantage and whether such an incompatibility would prevent the stable appearance of such strains in nature.

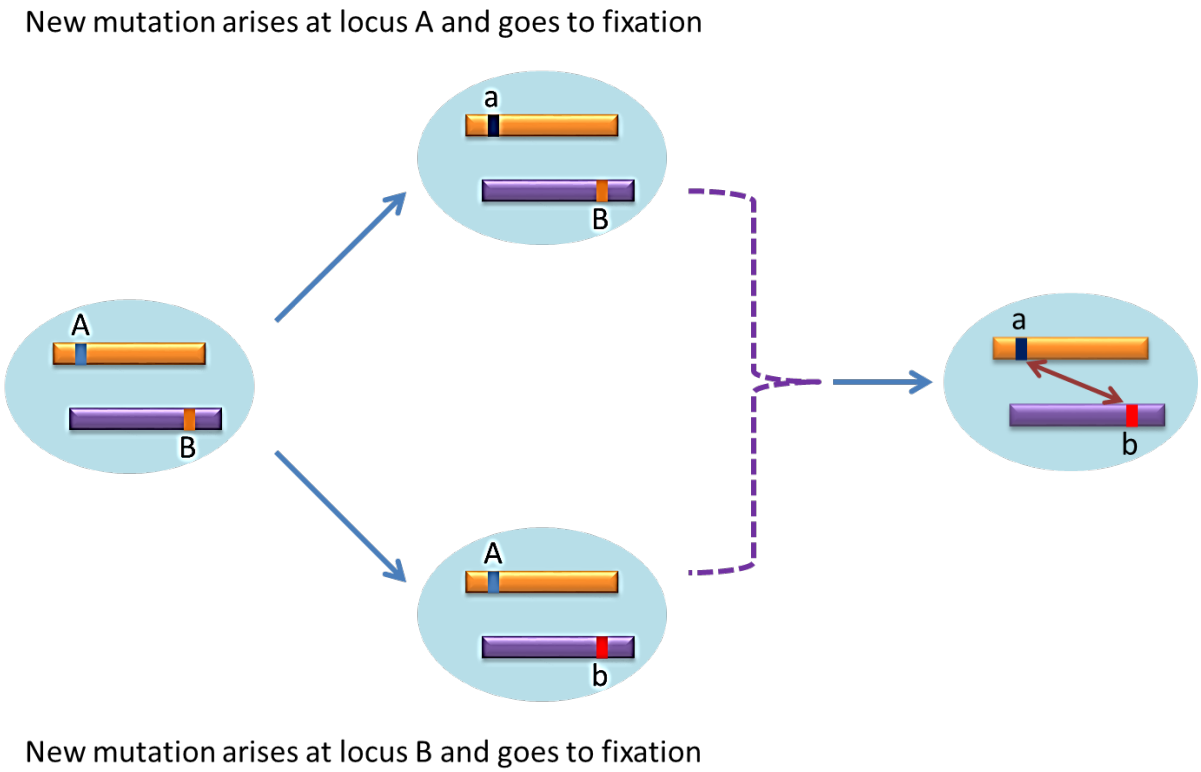

Figure 1.2. Dobzhansky-Muller model of hybrid incompatibility. Adapted from *Wu, C. & Ting, C. Genes and Speciation (2004)*. The original population has two loci A and B that are in an "ancestral state". In two diverging populations, a new allele (allele a) evolves at locus A in one population and a new allele b also arises and fixes independently (solid blue arrows) at locus B in the other population. The two alleles a and b confer a negative epistasis (shown in the two headed brown arrow) in the hybrid because neither the ancestral nor parental strains have experienced this genetic interaction during the course of adaptation.

A genetic incompatibility promotes adaptation in *Saccharomyces cerevisiae*

Work from the Alani laboratory, which identified negative epistasis involving MMR genes, encouraged me to test if such interactions could contribute to adaptive evolution. Baker's yeast is a very useful model to study genetic variation and natural selection. Stress conditions like high salt, low glucose, and treatment with antifungal drugs are used in many adaptive evolution studies [30,31]. Salt stress tolerance is a complex trait (influenced by many genes) that is attractive for evolutionary research because the physiological response to salt stress is well-characterized at the molecular level and the pathways governing it are highly-conserved [40]. In Chapter 2, I constructed isogenic compatible and incompatible *MLH1-PMS1* strains and subjected them to adaptive evolution assays in high salt.

I found that incompatible populations adapted more rapidly to high salt than compatible strains without displaying an apparent fitness cost. The evolved strains were subject to whole genome sequencing to identify which genes are involved in the adaptive phenotype. Several studies showed that yeast populations that adapted to high salt have mutations in genes encoding proteins involved in proton and ion exchange pathways such as proton efflux pump genes *PMA1*, the *ENA* genes encoding sodium efflux pumps, and the global transcriptional repressor gene *CYC8* which regulates *ENA* activity [38,41]. I initially looked at those genes to determine if my evolved strains had mutations at those sites; I did not find mutations at these loci in the evolved strains.

Surprisingly, I found that mutations in a single gene, *PMR1,* were the causative mutations for high salt resistance in incompatible populations. I also found that mutations in *PMR1* could subsequently arise in compatible populations. These observations demonstrate an adaptation race to obtain adaptive mutations to specific selective pressures.

Post adaptation strategy and its effect on long-term fitness

There are two main questions regarding adapted populations that use a mutator strategy: i) What fates await mutator populations after adaptation has been achieved? ii) Will adaptive mutations be maintained in populations, even if environments change back to non-extreme (non-challenging)? In Chapter 3, I mimic a natural scenario where most populations are heterogeneous. In this experiments, I included incompatible and compatible cells that acquired adaptive mutations to an environmental challenge, and incompatible and compatible cells that had not been adapted. I was interested in learning which populations would display a higher fitness. Previously in our lab, incompatibilities involving MMR genes *MLH1* and *PMS1* were shown to confer a long-term cost as measured by determining the spore viability of diploid strains that were propagated through extreme bottlenecks. Heck *et al.*, showed that incompatible strains have lower spore viability compared to compatible strains, indicating that they have accumulated more recessive lethal mutations [3]. In this study, I was interested in testing if a long-term fitness cost would be seen in competition experiments by measuring fitness differences of post adaptation incompatible strains compared to compatible strains (Chapter 3, Fig. 3.3).

MLH1-PMS1 Incompatibility in nature.

While the incompatible S288c *MLH1*-SK1 *PMS1* genotype was not found in nature in a small sample of strains assayed, it does arise through laboratory mating of derived yeast strains to create a mutator strain that shows a negative epistasis interaction between S288c *MLH1* and SK1 *PMS1* [23]. Heck *et al.,* showed that the incompatible strains have higher mutation rates and display a long-term fitness cost [23]. Consistent with this argument is the finding that incompatible S288c *MLH1*-SK1 *PMS1* genotypes were not observed in 65 strains isolated from

various parts of the world [42]. In Chapter 3, I performed a large-scale search for the incompatible combination by analyzing sequences of *MLH1* and *PMS1* genes among 1011 different yeast strains. Three clinical strains, YJM541, YJM554, and YJM555, were found that bear incompatible polymorphisms. Therefore, characterizing these strains provided a means to determine if incompatible combinations can be maintained in nature. As shown in Chapter 3, it is clear that novel strategies were developed to lower the mutation rate in these strains and thus allow them to escape long-term fitness cost.

Are MLH1-PMS1 incompatibilities a dead end?

As mentioned above, mismatch repair genes are exchanged between MMR defective bacterial genomes at higher than average rates, which is likely due to the hyper-recombination phenotypes exhibited by MMR-deficient strains [31]. Therefore, once adapted to an environment, the adapted individuals have the chance to receive functional MMR genes from the population and minimize long-term costs. While it would be relatively easy for an organism such as baker's yeast to lose MMR functions, horizontal gene transfer events in yeast that could restore such function are thought to be very rare [43]. However, in baker's yeast, the long-term fitness effects associated with the MMR hybrid incompatibility can be avoided by mating the adapted incompatible population to parental strains to regenerate, after sporulation, a compatible genotype. This idea is supported by DNA sequence analysis indicating that S288c and SK1 strains have exchanged information, indicating that they have mated naturally. Therefore, I also proposed that the incompatible combination probably exists in nature and is removed through mating and meiotic segregation [23,42].

Another strategy that a yeast population could use to suppress a mutator phenotype is to acquire a suppressor that reduces the mutation rate. It has been shown that mutator

populations in bacteria can acquire and fix mutations that could act as suppressor to reduce mutation load in the population [44]. Although in yeast, acquiring spontaneous mutations is rare compared to mating followed by chromosome segregation in meiosis, yeast populations in nature still grow in relatively large sizes, and thus an asexual strategy is feasible.

A Model for the Appearance and Disappearance of an MLH1-PMS1 Incompatibility

Based on the above observations, I created a model to explain how a genetic incompatibility could arise and disappear (Fig. 1.3). In this model, a common ancestral state can give rise to two strain backgrounds containing neutral or beneficial mutations in the *MLH1* and *PMS1* genes. On their own, these changes would not confer fitness effects. However, through mating between these strains, a hybrid can contain combinations that display negative epistasis, resulting in higher mutation rates. This interaction has the potential accelerate adaptive evolution. Once adapted to an environment, the adapted individuals have a chance to receive functional MMR genes from the population and minimize long-term fitness costs. While it would be relatively easy for an organism such as baker's yeast to lose MMR functions, horizontal gene transfer events in yeast that could restore such functions are thought to be very rare. However, in baker's yeast, the long-term fitness effects associated with the incompatibility can be avoided by mating the adapted incompatible population to parental strains to regenerate, after sporulation, a compatible genotype. This is an effective route for regaining a compatible MMR combination because: i) Outcrossing in yeast occurs in a much higher frequency compared to conferring spontaneous mutation [45]; ii) *MLH1, PMS1* and the locus involving adaptation *PMR1* are on different chromosomes. Therefore, the probability for a meiotic progeny to obtain a compatible combination and adaptive mutations through random segregation is high.

.

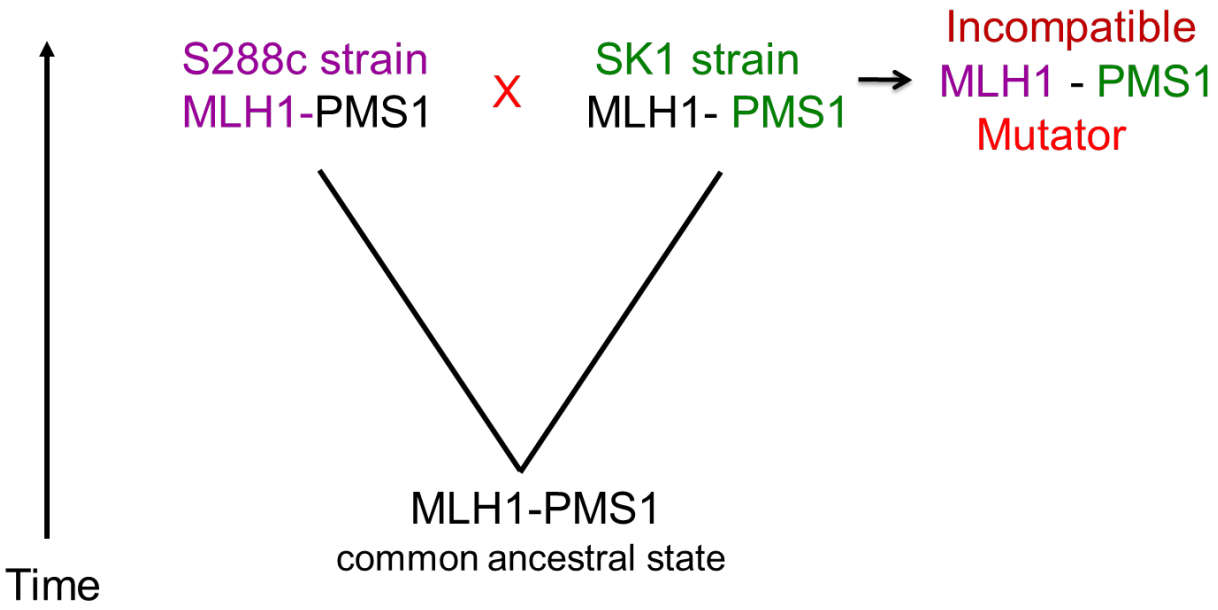

Figure 1.3. A model for the role of incompatibility in adaptive evolution involving MMR combinations of Mlh1-Pms1 in baker's yeast. From a common ancestral state, neutral or beneficial mutations occurred in Mlh1 and Pms1 and reach fixation in SK1 and S288c strains Mating between SK1 and S288c strains gives rise to an incompatible hybrid that displays a mutator phenotype. Such incompatible strains, being mutators, have the potential to adapt more quickly to extreme environments, but later show a fitness cost due to the accumulation of deleterious mutations. However, a portion of incompatible populations can mate back to either S288c or SK1 parental strains to reacquire a compatible combination of MMR genes or can obtain a suppressor of the mutator phenotype and thus avoid extinction.

Significance of understanding genetic variation and its relation to penetrance of HNPCC and other diseases.

Research focused on understanding MMR genes incompatibilities can allow for a better understanding of how mutations arise in cancers such as Hereditary Non-Polyposis Colorectal Cancer (HNPCC) and sporadic colon cancer. HNPCC is the most common form of hereditary colon cancer and is a syndrome characterized by a deficiency in MMR [46]. Mutations in both *MSH* and *MLH* genes have been linked to HNPCC and a subset of sporadic cancers [47,48]. A large percentage of MMR mutations and polymorphisms associated with HNPCC and sporadic cancers are missense mutations that can lead to either the loss of important interaction domains or disrupt protein structure [47,49]. Such mutations could alter MMR efficiency and eventually lead to tumor formation [50–52].

About 50% of all human MMR mutations that have been detected in HNPCC associated families are mutations in the *MLH1* gene [53] and mutations in MMR genes were shown in ~3,000-10,000 new cases of colorectal cancer diagnosed in Americans every year. At present the underlying genetic defects that are responsible for the remaining ~50% of HNPCC cases are not well understood [54,55]. Therefore, studying the penetrance of *mlh1* mutant alleles is very important for understanding the manner of segregation in HNPCC. Interestingly, genetic background can also alter the penetrance of the *mlh1* allele in yeast [56]. Heck *et al.* and Demogines *et al*. suggested that negative epistasis effects involving the *MLH1* and *PMS1* genes can reveal a mechanism to explain the occurrence of such driver mutators in sexually reproductive populations. In other words, sometimes a single mutation on its own would not have caused defects unless it occurs in a specific genetic background. This might explain some of the unaccounted causes for different types of cancer. The fact that around half of the families with HNPCC phenotypes do not have defined causative mutations in known MMR genes also support Heck and Demogines's hypothesis that genetic background effects could play an

important role [23,57]. My investigation into MMR incompatibilities involving natural polymorphisms allows for a better understanding of the effect of genetic background on disease penetrance. Knowledge about the effects of genetic background on phenotypic occurrence of abnormal growth and adaptation should help elucidate the causes of HNPCC and other cancers with deficient MMR.

REFERENCES

1. Sinha RP, Häder DP. UV-induced DNA damage and repair: a review. Photochem Photobiol Sci. 2002;1: 225–236. doi:10.1039/b201230h

2. Helleday T, Eshtad S, Nik-Zainal S. Mechanisms underlying mutational signatures in human cancers. Nat Rev Genet. Nature Publishing Group; 2014;15: 585–598. doi:10.1038/nrg3729

3. Roulston A, Marcellus RC, Branton PE. Viruses and Apoptosis. Annu Rev Microbiol. 1999; 577–628.

4. Ryan EL, Hollingworth R, Grand RJ. Activation of the DNA Damage Response by RNA Viruses. 2016; doi:10.3390/biom6010002

5. Lodish, H. et al. Molecular Biology of the Cell. 2004.

6. Lodish H, Berk A, Zipursky SL et al. DNA Replication, Repair, and Recombination. Molecular Cell Biology. New York: W. H. Freeman; 2004. p. chapter 12.

7. Kunkel T a, Erie D a. DNA mismatch repair. Annu Rev Biochem. 2005;74: 681–710. doi:10.1146/annurev.biochem.74.082803.133243

8. Nishant KT, Wei W, Mancera E, Argueso JL, Schlattl A, Delhomme N, et al. The baker's yeast diploid genome is remarkably stable in vegetative growth and meiosis. PLoS Genet. 2010;6: e1001109. doi:10.1371/journal.pgen.1001109

9. Zanders S, Ma X, Roychoudhury A, Hernandez RD, Demogines A, Barker B, et al. Detection of heterozygous mutations in the genome of mismatch repair defective diploid yeast using a Bayesian approach. Genetics. 2010;186: 493–503. doi:10.1534/genetics.110.120105

10. Brutlag D. Synthesis of Deoxyribonucleic. J Biol Chem. 1972;239: 222–232.

11. Lodish H, Berk A ZS. DNA Replication, Recombination, and Repair [Internet]. Molecular Cell Biology. New York: W. H. Freeman; 2016. doi:10.1007/978-4-431-55873-6

12. Marsischky GT, Richard D. Biochemical Characterization of the Interaction between the Saccharomyces cerevisiae MSH2-MSH6 Complex and Mispaired Bases in DNA. Chem, J Biol. 1999;274: 26668–26682.

13. Palombo F, Iaccarino I, Nakajima E, Ikejima M, Shimada T, Jiricny J. hMutSbeta, a heterodimer of hMSH2 and hMSH3, binds to insertion/deletion loops in DNA. Curr Biol. 1996;6: 1181–1184. doi:10.1016/S0960-9822(02)70685-4

14. Habraken Y, Sung P, Prakash L, Prakash S. ATP-dependent assembly of a ternary complex consisting of a DNA mismatch and the yeast MSH2-MSH6 and MLH1-PMS1 protein complexes. J Biol Chem. 1998;273: 9837–41. Available: http://www.ncbi.nlm.nih.gov/pubmed/9545323

15. Kolodner RD, Marsischky GT. Eukaryotic DNA mismatch repair. Curr Opin Genet Dev. 1999;9: 89–96. Available: http://www.ncbi.nlm.nih.gov/pubmed/10072354

16. Pluciennik A, Dzantiev L, Iyer RR, Constantin N, Kadyrov FA, Modrich P. PCNA function in the activation and strand direction of MutLα endonuclease in mismatch repair. 2010; 3–8. doi:10.1073/pnas.1010662107/-/DCSupplemental.www.pnas.org/cgi/doi/10.1073/pnas.1010662107

17. Lee JY, Chang J, Joseph N, Ghirlando R, Rao DN, Yang W. MutH complexed with hemi- and unmethylated DNAs: coupling base recognition and DNA cleavage. Mol Cell. 2005;20: 155–66. doi:10.1016/j.molcel.2005.08.019

18. Shell SS, Putnam CD, Kolodner RD. The N terminus of Saccharomyces cerevisiae Msh6 is an unstructured tether to PCNA. Mol Cell. 2007;26: 565–78. doi:10.1016/j.molcel.2007.04.024

19. Johnson RE, Kovvali GK, Guzder SN, Amin NS, Holm C, Habraken Y, et al. Evidence for Involvement of Yeast Proliferating Cell Nuclear Antigen in DNA Mismatch Repair. J Biol Chem. 1996;271: 27987–27990. doi:10.1074/jbc.271.45.27987

20. Ghodgaonkar MM, Lazzaro F, Olivera-Pimentel M, Artola-Borán M, Cejka P, Reijns MA, et al. Ribonucleotides misincorporated into DNA act as strand-discrimination signals in eukaryotic mismatch repair. Mol Cell. 2013;50: 323–32. doi:10.1016/j.molcel.2013.03.019

21. Sugawara N, Goldfarb T, Studamire B, Alani E, Haber JE. Heteroduplex rejection during single-strand annealing requires Sgs1 helicase and mismatch repair proteins Msh2 and Msh6 but not Pms1. Proc Natl Acad Sci U S A. 2004;101: 9315–9320. doi:10.1073/pnas.0305749101

22. Sugawara N, Pâques F, Colaiácovo M, Haber JE. Role of Saccharomyces cerevisiae Msh2 and Msh3 repair proteins in double-strand break-induced recombination. Proc Natl Acad Sci U S A. 1997;94: 9214–9219. doi:10.1073/pnas.94.17.9214

23. Heck JA, Argueso JL, Gemici Z, Reeves RG, Bernard A, Aquadro CF, et al. Negative epistasis between natural variants of the Saccharomyces cerevisiae MLH1 and PMS1 genes results in a defect in mismatch repair. Proc Natl Acad Sci U S A. 2006;103: 3256–61. doi:10.1073/pnas.0510998103

24. Ma X, Rogacheva M V, Nishant KT, Zanders S, Bustamante CD, Alani E. Mutation hot spots in yeast caused by long-range clustering of homopolymeric sequences. Cell Rep. The Authors; 2012;1: 36–42. doi:10.1016/j.celrep.2011.10.003

25. Leclerc JE, Li B, Payne WL, Cebula TA. High Mutation Frequencies Among Escherichia coli and Salmonella Pathogens S ~. 1996;9304958.

26. Giraud a, Matic I, Tenaillon O, Clara a, Radman M, Fons M, et al. Costs and benefits of high mutation rates: adaptive evolution of bacteria in the mouse gut. Science. 2001;291: 2606–8. doi:10.1126/science.1056421

27. Elena SF, Lenski RE. Evolution experiments with microorganisms: the dynamics and genetic bases of adaptation. Nat Rev Genet. 2003;4: 457–69. doi:10.1038/nrg1088

28. Lenski RE. letters to nature Evolution of high mutation rates in experimental populations of E . coli. 1997;606: 703–705.

29. Woods RJ, Barrick JE, Cooper TF, Shrestha U, Kauth MR, Lenski RE. Second-order selection for evolvability in a large Escherichia coli population. Science. 2011;331: 1433–6. doi:10.1126/science.1198914

30. Lang GI, Botstein D, Desai MM. Genetic variation and the fate of beneficial mutations in asexual populations. Genetics. 2011;188: 647–61. doi:10.1534/genetics.111.128942

31. Denamur E, Lecointre G, Darlu P, Tenaillon O, Acquaviva C, Sayada C, et al. Evolutionary implications of the frequent horizontal transfer of mismatch repair genes. Cell. 2000;103: 711–21. Available: http://www.ncbi.nlm.nih.gov/pubmed/11114328

32. Bhattacharyya NP, Skandalis A, Ganesh A, Groden J, Meuth M. Mutator phenotypes in human colorectal carcinoma cell lines. Proc Natl Acad Sci USA. 1994;91: 6319–6323. doi:10.1073/pnas.91.14.6319

33. Odmer WFB. The mutation rate and cancer. Proc Natl Acad Sci USA. 1996;93: 14800–14803.

34. Sohn K-J, Choi M, Song J, Chan S, Medline A, Gallinger S, et al. Msh2 deficiency enhances somatic Apc and p53 mutations in Apc+/-Msh2-/- mice. Carcinogenesis. 2003;24: 217–24. doi:10.1093/carcin/24.2.217

35. Bui DT, Dine E, Anderson JB, Aquadro CF, Alani EE. A Genetic Incompatibility Accelerates Adaptation in Yeast. PLoS Genet. 2015;11: e1005407. doi:10.1371/journal.pgen.1005407

36. Orr HA. Population Genetics of Speciation: 1995;

37. Wu C-I, Ting C-T. Genes and speciation. Nat Rev Genet. 2004;5: 114–22. doi:10.1038/nrg1269

38. Anderson JB, Funt J, Thompson DA, Prabhu S, Socha A, Sirjusingh C, et al. Determinants of divergent adaptation and Dobzhansky-Muller interaction in experimental yeast populations. Curr Biol. Elsevier Ltd; 2010;20: 1383–8. doi:10.1016/j.cub.2010.06.022

39. Berry DB, Guan Q, Hose J, Haroon S, Gebbia M, Heisler LE, et al. Multiple means to the same end: the genetic basis of acquired stress resistance in yeast. PLoS Genet. 2011;7: e1002353. doi:10.1371/journal.pgen.1002353

40. Dhar R, Sägesser R, Weikert C, Yuan J, Wagner A. Adaptation of Saccharomyces cerevisiae to saline stress through laboratory evolution. J Evol Biol. Blackwell Publishing; 2011;24: 1135–1153. doi:10.1111/j.1420-9101.2011.02249.x

41. Garciadeblas B, Rubio F, Quintero FJ, Bañuelos M a, Haro R, Rodríguez-Navarro a. Differential expression of two genes encoding isoforms of the ATPase involved in sodium efflux in Saccharomyces cerevisiae. Mol Gen Genet. 1993;236: 363–8. Available: http://www.ncbi.nlm.nih.gov/pubmed/8437581

42. Demogines A, Wong A, Aquadro C, Alani E. Incompatibilities involving yeast mismatch repair genes: a role for genetic modifiers and implications for disease penetrance and variation in genomic mutation rates. PLoS Genet. 2008;4: e1000103. doi:10.1371/journal.pgen.1000103

43. Liti G, Peruffo A, James S a, Roberts IN, Louis EJ. Inferences of evolutionary relationships from a population survey of LTR-retrotransposons and telomeric-associated sequences in the Saccharomyces sensu stricto complex. Yeast. 2005;22: 177–92. doi:10.1002/yea.1200

44. Wielgoss S, Barrick JE, Tenaillon O, Wiser MJ, Dittmar WJ, Cruveiller S, et al. Mutation rate dynamics in a bacterial population reflect tension between adaptation and genetic load. Proc Natl Acad Sci U S A. 2013;110: 222–7. doi:10.1073/pnas.1219574110

45. Ruderfer DM, Pratt SC, Seidel HS, Kruglyak L. Population genomic analysis of outcrossing and recombination in yeast. Nat Genet. 2006;38: 1077–81. doi:10.1038/ng1859

46. Timberlake WE, Frizzell MA, Richards KD, Gardner RC. A new yeast genetic resource for analysis and breeding. 2011; 63–80. doi:10.1002/yea

47. Jäger a C, Rasmussen M, Bisgaard HC, Singh KK, Nielsen FC, Rasmussen LJ. HNPCC mutations in the human DNA mismatch repair gene hMLH1 influence assembly of hMutLalpha and hMLH1-hEXO1 complexes. Oncogene. 2001;20: 3590–5. doi:10.1038/sj.onc.1204467

48. Peltomäki P, Vasen H. Mutations associated with HNPCC predisposition -- Update of ICG-HNPCC/INSiGHT mutation database. Dis Markers. 2004;20: 269–76. Available: http://www.ncbi.nlm.nih.gov/pubmed/15528792

49. Peltomaki P. Role of DNA Mismatch Repair Defects in the Pathogenesis of Human Cancer. J Clin Oncol. 2003;21: 1174–1179. doi:10.1200/JCO.2003.04.060

50. Fishel R. The Selection for Mismatch Repair Defects in Hereditary Nonpolyposis Colorectal Cancer : Revising the Mutator Hypothesis The Selection for Mismatch Repair Defects in

Hereditary Nonpolyposis Colorectal Cancer : Revising the Mutator Hypothesis 1. 2001; 7369–7374.

51. Jiricny J, Marra G. DNA repair defects in colon cancer. Curr Opin Genet Dev. 2003;13: 61–69. doi:10.1016/S0959-437X(03)00004-2

52. Radiobiology M, Forel-strasse A. Mismatch repair defects in cancer Josef Jiricny * and Minna Nyström-Lahti. 2000; 157–161.

53. Perrera C, Ra M, Panyushkina-seiler E, Marra G, Curci A, Quaresima B, et al. Functional Analysis of MLH1 Mutations Linked to. 2002;167: 160–167. doi:10.1002/gcc.1225

54. Dekker M, de Vries S, Aarts M, Dekker R, Brouwers C, Wiebenga O, et al. Transient suppression of MLH1 allows effective single-nucleotide substitution by single-stranded DNA oligonucleotides. Mutat Res. Elsevier B.V.; 2011;715: 52–60. doi:10.1016/j.mrfmmm.2011.07.008

55. Marti TM, Kunz C, Fleck O. DNA mismatch repair and mutation avoidance pathways. J Cell Physiol. 2002;191: 28–41. doi:10.1002/jcp.10077

56. Wanat JJ, Singh N, Alani E. The effect of genetic background on the function of Saccharomyces cerevisiae mlh1 alleles that correspond to HNPCC missense mutations. Hum Mol Genet. 2007;16: 445–52. doi:10.1093/hmg/ddl479

57. Peltomäki P. Deficient DNA mismatch repair: a common etiologic factor for colon cancer. Hum Mol Genet. 2001;10: 735–40. Available: http://www.ncbi.nlm.nih.gov/pubmed/11257106

58. Gary R, Park MS, Nolan JP, Cornelius HL, Kozyreva OG, Tran HT, et al. A novel role in DNA metabolism for the binding of Fen1/Rad27 to PCNA and implications for genetic risk. Mol Cell Biol. 1999;19: 5373–82. Available: http://www.pubmedcentral.nih.gov/articlerender.fcgi?artid=84380&tool=pmcentrez&rendertype=abstract

59. Tran HT, Degtyareva NP, Koloteva NN, Sugino A, Masumoto H, Gordenin DA, et al. Replication slippage between distant short repeats in Saccharomyces cerevisiae depends on the direction of replication and the RAD50 and RAD52 genes. Mol Cell Biol. 1995;15: 5607–17. Available: http://www.pubmedcentral.nih.gov/articlerender.fcgi?artid=230811&tool=pmcentrez&rendertype=abstract

CHAPTER 2.

A genetic incompatibility accelerates adaptation in yeast

* Research in this chapter was published in PLoS Genetics and cited as:

Bui DT, Dine E, Anderson JB, Aquadro CF, Alani EE (2015). A Genetic Incompatibility Accelerates Adaptation in Yeast. PLoS Genetics, 11(7), e1005407. http://doi.org/10.1371/journal.pgen.1005407.

This research was a collaborative effort with contributions from Duyen Bui, Elliot Dine, K.T. Nishant, Charles Aquadro, and Eric Alani. Contributions were as follows: D.B. performed adaptive evolution experiments and whole genome sequence (WGS) barcoding and WGS analyses. She also performed the *lys2-A*$_{14}$ and ONPG assays, and characterized the *pmr1* mutations. D.B., E.D. and N.K.T contributed to analyzing the DNA sequences of evolved strains. D.B., C.A. and E.A. contributed to analysis, ideas and interpretation of the research.

ABSTRACT

During mismatch repair (MMR) MSH proteins bind to mismatches that form as the result of DNA replication errors and recruit MLH factors such as Mlh1-Pms1 to initiate excision and repair steps. Previously we identified a negative epistatic interaction involving naturally occurring polymorphisms in the *MLH1* and *PMS1* genes of baker's yeast. Here we hypothesize that a mutagenic state resulting from this negative epistatic interaction increases the likelihood of obtaining beneficial mutations that can promote adaptation to stress conditions. We tested this by stressing yeast strains bearing mutagenic (incompatible) and non-mutagenic (compatible) mismatch repair genotypes. Our data show that incompatible populations adapted more rapidly and without an apparent fitness cost to high salt stress. The fitness advantage of incompatible populations was rapid, but disappeared over time. The fitness gains in both compatible and incompatible strains were due primarily to mutations in *PMR1* that appeared earlier in incompatible evolving populations. These data demonstrate a rapid and reversible role (by mating) for genetic incompatibilities in accelerating adaptation in eukaryotes. They also provide an approach to link experimental studies to observational population genomics.

INTRODUCTION

DNA mismatch repair (MMR) acts primarily during DNA replication in prokaryotes and eukaryotes to correct DNA polymerase misincorporation errors that include base substitutions, frameshift mutations, and insertions/deletions [1-3]. In *S. cerevisiae* MutS homolog (MSH) heterodimers can track with the replication fork to recognize and bind to DNA mismatches [4,5]. MSH-marked repair sites are recognized primarily by the MutL homolog (MLH) heterodimer Mlh1-Pms1. The resulting ternary complex interacts with downstream excision factors such as Exo1 to remove the newly replicated DNA strand where the misincorporation event had occurred.

Defects in MMR result in the accumulation of deleterious mutations and an overall loss in fitness (e.g. [6]). Interestingly, studies in microbes have shown that the mutation rate per base pair is inversely proportional to genome size, and that changes from the wild-type rate are selected against [7-10]. However, approximately 10% of natural *E. coli* isolates display a mutator phenotype with 1-3% displaying defects in the MMR pathway [11-12]. The finding that a high mutation rate is typically selected against, but that some bacterial isolates can be observed in populations have suggested that mutators may play an important role in adaptive evolution [11, 13-20]. One explanation for this observation is that mutators have an increased likelihood of acquiring the first adaptive mutations within a population. However, such a strategy is not sustainable due to the accumulation of deleterious mutations that ultimately outweigh beneficial mutations. Bacteria appear to solve this problem through horizontal transfer; mismatch repair genes are exchanged between genomes at higher than average rates, which is likely due to the hyper-recombination phenotypes exhibited by MMR-deficient strains [14].

Do eukaryotes also regulate MMR functions to adapt to new selective pressures? Previously Thompson et al. [21] showed that diploid baker's yeast lacking the *MSH2* MMR gene display an adaptive advantage when competed against diploid non-mutators. However, this advantage was not seen in haploids. Previously we hypothesized that MMR function could be modulated in eukaryotes through negative epistatic interactions [22]. This hypothesis was based on experiments in which we mated two *S. cerevisiae* strains, S288C and SK1, which show 0.7% sequence divergence, and identified one *MLH* genotype, S288c *MLH1*-SK1 *PMS1,* that conferred mutation rates 100-fold higher than wild type in an assay in which *mlh1* and *pms1* null strains display a 10,000-fold higher rate [22]. The S288c *MLH1*-SK1 *PMS1* combination was defined as 'incompatible', while the other three combinations, which did not display a mutator phenotype, were labeled 'compatible'. A single nucleotide polymorphism (SNP) in *PMS1* combined with a single SNP in *MLH1* were primarily responsible for the incompatibility [22].

Dobzhansky and Muller proposed a model to explain how hybrid incompatibilities can arise without causing defects within parental strains or species [23-26]. As described previously [22,27], the evolution of the S288c *MLH1*-SK1 *PMS1* MMR incompatibility (Fig. 2.1) fits this model. Mating of S288C and SK1, followed by sporulation and segregation of gene variants within progeny, creates an S288c *MLH1*-SK1 *PMS1* genotype that shows negative epistasis and has not been sampled in set of 65 *S. cerevisiae* strains (Fig. 2.1; [27]). Such negative epistasis is similar to the interactions thought to underlie hybrid incompatibility between established [28-32] or incipient species [33].

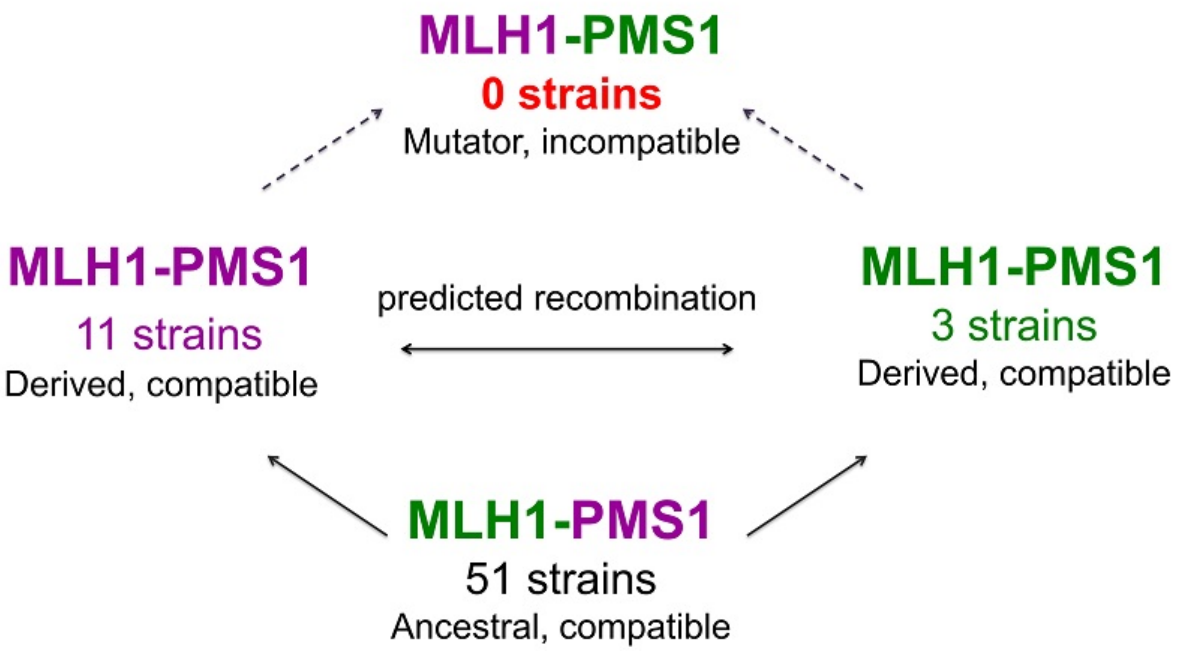

Figure 2.1. A model for how MMR incompatible populations arise in nature [22,27]. In this cartoon, a common ancestor bearing the Mlh1 Gly 761 and Pms1 Arg 818/822 alleles can sustain mutations, neutral or beneficial, that give rise to the derived S288c (purple, Asp 761, Arg 818/822) and SK1 (green, Gly 761, Lys 818/822) group strains. Mating between the derived strains can yield an allele combination (Mlh1 Asp 761, Pms1 Lys 818/822) that had not been selected for function, leading to a negative epistatic interaction and a mutator phenotype. Sequencing analysis of a 32-kb region in the derived groups provided evidence for recombination between the two, supporting the idea that these two groups can meet in nature, exchange genetic information, and form a hybrid mutator [22].

DNA sequence analyses of natural and laboratory yeast strains indicated that S288c and SK1 strains have mated naturally [22]. This finding suggests that incompatible combinations were likely to have been created in nature but were not maintained due to losses in fitness associated with defects in MMR (e.g. [3,22,27]). We hypothesize that negative epistasis involving MMR gene variants provides a transient advantage critical for adaptive evolution. To test this idea we constructed isogenic compatible and incompatible *MLH1-PMS1* strains and subjected them to adaptive evolution in high salt. We found that incompatible populations adapted more rapidly to high salt than compatible strains without displaying an apparent fitness cost. Furthermore, we show that mutations in *PMR1* were causative for high salt resistance in incompatible populations. Interestingly, mutations in this same gene, *PMR1*, subsequently arose in compatible populations though at a slower rate. Together these observations demonstrate an experimentally validated role for genetic incompatibilities in accelerating adaptation to environmental challenges in eukaryotes.

MATERIAL AND METHODS

Media, plasmids and strains.

Yeast strains, all isogenic to the FY/S288c background, were grown in YPD (yeast extract, peptone, dextrose), YPD + 1.2 M sodium chloride (NaCl), or YPD + 0.4 M lithium chloride (LiCl) (Table 2.1; [65,66]). DNA fragments containing S288c or SK1 derived *MLH1* and *PMS1* genes *(MLH1:KANMX, MLH1::NATMX*, and *PMS1::HIS3)* were introduced into S288c-background strains by gene replacement (Table 2.1; [22,67]). S288c derived *pmr1::URA3* alleles (*URA3* is located 500 bp upstream of *PMR1*) were also introduced into S288c background strains by gene replacement (Table 2.1, pEAA602-606 digested with *Not*I and

*Xho*I). Integrations were confirmed by PCR amplification of yeast chromosomal DNA, prepared as described by Holm et al. [68] using primers located outside of the ends of the DNA fragments used for integration. Allele integrations were confirmed by sequencing the relevant PCR products using the Sanger method. pMZ11 (*UPRE::lacZ, ARS-CEN, TRP1*, reporter to measure the unfolded protein response) and pKC201 (*pmr2::lacZ, 2μ*, *URA3* reporter to measure *PMR2* expression) were generously provided by Jeff Brodsky and Kyle Cunningham, respectively.

Adaptive evolution assays.

Single colonies of *Saccharomyces cerevisiae* were inoculated into 6 ml of YPD and grown for 24 hrs at 30°C in 20 ml glass tubes in a New Brunswick G25 shaker run at 250 RPM. Approximately 2 x 10^7 of each culture were then transferred into fresh 6 ml YPD or YPD + 1.2 M NaCl (to achieve an initial OD_{600} of 0.1, Shimadzu UV-1201 spectrophotometer) and then grown for 24 hrs. This procedure was repeated for up to 20 transfers. The number cell generations completed per transfer was determined using the equation $\log_2 (N_t/N_o)$, where N_o = total cell count at 0 hrs and N_t = total cell count at 24 hrs post transfer. A Wilcoxon sign-ranked test was used to compare growth of independent cultures [69].

Competition assays.

Incompatible and compatible *MLH1-PMS1* strains were created in which the *MLH1* gene was marked with *KANMX* or *NATMX* (Table 2.1). These markers were shown previously to not affect fitness [70,71]. After 7, 10, and 16 transfers in YPD or YPD + 1.2 M NaCl (approximately 50, 70 and 110 generations respectively), incompatible and compatible populations were mixed at a 1:1 ratio (1 x 10^7 cells each inoculated into 5 ml YPD or YPD + 1.2 M NaCl) and grown for

an additional 24 hours. The ratio of incompatible and compatible populations was assessed by replica plating YPD plates containing ~ 200 yeast colonies (plated prior to, or after 24 hours of growth) onto YPD-G418 and YPD-nourseothricin plates [70].

Fitness values (Table 2.3) were separately determined after competition experiments in which evolved cultures were randomly mixed at a 1:1 ratio and grown for an additional 24 hours (estimated to be 7 generations) in YPD or YPD + 1.2 M NaCl. Fitness (w) [34,35] of the incompatible cells relative to the compatible cells was calculated as $w = ((p_t/q_t)/(p_o/q_o))^{1/t}$, where p_o and q_o are the number of incompatible and compatible cells, respectively at 0 hrs and p_t and q_t are the number of incompatible and compatible cells, respectively, at 24 hrs, with t = 7 generations of growth. Fitness differences were analyzed for significance using one-way ANOVA [36].

lys2-A$_{14}$ reversion assays.

lys2-A$_{14}$ strains (Table 2.1; $(A)_{14}$ inserted into the *LYS2* gene) were analyzed for reversion to Lys^+ as described previously [27,72]. All strains were inoculated in YPD overnight and plated onto LYS drop out and synthetic complete plates. The 95% confidence intervals were determined as described by Dixon and Massey [73]. Pair-wise Kruskal–Wallis tests were performed between each pair of incompatible and compatible strains to determine the significance of the differences in median reversion rates.

Bulk segregation analysis.

Individual $NaCl^r$ clones isolated from incompatible and compatible strains grown for 10 transfers were phenotyped and then crossed to isogenic, unevolved strains. The resulting diploids were first struck onto YPD + 1.2 M NaCl plates to determine if the $NaCl^r$ phenotype

observed in the evolved haploid strain was dominant or recessive. The diploids were then sporulated using either liquid or solid media containing 1% potassium acetate. Tetrads were dissected and spore clones were germinated on YPD were struck onto YPD + 1.2 M NaCl to assess NaCl resistance. The resulting $NaCl^r$ and $NaCl^s$ spore clones, at least 18 of each, were pooled in equal cell amounts to create resistant and sensitive bulk pools that were subjected to whole genome sequencing.

Whole genome sequencing.

Parental, $NaCl^r$ evolved compatible and incompatible clones, and the bulk pools described above, were grown in 8 ml cultures. Chromosomal DNA was isolated using Affymetrix Prep-Ease kit and quantified using the Qubit® dsDNA HS Assay Kit (Life Technologies). This DNA was then barcoded using Illumina Nextera XT. High throughput sequencing of chromosomal DNA was performed on an Illumina HiSeq 2500 at the Cornell Biotechnology Resource Center.

GATK was used as a platform-independent Java framework. The core system uses the standard sequence alignment program BWA against a reference sequence to create SAM format files [74]. We used the S288c reference sequence in this study (SGD: http://www.yeastgenome.org/) because our strains are isogenic to this background.

All differences between our starting unevolved strain and the reference were subtracted. A binary alignment version of the SAM format, called binary alignment/map (BAM), was then compressed and indexed using picard (http://picard.sourceforge.net). Finally, BAM files were analyzed by GATK to optimize the genotyping analysis toolkit (http://www.broadinstitute.org/gsa/wiki/index.php/The_Genome_Analysis_Toolkit). SNPs with quality scores of less than 75 were removed from the analysis. Uniprot was used to predict the

topology of Pmr1 (http://www.uniprot.org/).

Beta-galactosidase assays.

pKC201 (*pmr2::lacZ, 2μ*, *URA3;* [41]) was transformed into evolved strains to determine if mutations in *PMR1* activated *ENA1/PMR2* expression. Transformants were grown overnight in uracil dropout media in the presence or absence of 1.2 M NaCl and then analyzed in liquid assays for beta-galactosidase activity (permeabilized yeast cell assay, [51]). pMZ11 (*UPRE::lacZ, ARS-CEN, TRP1;* [44]) was transformed into evolved strains to determine if mutations in *PMR1* activated the unfolded protein response pathway. Transformants were grown for the indicated times in tryptophan dropout media with or without 1.2 M NaCl and then analyzed in liquid assays for beta-galactosidase activity. DTT was included at 5 mM to serve as a positive control for the unfolded protein response.

RESULTS

***MLH1-PMS1* Incompatible strains display a fitness advantage when evolved in high salt.**

We tested if the negative epistasis phenotype seen in yeast bearing the S288c *MLH1*-SK1 *PMS1* genotype confers an adaptive advantage during stress. This study was initiated by constructing isogenic compatible and incompatible *MLH1-PMS1* strains that displayed, prior to adaptation, similar fitness levels in YPD and YPD + 1.2 M NaCl media as measured in growth and competition assays (Materials and Methods; Table 2.1; Fig. 2.2).

Table 2.1. Strains and plasmids used in this study. S288c derived genes are referred to as "c" and SK1 derived genes as "k."

Strains	
FY23	*MATa, ura3-52, leu2Δ1, trp1Δ63*
FY86	*MATalpha, ura3-52, leu2Δ1, his3Δ200*
EAY1366	*MATa, leu2, ura3, trp1, his3, lys2::InsE-A14, mlh1Δ::KANMX*
EAY1369	*MATalpha, ura3-52, leu2Δ1, trp1Δ63, his3Δ200, lys2::insE-A14, cPMS1::HIS3*
EAY1370	*MATalpha, ura3-52, leu2Δ1, trp1Δ63, his3Δ200, lys2::insE-A14, kPMS1::HIS3*
EAY3191	*MATa, ura3-52, leu2Δ1, trp1Δ63, his3Δ200, kMLH1::KANMX, kPMS1::HIS3*
EAY3193	*MATalpha, ura3-52, leu2Δ1, trp1Δ63, his3Δ200, kMLH1::KANMX, kPMS1::HIS3,*
EAY3197	*MATalpha, ura3-52, leu2Δ1, trp1Δ63, his3Δ200, cMLH1::NATMX, kPMS1::HIS3*
EAY3225	*MATalpha, ura3-52, leu2Δ1, trp1Δ63, his3Δ200, lys2::insE-A14, kMLH1::NATMX, cPMS1::HIS3*
EAY3230	*MATalpha, ura3-52, leu2Δ1, trp1Δ63, his3Δ200, kMLH1::NATMX, cPMS1::HIS3*
EAY3233	*MATalpha, ura3-52, leu2Δ1, trp1Δ63, his3Δ200, cMLH1-KANMX, cPMS1::HIS3*
EAY3234	*MATa, ura3-52,leu2Δ1, trp1Δ63, his3Δ200, lys2::insE-A14, cMLH1-KANMX, cPMS1::HIS3*
EAY3235	*MATa, ura3-52, leu2Δ1, trp1Δ63, his3Δ200, lys2::insE-A14, cMLH1::KANMX, kPMS1::HIS3*
EAY3236	*MATalpha, ura3-52,leu2Δ1, trp1Δ63, his3Δ200, cMLH1::KANMX, kPMS1::HIS3*
EAY3239	*MATalpha, ura3-52, leu2Δ1, trp1Δ63, his3Δ200, kMLH1::NATMX, kPMS1::HIS3*
EAY3241	*MATa, ura3-52, leu2Δ1, trp1Δ63, his3Δ200, kMLH1::NATMX, kPMS1::HIS3*
EAY3242	*MATalpha ura3-52, leu2Δ1, trp1Δ63, his3Δ200, kMLH1::NATMX, kPMS1::HIS3*
EAY3246	*MATa, ura3-52,leu2Δ1, trp1Δ63, his3Δ200, lys2::insE-A14, kMLH1::NATMX, kPMS1::HIS3*
EAY3247	*MAT alpha, ura3-52, leu2Δ1, trp1Δ63, his3Δ200, lys2::insE-A14, kMLH1::NATMX kPMS1::HIS3*
EAY3684	*EAY3242, pmr1-T412C::URA3*
EAY3685	*EAY3242, pmr1-T2G::URA3*
EAY3686	*EAY3242, pmr1-A557G::URA3*
EAY3687	*EAY3242, pmr1-C554T::URA3*
EAY3688	*EAY3242, PMR1::URA3*
Plasmids	
pRS416	*ARS-CEN, URA3*
pEAA588	*ARS-CEN, URA3, PMR1*
pEAA589	*ARS-CEN, URA3, pmr1-C2027T*
pEAA590	*ARS-CEN, URA3, pmr1-T459A*
pEAA591	*ARS-CEN, URA3, pmr1-T412C*
pEAA592	*ARS-CEN, URA3, pmr1-T2G*
pEAA594	*ARS-CEN, URA3, pmr1-G2031T*
pEAA595	*ARS-CEN, URA3, pmr1-A557G*
pEAA600	*ARS-CEN, URA3, pmr1-658AAinsertion*
pEAA601	*ARS-CEN, URA3, pmr1-A778C*

Table 2.1. Strains and plasmids used in this study. (continued)

pEAA602	*ARS-CEN, URA3, PMR1::URA3*
pEAA603	*ARS-CEN, URA3, pmr1-T412C::URA3*
pEAA604	*ARS-CEN, URA3, pmr1-T2G::URA3*
pEAA605	*ARS-CEN, URA3, pmr1-A557G::URA3*
pEAA606	*ARS-CEN, URA3, pmr1-C554T::URA3*
pMZ11	*ARS-CEN, TRP1, UPRE::lacZ*
pKC201	*2 micron, URA3, pmr2A::lacZ*

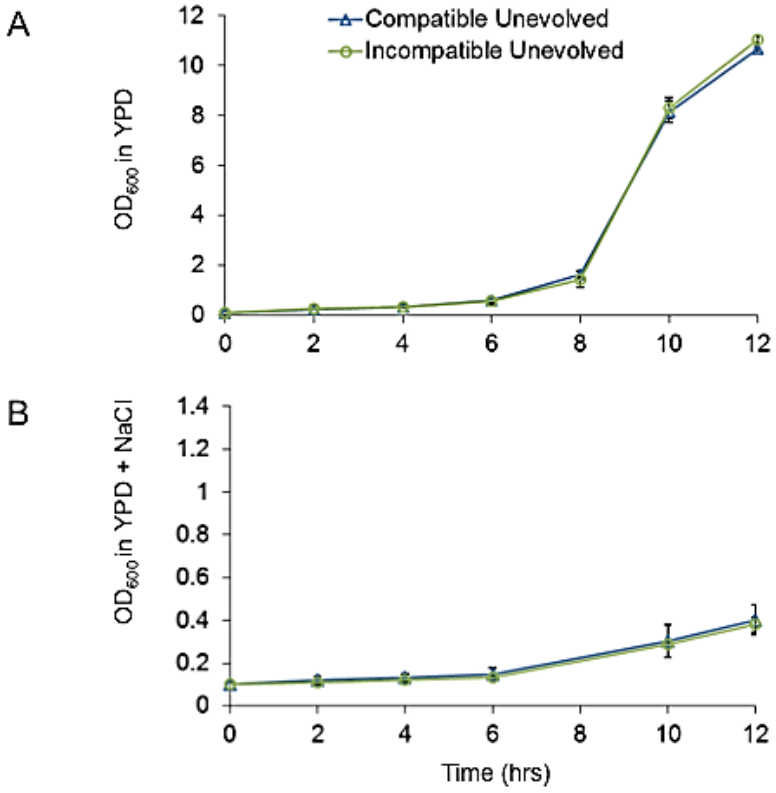

Figure 2.2. Initial fitness of incompatible and compatible strains are similar. Independent growth curves measured by OD 600 of both incompatible and compatible strains are not significantly different in either A, rich environment (YPD) or in B challenging environment (YPD + NaCl)

Table 2.2. Mutation rates in in unevolved and evolved compatible and incompatible *MLH1-PMS1* strains.

MLH1-PMS1 genotype	Lys^+ reversion rate (10^{-7}), (95% CI)		Relative Rate	(n)
Compatible (c-c)	1.55	(1.14-1.96)	1	35
Compatible (c-c), Transfer 10:				
Clone 1	1.58	(1.21-2.57)	1.0	19
Clone 2	2.43	(2.2-3.3)	1.7	5
Clone 3	2.8	(2.27-3.23)	1.9	10
Compatible (k-k)	11.1	(8.9-13.8)	7.2	30
Compatible (k-k), Transfer 10:				
Clone 1	5.67	(1.24-19.3)	3.7	10
Clone 2	11.1	(7.4-15.2)	7.7	5
Clone 3	10.6	(6.8-16.7)	7.3	5
Compatible (k-k), Transfer 16:				
Clone 1	15.8	(13-25.3)	10.9	15
Clone 2	10.9	(8.7-20.6	7.5	5
Clone 3	8.4	(5.3-6.46)	5.8	10
Incompatible (c-k)	183	(162-335)	118	44
Incompatible (c-k), Transfer 10:				
Clone 1	89.3	(46.2-160)	57.6	20
Clone 2	88.8	(60.0-191)	57.3	10
Clone 3	93.8	(43.5-149)	60.5	15

Table 2.2. Mutation rates in in unevolved and evolved compatible and incompatible *MLH1-PMS1* strains (Continued)

MLH1-PMS1 genotype	Lys$^+$ reversion rate (10^{-7}), (95% CI)		Relative Rate	(n)
Incompatible (c-k), Transfer 16:				
Clone 1	119.4	(85.5-185)	77	15
Clone 2	169	(119-244)	116.6	8
Clone 3	151	(104-200)	104.1	5
Compatible (k-c)	1.07	(0.70-1.92)	0.7	15
*mlh1Δ**	31,950	(15,900-60,150)	20,600	25

The *lys2:InsE-A$_{14}$* strains EAY3234 (*cMLH1-cPMS1, compatible, c-c*), EAY3225 (*kMLH1-cPMS1, compatible, k-c*), EAY3246 (*kMLH1-kPMS1, compatible, k-k*), EAY3235 (*cMLH1-kPMS1, incompatible, c-k*), and evolved NaCl-resistant clones from these strains obtained from Transfer 10 were examined for reversion to Lys$^+$. n, the number of independent cultures tested. Median mutation rates are presented with 95% confidence intervals, and relative mutation rates compared to the wild type strain are shown. *Data for *mlh1Δ* (EAY1366) were obtained from Wanat et al. [75].

We assessed the mutator phenotype of compatible and incompatible strains using the *lys2-A*$_{14}$ reversion assay. Compared to SK1 *MLH1*-SK1 *PMS1* compatible strains, S288c *MLH1*-SK1 *PMS1* incompatible strains showed increased reversion rates similar to that seen in previously constructed incompatible strains (100 to 120-fold higher than S288c *MLH1*-S288c *PMS1*; Table 2.2; [22]).

Compatible and incompatible lines were analyzed for adaptation to high salt conditions by growing them in YPD media containing 1.2 M NaCl as described in the Materials and Methods. In YPD media both compatible and incompatible lines completed 8-9 generations per transfer. In YPD + 1.2 M NaCl media both compatible and incompatible lines completed ~5.5 generations after the first transfer. A steady rise in the number of generations completed, from ~6.0 to ~6.8, was seen after Transfers 2 to 20. Cultures obtained after 7 (~50 generations), 10 (~70 generations), and 16 (~120 generations) transfers showed the maximal fitness advantage gained by incompatible lines. Growth rate was determined by measuring the OD_{600} of cultures every two hours following dilution into YPD + 1.2 M NaCl. Pair-wise competition experiments were performed by mixing equal amounts of cells obtained from randomly chosen incompatible and compatible cultures. The proportion of cells in each culture was determined at T = 0 and T = 24 hrs following mixing (Materials and Methods).

We assessed the growth of isogenic compatible and incompatible lines in YPD and YPD + 1.2 M NaCl. These lines could be distinguished from each other in experimental cultures because they contained different antibiotic resistance markers (*KANMX*, resistance to G418, and *NATMX*, resistance to nourseothricin) linked to the *MLH1* locus (Table 2.1). The markers could be switched between compatible and incompatible strains without an effect on fitness in growth and competition assays, indicating that the antibiotic markers did not confer a selective advantage. As shown in Fig. 2.3, incompatible lines displayed a faster growth rate in YPD + 1.2 M NaCl after Transfer 7 (~50 generations). This advantage was more apparent after Transfer

10 (~70 generations; $p < 0.0001$, n =25), but was not seen after Transfer 16 (~120 generations; $p > 0.05$; n=8).

In addition to direct growth measurements, we measured fitness in competition assays in which cells from randomly chosen compatible and incompatible evolved lines were mixed together at an approximately 1:1 ratio. These competitions involved cells adapted in YPD + 1.2 M NaCl that had undergone the same number of transfers. After mixing, the lines were grown in YPD or YPD + 1.2 M NaCl for 24 hrs (seven generations) and the proportion of each type was determined (Materials and Methods). As shown in Table 2.3 and Fig. 2.4 (left panels), neither compatible nor incompatible lines showed a competitive advantage in YPD media. In YPD + 1.2 M NaCl media, neither of the two lines showed a competitive advantage after Transfer 7. However, incompatible lines displayed a competitive advantage in this media after Transfer 10 ($p = 0.0031$), with an average fitness advantage of 16% over compatible lines. This advantage was lost after Transfer 16 ($p = 0.39$) (Table 2.3 and Fig 2.4 (right panels). Together, these data indicate that a MMR incompatibility generated by recombination involving naturally occurring variants in *PMS1* and *MLH1* can lead to an elevated rate of occurrence of adaptive mutations, and thus accelerate adaptation in a eukaryote.

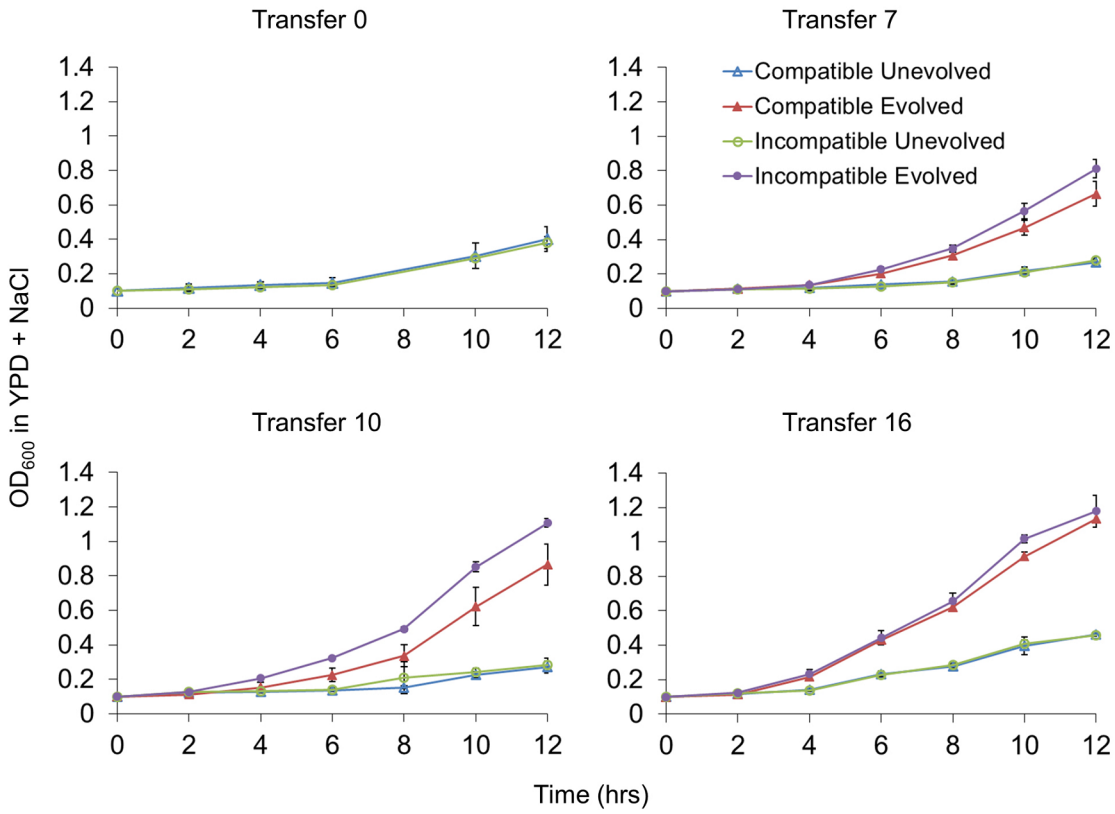

Figure 2.3. Incompatible strains display a fitness advantage in high salt media. Independent cultures of compatible (*kMLH1-kPMS1*, EAY3242) and incompatible (*cMLH1-kPMS1*, EAY3236) strains were grown for up to Transfer 16 (~ 2 x 10^7 cells per transfer) in YPD (unevolved) or YPD + 1.2 M NaCl (evolved). Cultures at the indicated transfers were diluted to an OD_{600} of 0.1 (~ 2 x 10^7 cells per transfer) in YPD + 1.2 M NaCl and monitored for growth for 12 hrs. A representative experiment involving three replicates for each genotype is shown. Mean OD_{600}, +/- standard deviation, is presented for each time point. See Materials and Methods for details.

Table 2.3. Fitness of incompatible relative to compatible strains following competition.

	Fitness, *w* +/-SEM, (n)		ANOVA
Transfer	YPD	YPD+NaCl	(p-value)
0	0.99 ± 0.02 (10)	0.95 ± 0.01 (10)	0.1417
7	0.98 ± 0.02 (12)	1.01 ± 0.02 (12)	0.3806
10	0.99 ± 0.01 (16)	1.16 ± 0.04 (16)	0.0031 *
16	0.96 ± 0.03 (6)	0.90 ± 0.06 (6)	0.3905

Independent cultures of compatible (*kMLH1-kPMS1*, EAY3242) and incompatible (*cMLH1-kPMS1*, EAY3236) strains were grown for the indicated number of transfers in YPD + 1.2 M NaCl. Fitness values were separately determined after competition experiments in which evolved cultures were randomly mixed at a 1:1 ratio and grown for an additional 24 hours in YPD or YPD + 1.2 M NaCl (see examples of the raw data in Fig. 2.4). Fitness (*w*) [34,35] was calculated as $w = ((p_t/q_t)/(p_o/q_o))^{1/t}$, where t equals the number of generations after 24 hrs of competition (7 generations), p_o and q_o are the number of incompatible and compatible cells, respectively at 0 hrs, and p_t and q_t are the number of incompatible and compatible cells, respectively, at 24 hrs. n is the number of unique competitions performed for each data set. One-way ANOVA [36] was used to test whether mean fitness values are different in YPD + 1.2M NaCl vs. YPD.

Figure 2.4. Representative competition experiments showing that incompatible strains display a transient fitness advantage in adapting to NaCl. Independent cultures of compatible (*kMLH1-kPMS1*, EAY3242) and incompatible (*cMLH1-kPMS1*, EAY3236) strains were subjected to 0 (Panel A, initial strains) 7 (B), 10 (C), and 16 (D) transfers (2 x 10^7 cells per transfer) in YPD (left) or YPD + 1.2 M NaCl (right). Left panels: incompatible and compatible cultures transferred in YPD were randomly mixed at a 1:1 ratio and grown for an additional 24 hours in YPD. Right panels: Incompatible and compatible cultures transferred in YPD + 1.2 M NaCl were randomly mixed at a 1:1 ratio and grown for an additional 24 hours in YPD + 1.2 M NaCl. In both sets of experiments, the ratio of incompatible to compatible populations is presented prior to and after 24 hrs of growth. See Materials and Methods for details.

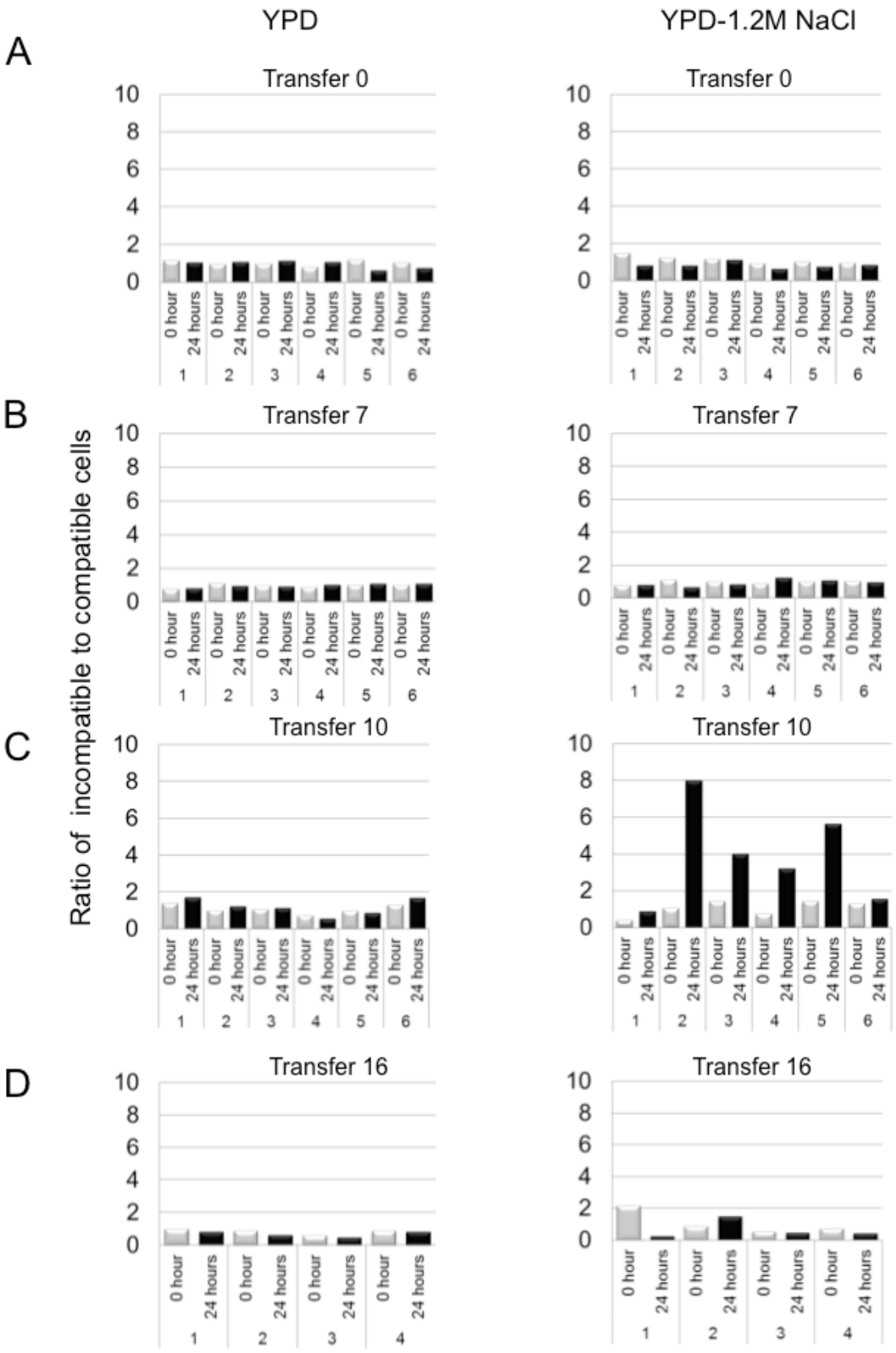
YPD
YPD-1.2M NaCl
A
B
C
D
Transfer 0
Transfer 7
Transfer 10
Transfer 16
Ratio of incompatible to compatible cells
0 hour
24 hours

The fitness advantage seen in incompatible strains depends on mutation supply.

How can we explain the temporal rise in fitness advantage seen in incompatible versus compatible lines? The most straightforward explanation is that the supply of mutations in the incompatible lines is higher than in the compatible lines, thus providing a greater likelihood for obtaining beneficial mutations that reach a high enough frequency to be selected and maintained in a population (e.g. [20,21,37]). The mutation supply available is a function of the mutation rate and the population size (N). To test this idea, we lowered the mutation supply by reducing the number of cells (and thus population size) per transfer in YPD-1.2 M NaCl by ten-fold to ~2 x 10^6 cells per transfer. We then performed cell growth and competition assays. In this experiment we were unable to observe a statistically significant advantage ($p > 0.05$) in fitness for the incompatible strains even though the number of generations completed, 70 to 75 after Transfer 10, were similar. In this experiment w = 0.99 +/-0.04 (SEM, n=4) in YPD, and w= 0.96 +/- 0.02 (SEM, n =4) in YPD-1.2 M NaCl (see also Fig. 2.5). These observations thus support the premise that mutation supply is critical to achieve the fitness advantage seen in incompatible strains.

Why was a fitness advantage in high salt seen in incompatible strains at Transfer 10 but not at Transfer 16? One possibility is that compatible populations adapt more slowly due to a lower mutation supply, but eventually obtain beneficial mutations that are selected for and maintained in the population. Alternatively, and/or in conjunction, incompatible populations accumulate a greater number of deleterious mutations and lose fitness over time. As shown in Table 2.3 and Fig. 2.4, the fitness of compatible and incompatible cultures was similar in YPD media even after 16 transfers, when the fitness advantage for incompatible lines in YPD + 1.2 M NaCl media was no longer apparent. Together these observations and the mutation supply experiments presented above and Fig. 2.5 indicate that the speed by which compatible and incompatible populations adapt is dependent on the mutation supply rate, which is higher in the incompatible strains.

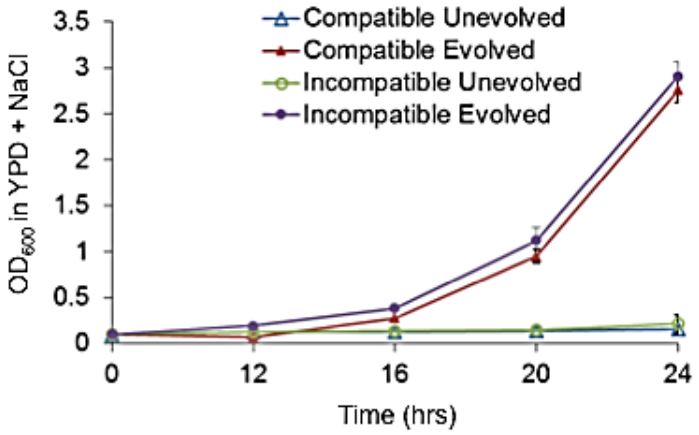

Figure 2.5. Incompatible fitness advantage is not observed when the amount of cells transferred is reduced 10-fold. Independent cultures of compatible (*kMLH1-kPMS1*, EAY3242) and incompatible (*cMLH1-kPMS1*, EAY3236) strains were grown for up to 16 transfers (~ 2 x 10^6 cells per transfer) in YPD (unevolved) or YPD + 1.2 M NaCl (evolved). In A, data are shown in which cultures after Transfer 10 were diluted to an OD_{600} of 0.1 in YPD + 1.2 M NaCl and monitored for growth for 12 hrs. A representative experiment involving three replicates for each genotype is shown. Mean OD_{600}, +/- standard deviation, is presented for each time point.

Mutations in *PMR1* were identified in both compatible and incompatible lines grown in high salt.

Are mutant alleles of the same genes responsible for salt resistance in incompatible and compatible populations? We answered this question by isolating salt-resistant clones (one per line) from independent incompatible and compatible lines. NaCl resistance in evolved strains can be easily phenotyped on YPD + NaCl plates because they grow to larger colony sizes relative to unevolved strains (Fig 2.6B, left panel). To determine the complexity of the NaCl resistant phenotype, we mated these clones (primarily from transfer 10) to unevolved strains of the opposite mating type (Fig 2.6) to form diploids. While most (five of eight tested) of the diploid strains were sensitive to NaCl, indicating recessive transmission, three of the eight displayed a semi-dominant phenotype (example in Fig 2.6B, left panel). Four diploids created by mating evolved and unevolved strains were then sporulated and phenotyped for salt resistance. Interestingly, all four strains displayed primarily a 2 $NaCl^r$:2 $NaCl^s$ segregation phenotype on YPD + NaCl plates, indicating that a single locus in the evolved strain was causative. At least 18 $NaCl^r$ and 18 $NaCl^s$ spore clones derived from each of the four matings were pooled separately and subsequently analyzed by whole-genome sequencing using a bulk segregation strategy (Materials and Methods). As shown in Table 2.4, only one to three mutations were identified in each of the four clones. Interestingly, in all four clones only one locus, *PMR1*, displayed strong linkage, as measured in sequence read counts, to the $NaCl^r$ phenotype ($p < 10^{-5}$ for all linkages to *PMR1*). As described in further detail below, *PMR1* encodes a membrane-bound P-type Ca^{2+} dependent ATPase involved in transporting Mn^{2+} and Ca^{2+} into the Golgi [38]. In subsequent paragraphs we describe a detailed analysis of *pmr1* mutants identified in evolved cultures, with the goal of explaining the genetic basis of adaptation to a defined stress, in this case, high salt.

Figure 2.6. **A single locus is likely responsible for high salt adaptation in compatible and incompatible strains.** A, High salt resistant clones (red) isolated from evolved compatible and incompatible cultures were crossed to an unevolved strain (blue). Diploids were selected and streaked onto YPD + 1.2 M NaCl plates to determine if $NaCl^r$ in the evolved strain was dominant or recessive. Subsequently, diploids were sporulated and tetrad dissected, and spore clones were analyzed for resistance to NaCl. B. Left panel. An evolved NaCl resistant clone showing a dominant phenotype. Growth of the indicated haploid and diploid strains on YPD + 1.2 M NaCl plates is shown. Right panel, example of 2:2 $NaCl^r$:$NaCl^s$segregation. Growth on YPD + 1.2 M NaCl plates is shown for the spore clones of a single tetrad obtained by mating an evolved $NaCl^r$ clone to an unevolved strain. C. The indicated incompatible and compatible evolved $NaCl^r$ clones were each mated to an unevolved haploid strain and analyzed for segregation of NaCl resistance in tetrad analysis. For each mating the vast majority displayed 2:2 segregation of resistance to sensitivity. In total nine tetrads deviated from this pattern ("other" category) with eight showing 3:1 or 1:3 segregation and one showing 4:0 segregation.

A

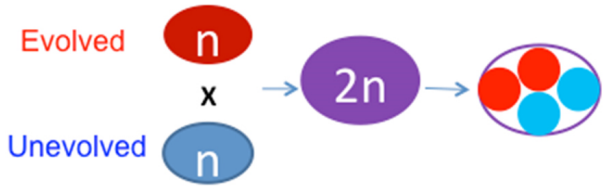

B

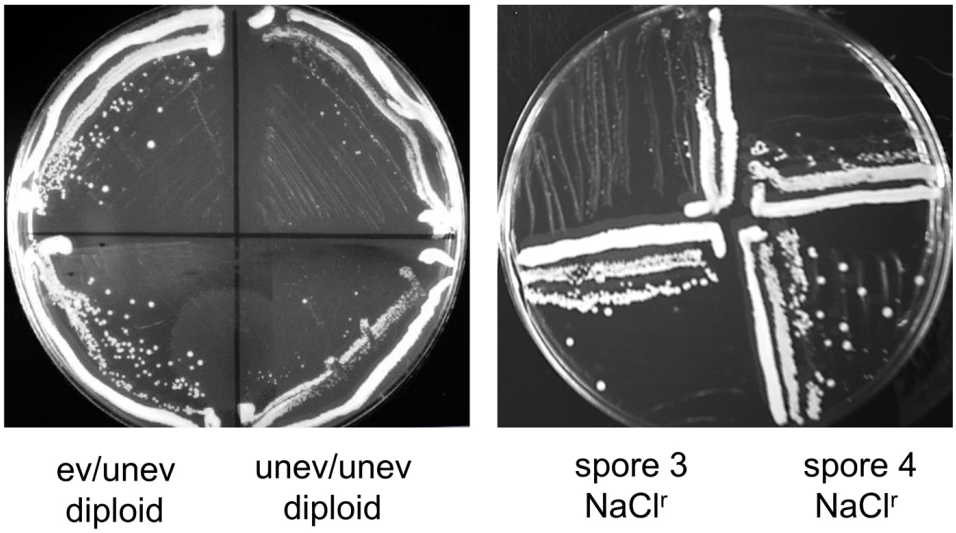

C

Genotype	evolved haploid	tetrads	2:2 $NaCl^r$:$NaCl^s$	other
Incompatible	I10A	22	19	3
	I10B	18	17	1
	I10C	12	10	2
Compatible	C10A	18	15	3

Table 2.4. Whole genome sequencing indicates *PMR1* linkage to NaCl resistance.

Line	SGD locations	*pmr1* mutation	WT/ SNP	$NaCl^r$ pool		$NaCl^s$ pool		linkage
				WT	SNP	WT	SNP	
I10A incompatible	chrVII:190010	T459A	A/T	1	58	54	1	Yes
	chrVIII:555937		A/G	29	13	29	35	No
I10B incompatible	chrII:48117		C/T	42	51	29	28	No
	chrVII:190057	T412C	A/G	0	91	50	0	Yes
I10C incompatible	chrIV:13937		G/A	50	40	55	46	No
	chrVII:190467	T2G	A/C	0	14	91	0	Yes
	chrXIII:908203		G/A	11	18	86	61	No
C10A incompatible	chrVII:188442	C2027T	G/A	0	70	104	6	Yes

The indicated evolved clones obtained from Transfer 10 were each mated to an unevolved compatible strain (EAY3241 for mating to incompatible evolved, EAY3191 for mating to compatible evolved). The resulting diploids were sporulated and tetrad dissected and germinated spore clones were analyzed for growth on YPD containing 1.2 M NaCl. For each mating at least 18 $NaCl^r$ and 18 $NaCl^s$ spore clones were separately pooled. The resistant and sensitive pools were then analyzed by whole genome sequencing (Materials and Methods). The sequence for the indicated position is shown for the unevolved reference (WT) and the evolved strains (SNP), followed by the number of WT and SNP reads detected in each pool. Using the Fisher Exact test, all SNPs we found that were defined as linkage differ from random segregation with a p value <0.0001.

We sequenced in total 37 clones obtained from independent compatible or incompatible lines grown in YPD +1.2 M NaCl. Twelve of these were subjected to whole genome sequencing. For 25 clones Sanger sequencing was performed on the PCR-amplified *PMR1* locus. As shown in Table 2.5 and Fig 2.7, 21 different mutations in *PMR1* were identified in the 37 clones that mapped to the predicted cytoplasmic domain of Pmr1. While most mutations resulted in amino-acid substitutions in the 950 amino acid Pmr1 protein sequence, two involved start codon disruptions, and one was a frameshift mutation predicted to disrupt the reading frame beginning at amino acid 220.

The following observations suggested that *pmr1* mutations conferred strong adaptive advantages earlier in incompatible populations due to a higher mutation supply. 1. Almost all of the evolved incompatible clones isolated from evolved lines that completed 10 (twelve of fourteen) or 16 transfers (seven of eight) contained *pmr1* mutations. 2. Only two of ten such clones from compatible lines after Transfer 10 contained a *pmr1* mutation. 3. For compatible lines at Transfer 16, six of six such clones contained *pmr1* mutations (Table 2.5).

We also sequenced clones isolated from the same line, but at different transfers. For two compatible lines (lines A, N) and three incompatible lines (B, F, I) the same mutation was identified in clones isolated after Transfers 10 and 16 (Table 2.5). However, for an incompatible line D two different *pmr1* mutations were identified in clones isolated after Transfer 10 (*pmr1-T2213C*) and 16 (*pmr1-G3T*). Whole genome analysis of these clones showed that two indel mutations were present in both Transfer 10 and 16, suggesting that these mutations reached fixation prior to Transfer 10 (Table 2.6). We then sequenced additional clones from line D incompatible line at Transfers 10 and 16. For Transfer 10, the *PMR1* gene was sequenced in nine clones; eight of these contained the T2213C mutation and one contained the wild-type sequence. For Transfer 16, all three clones that were sequenced contained the G3T mutation. Together these observations are consistent with the *T2213C* mutation being adaptive, but before it could fix the *G3T* mutation appeared in the population and swept to fixation.

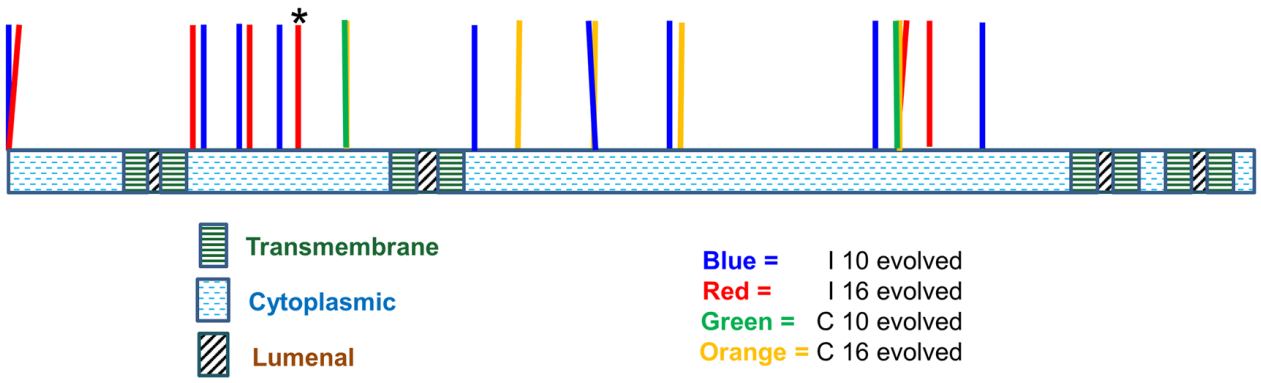

Figure 2.7. Location of *pmr1* mutation alleles found in evolved strains. 21 *pmr1* mutations (see Table 2.5 for the exact locations) identified in this study were mapped onto the Pmr1 structure predicted by Uniprot (Materials and Methods). * indicates the presence of a frameshift mutation.

Table 2.5. *pmr1* mutations identified in this study.

Evolved clone		Sequencing method	*pmr1* mutation	Amino acid change
C10	A	WGS	C2027T	A676V
C10	B	WGS	None	n/a
C10	C	WGS	None	n/a
C10	D	Sanger, *PMR1* PCR	None	n/a
C10	E	Sanger, *PMR1* PCR	None	n/a
C10	F	Sanger, *PMR1* PCR	None	n/a
C10	K	Sanger, *PMR1* PCR	None	n/a
C10	L	Sanger, *PMR1* PCR	None	n/a
C10	M	Sanger, *PMR1* PCR	None	n/a
C10	N	Sanger, *PMR1* PCR	A778C	T260P
C16	A	WGS	C2027T	A676V
C16	G	WGS	T-220A*	
C16	H	Sanger, *PMR1* PCR	G1348T	D450Y
C16	I	Sanger, *PMR1* PCR	G1121T	G374V
C16	J	Sanger, *PMR1* PCR	C1532T	S511F
C16	N	Sanger, PMR1 PCR	A778C	T260P
I10	A	WGS	T459A	C153→stop codon
I10	B	WGS	T412C	S138P
I10	C	WGS	T2G	start codon disruption
I10	D	WGS	T2213C	F738S
I10	E	WGS	A1349T	D450V

Table 2.5. *pmr1* mutations identified in this study. (continued)

Evolved clone		Sequencing method	*pmr1* mutation	Amino acid change
I10	F	Sanger, *PMR1* PCR	A557G	D186G
I10	G	Sanger, *PMR1* PCR	G533C	R178T
I10	I	Sanger, *PMR1* PCR	+ 2(AA) at bp 658	frameshift, amino acid 220
I10	J	Sanger, *PMR1* PCR	A631G	K211E
I10	K	Sanger, *PMR1* PCR	A1981C	K661Q
I10	L	Sanger, *PMR1* PCR	C1508T	A503V
I10	M	Sanger, *PMR1* PCR	G1051C	A351P
I10	Q	Sanger, *PMR1* PCR	None	n/a
I10	O	Sanger, *PMR1* PCR	None	n/a
I16	F	Sanger, *PMR1* PCR	A557G	D186G
I16	H	WGS	C554T	A185V
I16	D	WGS	G3T	start codon disruption
I16	B	Sanger, *PMR1* PCR	T412C	S138P
I16	I	Sanger, *PMR1* PCR	+ 2(AA) at bp 658	frameshift, amino acid 220
I16	N	Sanger, *PMR1* PCR	T2062G	L688V
I16	O	Sanger, *PMR1* PCR	None	n/a
I16	P	Sanger, *PMR1* PCR	G2031T	M677I

Clones from the indicated compatible (C) and incompatible (I) lines at Transfer 10 or 16 were analyzed by DNA sequencing. WGS indicates whole genome sequencing that was confirmed by Sanger sequencing the PCR-amplified *PMR1* locus. "Sanger, *PMR1* PCR" indicates that the *PMR1* locus was amplified by PCR and sequenced by the Sanger method. *pmr1* mutations are indicated by the wild-type sequence, followed by base pair or amino acid position, and then the mutant sequence. n/a, not applicable. *T to A substitution 220 bp upstream of the *PMR1* start codon.

Table 2.6. Whole genome sequencing of mutations in single clones isolated from evolved strains.

evolved clone			SNPs, location of mutations	Indels, location of mutations		Average SNPs + INDELs
C10	A	1	chrVII 188442 *PMR1*	0		3.3
C10	B	1	chrXI, 83451, *CNB1*	2	chrIV, 966520, *RMD5*	
					chrXV, 444498, *RPL3*	
C10	C	1	chrIV, 1028956, *GCN2*	1	chrXII, 1054059, YLR455W	
C16	A	2	chrVI, 113096, *HXT10*	0		5
			chrVII, 188842, *PMR1*			
C16	G	2	chrIV, 822440, *SCC1*	2	chrI, 70179, nc	
			chrVII, 190689 (221 bp upstream of *PMR1* start codon and 440 bp upstream of the *CUP2* start codon)		chrXI, 68454, *PTK1*	
I10	A	4	chrVII, 190010, *PMR1*	4	chrI, 9052, nc, 32 bp upstream of *SEO1* start codon	7.3
			chrVIII, 555937, *IMD2*		chrIII, 315517, nc	
			chrXI, 381005, *IXR1*		chrIV, 977331, nc	
			chrXVI, 50390, *RAD1*		chrXIII, 858326, IBI2	
I10	D	3	chrVII, 188256, *PMR1*	6	chrII, 602369, nc (265 upstream of the *GDT1* start codon)	
			chrIX, 101521, *FKH1*		chrII, 767793, nc (187 bp upstream of the *DUG2* start codon)	
			chrXV, 63262, *RTC1*		chrIII, 264555, nc	
					chrV 33475,nc (9 bp upstream of the *CAN1* start codon)	
					chrXIII, 21958, nc	
					chrXV, 397478, protein of UF	
I10	E	3	chrIV, 238498, *CDC48*	3	chrXV, 721829, nc	
			chrVII, 189120, *PMR1*		chrI, 143575, nc (132 bp upstream of the *VPS8* start codon)	
			chrVII, 685650, *ESP1*		chrX, 59054, nc	

Table 2.6. Whole genome sequencing of mutations in single clones isolated from evolved strains. (Continued)

evolved clone		SNPs, location of mutations		Indels, location of mutations		Average SNPs + INDELs
I16	H	3	chr IV, 1263974, *SXM1* chrVII, 189915, *PMR1* chrXVI 454870 *LGE1*	4	chrI, 35113, nc chrXII, 253323, nc (538 bp upstream of the *ERG3* start codon) chrXII, 704138, nc chrXV, 1049251, nc	10
I16	D	3	chrVII, 190466, *PMR1* chrVII, 245858, *FLD1* chrVII, 1027871, *YTA7*	7	chrII, 767793 (187 bp upstream to *DUG2* start codon) chrIX, 127338, nc (324bp upstream of the *SIM1* start codon) chrX, 269905, nc (90 bp downstream of the *ARG3* stop codon, 97 bp downstream of the *TRL1* stop codon) chrXII, 807323 (62 bp upstream of the *SPO77* start codon) chrXII, 823566, nc chrXIV, 235881, *ALG9* chrXV, 397478, protein of unknown function	

SNP and Indel mutations were identified by whole genome sequencing of one individual clone purified from each of ten independently evolved populations (Materials and Methods). The individual clones (A, B, C, etc.) are indicated as being from incompatible (I) or compatible (C) strains evolved for 10 or 16 transfers. nc indicates a SNP or indel was detected in a non-coding region.

Clones obtained from the compatible and incompatible evolved populations showed mutation rates that were similar to those measured in the corresponding unevolved lines (Table 2.2). Thus it is not surprising that the total number of mutations detected in the evolved lines were consistent with the genotype of the line (compatible vs incompatible). On average 2.4 mutations were identified per compatible line vs. 8.0 mutations per incompatible line ($p < 0.0002$). Interestingly, the vast majority of indel mutations (~90%) detected in this study were in homopolymeric runs, with five times as many indels detected per line in incompatible compared to compatible lines. The latter comparison is consistent with the mutation spectra seen in *mlh1*^{ts} strains grown at the non-permissive temperature [3,6].

Gene replacement analysis shows that *pmr1* mutations identified in compatible and incompatible lines are causative for evolved salt tolerance.

PMR1 encodes a P-type Ca^{2+} dependent membrane ATPase involved in protein sorting and calcium homeostasis. It is primarily localized to the Golgi membrane and is involved in transporting Mn^{2+} and Ca^{2+} into the Golgi lumen [38]. An uncharacterized *pmr1* mutation was identified by Park et al. [39] that conferred increased tolerance to NaCl. The authors proposed that such NaCl tolerance occurred because increased levels of cytosolic calcium in the *pmr1* mutant activated calcineurin, a calcium/calmodulin-dependent phosphatase. This activation increased expression of *ENA1*, a gene encoding a P-type ATPase pump that functions in sodium and lithium efflux to permit salt tolerance [39,40]. In such a model it is not surprising that *pmr1* null and hypomorph strains are also both resistant to lithium (Fig. 2.8). However, if only this pathway is involved then the *pmr1Δ* mutation should also confer NaCl tolerance. In fact, *pmr1Δ* confers NaCl hypersensitivity in isogenic cell lines as well as in the S288c yeast knockout collection (Fig. 2.8). We do not have a clear explanation for why the *pmr1* alleles identified in this study confer NaCl resistance while the *pmr1* null confers hypersensitivity. One

possibility, suggested by Park et al. [39] is that factors that act in calcium homeostasis are differentially regulated in the presence or absence of full or partial-length Pmr1, and thus may differentially regulate pumps that function in sodium and lithium efflux.

To further characterize the mutations in *PMR1* and their phenotype related to salt resistance, we replaced the wild type *PMR1* gene in unevolved strains with constructs containing *pmr1* alleles identified in our studies (Fig. 2.8). All assessed alleles (*pmr1-T412C, pmr1-T2G, pmr1-A557G, pmr1-C554T)* conferred $NaCl^r$ and $LiCl^r$ phenotypes in the unevolved strains that were identical to the phenotypes observed in the corresponding evolved strains (Fig. 2.8). These results indicate that the phenotypes identified in evolved lines can be completely explained by mutations in *PMR1*, supporting the data shown in the bulk segregation experiments (Table 2.4).

To obtain a better mechanistic explanation for why *pmr1* point, frameshift, and initiation codon mutations, but not *pmr1Δ* conferred $NaCl^r$, we transformed two reporter constructs, pKC201 and pMZ11, into wild-type, *pmr1Δ,* and *pmr1* allele strains. pKC201 is a *pmr2/ena1::lacZ* reporter plasmid used to measure expression levels of the Pmr2/Ena1 ion pump, a major P-type ATPase required for sodium ion flux. *pmr2Δ/ena1Δ* strains are sensitive to NaCl but strains containing increased copy number or expression of this locus display increased resistance [41-43]. pMZ11 is a *UPRE::lacZ* reporter used to monitor the unfolded protein response, a signaling pathway that improves endoplasmic reticulum (ER) function during ER stress [44].

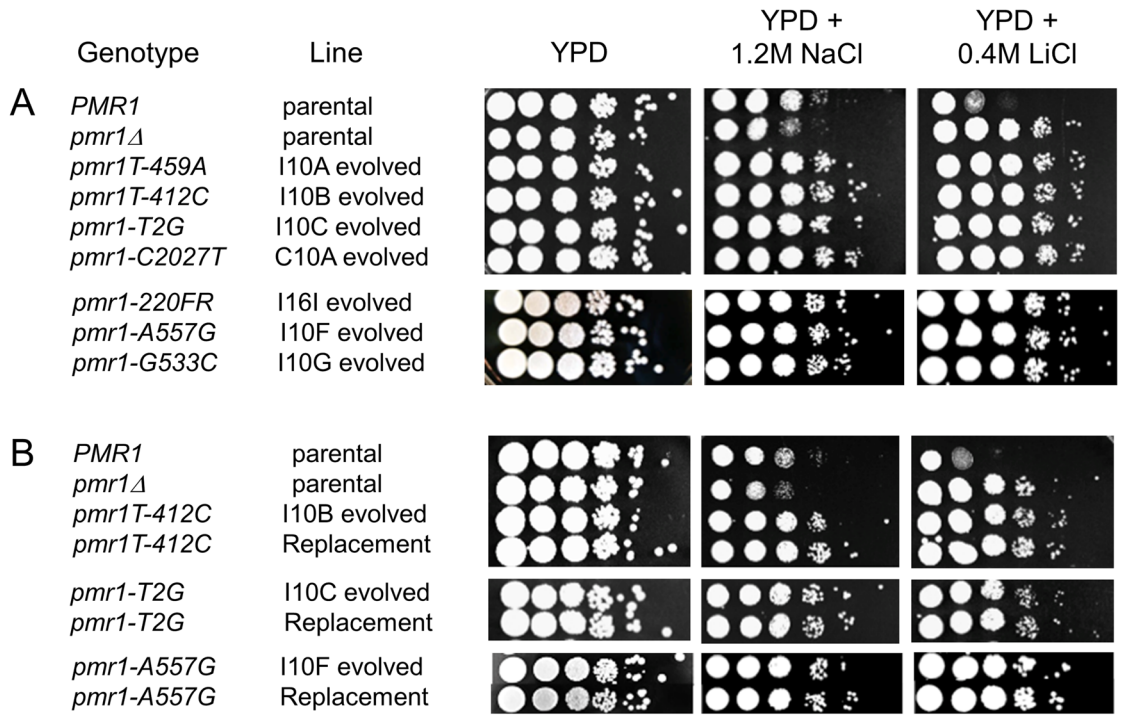

Figure 2.8. *pmr1* mutations identified in evolved lines are causative for resistance to 1.2 M NaCl and 0.4 M LiCl. In both A and B, wild type and *pmr1Δ* unevolved strains were plated in 10-fold serial dilutions onto YPD, YPD + 1.2 M NaCl, and YPD + 0.4 M LiCl plates. In panel A, representative NaCl-evolved strains (I, incompatible, C, compatible, with the Transfer indicated) bearing *pmr1* mutations are shown. In panel B, unevolved strains transformed to contain the indicated *pmr1* alleles (Replacement) are shown, with the corresponding evolved strain plated side by side.

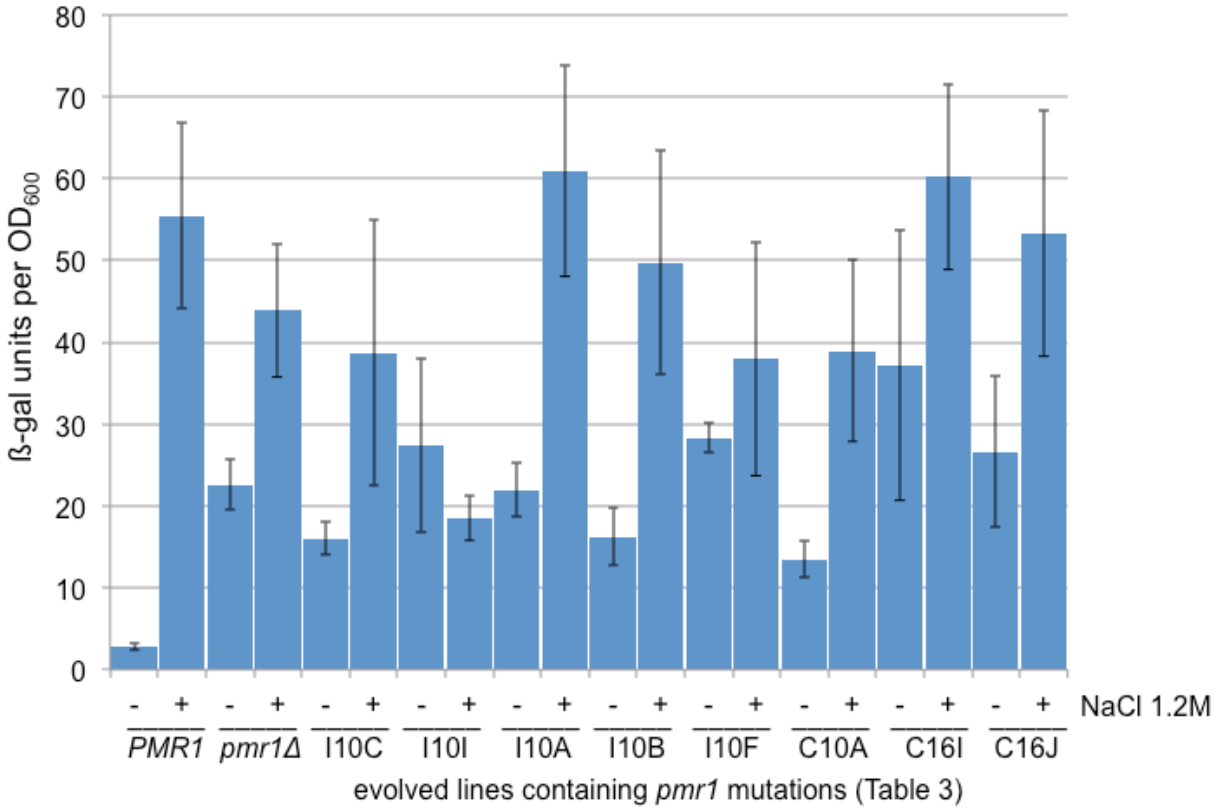

Figure 2.9. *pmr1* mutant strains constitutively induce expression of *ENA1/PMR2*. Wild-type, *pmr1Δ,* and NaCl^r strains bearing the indicated *pmr1* mutations were transformed with the *ena1::LACZ* reporter pKC201 to measure Ena1 expression. Transformants were analyzed in the presence or absence of NaCl for beta-galactosidase activity as described in the Materials and Methods. The standard deviation of 4-8 independent measurements is presented.

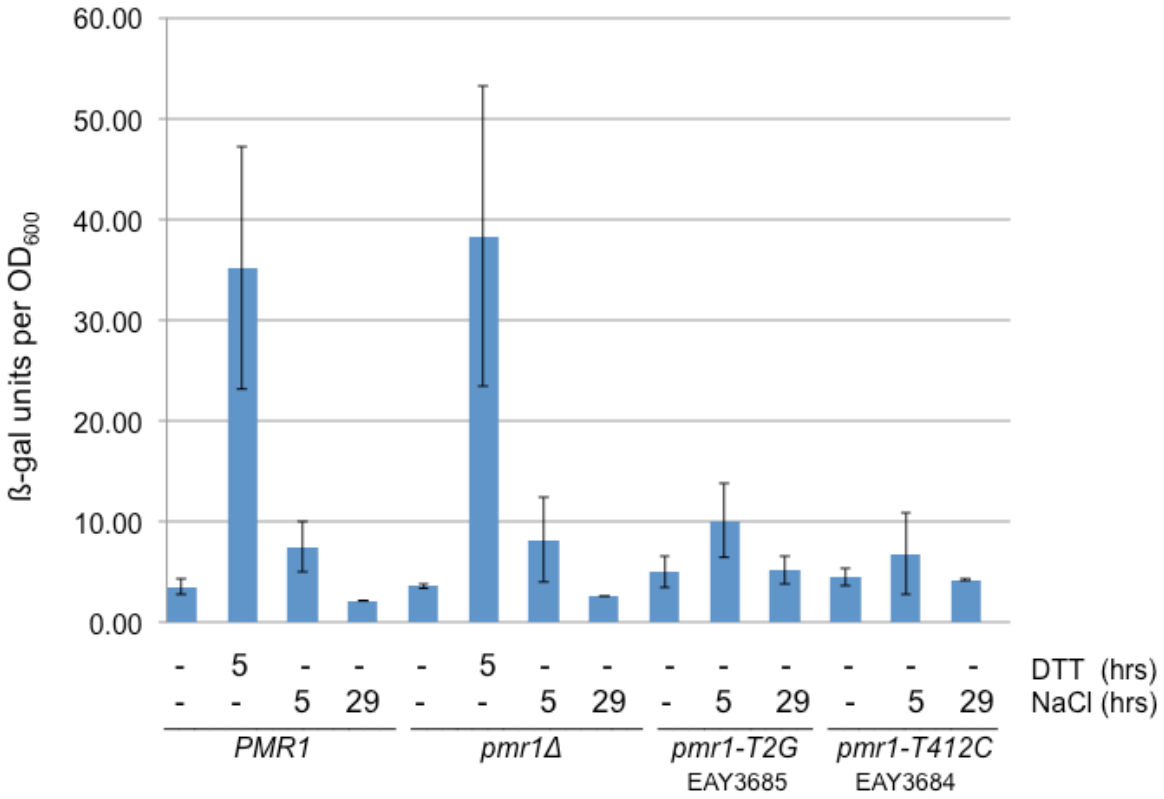

Figure 2.10. *pmr1* mutant strains do not appear to be induced for the unfolded protein response. Wild-type, *pmr1Δ,* and NaCl^r strains bearing the indicated *pmr1* mutations were transformed with the *UPRE::LACZ* reporter pMZ11 to measure the unfolded protein response. Transformants were analyzed for beta-galactosidase activity as described in the Materials and Methods. DTT was included at a final concentration of 5 mM and NaCl was added at a final concentration of 1.2 M for the number of hours indicated. The standard deviation of 2-7 independent measurements is presented.

As shown in Fig. 2.9, *pmr1Δ* and evolved *pmr1* strains each displayed constitutive expression of Pmr2/Ena1 at levels that were higher in the absence of NaCl than seen in wild-type. Using the pMZ11 reporter, we found that *pmr1* and *pmr1Δ* strains displayed similar phenotypes with respect to the unfolded protein response (Fig. 2.10). Together these results suggest that *ENA1* overexpression or the induction of the unfolded protein response cannot explain the different $NaCl^r$ phenotypes seen in *pmr1* and *pmr1Δ* strains. At present, we favor the idea that factors acting in calcium homeostasis are differentially regulated in the presence or absence of regulatory sequences during translation of Pmr1 or in the Pmr1 polypeptide, and may differentially regulate pumps that function in sodium and lithium efflux.

It is important to note that not all clones that showed salt resistance contained mutations in *PMR1*. In fact, most $NaCl^r$ clones obtained from compatible lines that had undergone 10 transfers did not contain *pmr1* mutations (Table 2.6; Fig. 2.11).

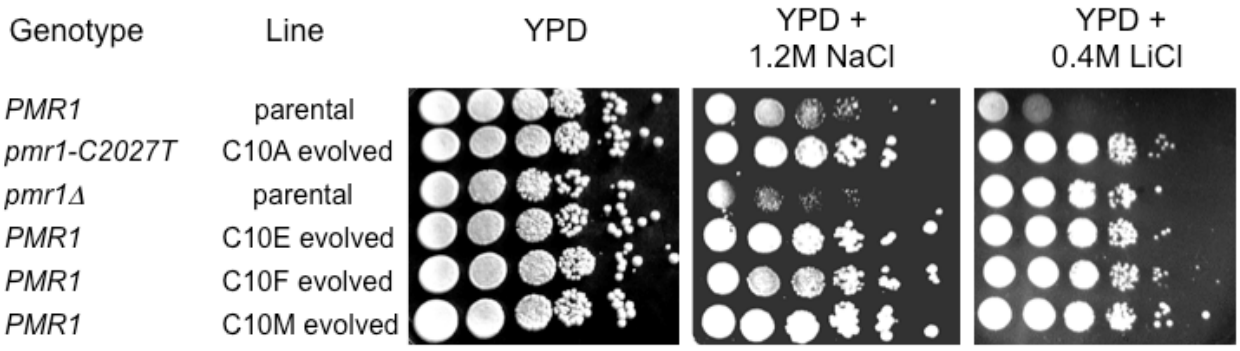

Figure 2.11. Growth of compatible lines on salt media. $NaCl^r$ clones (Table 2.4) obtained from Transfer 10 compatible lines were plated in 10-fold serial dilutions onto YPD, YPD + 1.2 M NaCl and YPD + 0.4 M LiCl plates.

Whole genome sequencing identified mutations in other candidate genes that may be causative. For example, clone C10B isolated from the compatible line at transfer 10 (C10B) contains a mutation in *CNB1.* Cnb1 is a regulatory subunit of calcineurin that is linked to stress responses ([45]; see below). While *cnb1* null mutants show sensitivity to NaCl, mutations in *CNB1* were previously identified in lines evolved in NaCl [46]. A clone isolated from a compatible line that had completed 10 transfers (C10C) contained a mutation in *GCN2* and a clone isolated from a compatible line that had completed 16 transfers (C16B) contained a mutation in *PTK1*. Gcn2 is a protein kinase that phosphorylates the alpha-subunit of translation initiation factor eIF2 in response to starvation and Ptk1 is a putative kinase that is involved in polyamine transport [47,48]. Gene replacement approaches will be required to test whether these or other mutations identified in these clones are causative.

DISCUSSION

In this study we showed that *S. cerevisiae* populations bearing an incompatible Mlh1-Pms1 combination display an adaptive advantage when challenged to adapt to a high salt growth media. The advantage, which was rapid, but transient, was due to the greater mutation supply in incompatible populations. While *pmr1* mutations were first seen at high frequency in incompatible lines, they were eventually detected at high frequency in compatible lines. The initial fitness advantage of incompatible lines in which *pmr1* mutations had occurred no longer existed when these lines were later competed against compatible lines in which *pmr1* mutations had subsequently also arisen. Taken together, these observations suggested that the two loci MMR incompatibility genotype (*MLH1, PMS1*) generated by recombination among naturally occurring variants at these genes accelerated the appearance of highly beneficial mutations within our yeast populations.

Why did incompatibility accelerate adaptation? The most likely explanation is that the moderate mutator phenotype seen in incompatible strains resulted in a higher rate of mutation (including those that were neutral, deleterious, and beneficial), with strains bearing beneficial mutations selected in our high salt stress condition. Such a model fits observations seen for bacterial populations maintained in stress or selection conditions; in these experiments bacteria displaying high mutation rates were identified at high frequency (e.g. [49]). In one such study *E. coli* populations displaying high mutation rates, primarily due to MMR defects, showed short-term fitness advantages that were not sustainable [19]. The simplest explanation is that the lack of a long-term fitness advantage was due to the accumulation of deleterious mutations elsewhere in the genomes containing the beneficial mutations [19,50-52]. As indicated in the Introduction, bacterial populations appear to overcome long-term fitness costs associated with high mutation rates by reacquiring functional MMR genes and thus normal mutation rates through horizontal gene transfer [14,19].

Several groups have examined whether a mutator phenotype in eukaryotes confers a fitness advantage when adapting to a stress environment (e.g. [21,37]). Some of the best-known examples involve cancer cells that display mutator phenotypes and/or high rates of genome instability [53]. Such work has suggested that over time mutator populations lose their initial advantage due to fitness costs and clonal interference (e.g. [37]). Fitness costs associated with high mutation rates can occur rapidly; for example, Ma et al. [6] showed that, following 160 generations of growth in non-permissive conditions, a diploid *mlh1*^{ts} yeast strain accumulated 92 heterozygous mutations, including five in essential genes, and that these mutations account for the poor spore viability (3%) seen in the strain. In addition, even a moderate mutator can quickly display a fitness defect. Relevant to this study, Heck et al. [22] showed that the *S288c MLH1-SK1 PMS1* incompatible genotype conferred a subtle but significant fitness cost, as measured by decreased spore viability, in diploids grown in rich

media for 160 generations. These observations suggest that an adaptive advantage seen in a mutator population is not sustainable. Furthermore, horizontal gene transfer is very rare in yeast [54], indicating that MMR is unlikely to be recovered through such a mechanism.

In our studies the incompatibility seen in *S288c MLH1-SK1 PMS1* strains provided an initial adaptive advantage prior to observing a detectable fitness cost. Such an advantage was likely due to incompatible strains displaying a modest mutator phenotype in conjunction with relatively large population sizes of the yeast undergoing serial transfer. How can adapted eukaryotic strains that are mutators escape long-term fitness costs? Sequencing analysis of a 32 kb genomic region provided evidence for recombination between SK1 and S288c strain groups [22]. This observation suggests that an incompatibility could be generated through mating and that adapted incompatible populations can mate back to other strains available in the environment to regain a compatible MMR combination, thus avoiding long-term fitness costs. Several factors are thought to contribute to the likelihood of such a scenario: 1. The frequently of meiotic cycles in wild populations. 2. The number of clonal generations experienced between an outcross. 3. The effects of post-zygotic barriers on the formation of viable progeny. 4. The effect of a stress condition on mating and meiotic cycles.

The ratio between mitotic and meiotic cycles in wild populations of *S. cerevisiae* is not known, although in *S. paradoxus*, population genetics approaches have shown that this organism undergoes a sexual cycle approximately once every 1,000 asexual cycles [55]. Magwene et al. [56] used a molecular clock analysis of genomic sequences between yeast strains to estimate the number of clonal generations that two strains would have experienced prior to outcrossing. Their estimates, in conjunction with recombination frequency estimates performed by Ruderfer et al. [57], suggested one outcrossing event per 12,500 to 62,500 generations. Importantly, random mating between spores in natural strains can occur at high rates in the laboratory, and outbreeding was shown to be elevated when spores from different

strains were passaged through the fruit fly gut [58,59]. Therefore, mating behaviors are likely to be affected by yeast lifestyle conditions that include selection/stress conditions, MMR defects, and population size. Thus it is not difficult to imagine outcrossing restoring MMR compatibility in a large population subjected to strong selection.

Mutations in *PMR1* confer a striking adaptive advantage to NaCl tolerance.

The majority of mutations that conferred salt tolerance mapped to the *PMR1* locus (Table 2.4 and Fig. 2.8). Previously Anderson et al. [42] identified mutations in other loci that are linked to NaCl tolerance including *PMA1*, which encodes a proton efflux pump, *ENA1*, which encodes a sodium efflux pump, and *CYC8*, which encodes a global transcriptional repressor that regulates ENA1 activity [42]. Possible reasons for why different loci were targeted in the two studies include: 1. The strains used in the two studies were not identical and were likely to have different background mutations. 2. We imposed a stronger selection for NaCl tolerance (1.2 M) than Anderson et al. (1.0 M) [42]. 3. We screened for adaptive advantages at earlier generations (70-100) than Anderson et al. (100-500) [42]. This is of interest because of recent observations made by Lang et al. [60], who studied the appearance of beneficial sterility mutations in haploid *S. cerevisiae*. In their system they estimated that roughly 100 generations of adaptation were required to generate a threshold level of genetic diversity upon which beneficial mutations could be selected. Thus different target genes might be identified depending on when adaptation is measured. 4. The effective population size per transfer is different in the two studies; we used a 10-fold higher number of cells than Anderson et al. [42]. Such a difference would likely alter the frequency and likelihood that mutations in any one locus would emerge. It is important to note that despite the differences in genes identified between the two studies there is a nice commonality in that $NaCl^r$ in both studies is likely to involve altered regulation of the Ena1 efflux pump (Fig. 2.9).

Negative epistasis in MMR genes as a possible adaptation strategy.

Epistatic effects involving interacting alleles have been detected for specific fitness measurements between individuals within a population (e.g. [61]). One of the best demonstrations of such effects in yeast was obtained by Brem et al. [62], who crossed two strains of baker's yeast and then searched for genetic interactions by measuring the levels of all transcripts in a large number of spore progeny. In their analysis they identified statistically significant interactions between locus pairs for 225 transcripts. Based on a population survey of *MLH1* and *PMS1* alleles, we argued previously that the incompatibility that was identified between MMR genes is similar to epistatic interactions seen in hybrids formed from established or incipient species ([28,29]; see examples in [22]). Support for such an idea is based on the fact that mild reproductive barriers have already been shown to exist between some *S. cerevisiae* strains [22], and the MMR machinery has been shown to contribute to reproductive isolation when *S. cerevisiae* strains with sequence divergence are mated [63,64]. The experiments presented in this paper provide an interesting twist to this idea because the incompatibility involving *MLH1* and *PMS1* might also provide opportunities for adaptive evolution by moderately increasing mutation rates.

ACKNOWLEDGEMENTS

We thank members of the Alani lab, Andrew Clark, Richard Lenski, and Jeff Brodsky for helpful comments and technical advice. We would also like to thank Dr. Anthony Hay, Dr. Qi Sun of the Cornell University Bioinformatics Core Facility, and Dr. K.T. Nishant of the Indian Institute of Science, Education, and Research for their advice regarding whole genome sequencing procedures.

REFERENCES

1. Kunkel TA. Erie DA (2005) DNA mismatch repair. Annu Rev Biochem 74: 681–710. PMID :15952900 doi: 10.1146/annurev.biochem.74.082803.133243

2. Nishant KT, Wei W, Mancera E, Argueso JL, Schlattl A, et al. (2010) The baker's yeast diploid genome is remarkably stable in vegetative growth and meiosis. PLoS Genet 6: e1001109. doi: 10.1371/journal.pgen.1001109. PMID :20838597

3. Zanders S, Ma X, Roychoudhury A, Hernandez RD, Demogines A, Barker B et al. (2010) Detection of heterozygous mutations in the genome of mismatch repair defective diploid yeast using a Bayesian approach. Genetics 186: 493–503. doi: 10.1534/genetics.110.120105. PMID :20660644

4. Hombauer H, Campbell CS, Smith CE, Desai A, Kolodner RD (2011) Visualization of eukaryotic DNA mismatch repair reveals distinct recognition and repair intermediates. Cell 147: 1040–1053. doi: 10.1016/j.cell.2011.10.025. PMID :22118461

5. Jiricny J (2013) Postreplicative mismatch repair. Cold Spring Harb Perspect Biol 5: a012633. doi: 10.1101/cshperspect.a012633. PMID :23545421

6. Ma X, Rogacheva MV, Nishant KT, Zanders S, Bustamante CD, Alani E. (2012) Mutation hot spots in yeast caused by long-range clustering of homopolymeric sequences. Cell Rep 1: 36–42. doi: 10.1016/j.celrep.2011.10.003. PMID :22832106

7. Lynch M. (2010) Evolution of the mutation rate. Trends in Genetics 26: 345–352. doi: 10.1016/j.tig.2010.05.003. PMID :20594608

8. Drake JW (1991) A constant rate of spontaneous mutation in DNA-based microbes. Proc Natl Acad Sci USA 88: 7160–7164. PMID :1831267 doi: 10.1073/pnas.88.16.7160

9. Drake JW, Charlesworth B, Charlesworth D, Crow JF (1998) Rates of Spontaneous Mutation. Genetics 148: 1667–1686. PMID :9560386

10. Zeyl C, DeVisser JA (2001) Estimates of the rate and distribution of fitness effects of spontaneous mutation in Saccharomyces cerevisiae. Genetics 157: 53–61. PMID :11139491

11. LeClerc JE, Li B, Payne WL, Cebula TA (1996) High mutation frequencies among Escherichia coli and Salmonella pathogens. Science 274: 1208–1211. PMID :8895473 doi: 10.1126/science.274.5290.1208

12. Matic I, Radman M, Taddei F, Picard B, Doit C, et al. (1997) Highly variable mutation rates in commensal and pathogenic Escherichia coli. Science 277: 1833–1834. PMID :9324769 doi: 10.1126/science.277.5333.1833

13. Boe L, Danielsen M, Knudsen S, Petersen JB, Maymann J, et al. (2000) The frequency of mutators in populations of Escherichia coli. Mutat Res 448: 47–55. PMID :10751622 doi: 10.1016/s0027-5107(99)00239-0

14. Denamur E., Lecointre G, Darlu P, Tenaillon O, Acquaviva C et al. (2000) Evolutionary implications of the frequent horizontal transfer of mismatch repair genes. Cell 103: 711–721. PMID :11114328 doi: 10.1016/s0092-8674(00)00175-6

15. Sniegowski PD, Dombrowski PG, Fingerman E (2002) Saccharomyces cerevisiae and Saccharomyces paradoxus coexist in a natural woodland site in North America and display different levels of reproductive isolation from European conspecifics. FEMS Yeast Res 1: 299–306. PMID :12702333 doi: 10.1111/j.1567-1364.2002.tb00048.x

16. Taddei F, Radman M, Maynard-Smith J, Toupance B, Gouyon PH, et al. (1997) Role of mutator alleles in adaptive evolution. Nature 387: 700–702. PMID :9192893 doi: 10.1038/42696

17. Tanaka MM, Bergstrom CT, Levin BR (2003) The evolution of mutator genes in bacterial populations: the roles of environmental change and timing. Genetics 164: 843–854. PMID :12871898

18. Townsend JP, Nielsen KM, Fisher DS, Hartl DL (2003) Horizontal acquisition of divergent chromosomal DNA in bacteria: effects of mutator phenotypes. Genetics 164: 13–21. PMID :12750317

19. Giraud A, Matic I, Tenaillon O, Clara A, Radman M, et al. (2001) Costs and benefits of high mutation rates: adaptive evolution of bacteria in the mouse gut. Science 291: 2606–2608. PMID :11283373 doi: 10.1126/science.1056421

20. Chao L, Cox EC (1983) Competition between high and low mutating strains of Escherichia coli. Evolution 37: 125–134. doi: 10.2307/2408181

21. Thompson DA, Desai MM, Murray AW. (2006) Ploidy controls the success of mutators and nature of mutations during budding yeast evolution. Curr Biol 16: 1581–1590. PMID :16920619 doi: 10.1016/j.cub.2006.06.070

22. Heck JA, Argueso JL, Gemici Z, Reeves RG, Bernard A, et al. (2006) Negative epistasis between natural variants of the Saccharomyces cerevisiae MLH1 and PMS1 genes results in a defect in mismatch repair. Proc Natl Acad Sci USA 103: 3256–3261. PMID :16492773 doi: 10.1073/pnas.0510998103

23. Muller HJ, Pontecorvo G (1940) Recombinants between Drosophila Species the F1 Hybrids of which are sterile. Nature 146: 199–200. doi: 10.1038/146199b0

24. Muller HJ (1939) Reversibility in evolution considered from the standpoint of genetics. Biol Rev Camb Philos Soc 14: 261–280. doi: 10.1111/j.1469-185x.1939.tb00934.x

25. Orr HA (1995) The population genetics of speciation: the evolution of hybrid incompatibilities. Genetics 139: 1805–1813. PMID :7789779

26. Dobzhansky T (1936) Studies on Hybrid Sterility. II. Localization of Sterility Factors in Drosophila Pseudoobscura Hybrids. Genetics 21: 113–135. PMID :17246786

27. Demogines A, Wong A, Aquadro C, Alani E (2008) Incompatibilities involving yeast mismatch repair genes: a role for genetic modifiers and implications for disease penetrance and variation in genomic mutation rates. PLoS Genetics 4: e1000103. doi:10.1371/journal.pgen. 1000103. PMID :18566663

28. Wu CI, Ting CT (2004) Genes and speciation. Nat Rev Genet 5: 114–122. PMID :14735122 doi: 10.1038/nrg1269

29. Coyne JA, Orr HA (2004) Speciation, Sinauer Associates, Sunderland, MA.

30. Ting CT, Tsaur SC, Wu ML, Wu CI (1998) A rapidly evolving homeobox at the site of a hybrid sterility gene. Science 282: 1501–1504. PMID :9822383 doi: 10.1126/science.282.5393.1501

31. Barbash DA, Siino DF, Tarone AM, Roote J (2003) A rapidly evolving MYB-related protein causes species isolation in Drosophila. Proc Natl Acad Sci USA 100: 5302–5307. PMID :12695567 doi: 10.1073/pnas.0836927100

32. Wittbrodt J, Adam D, Malitschek B, Maueler W, Raulf F et al. (1989) Novel putative receptor tyrosine kinase encoded by the melanoma-inducing Tu locus in Xiphophorus. Nature 341: 415–421. PMID :2797166 doi: 10.1038/341415a0

33. Rawson RD, Burton RS (2002) Functional coadaptation between cytochrome c and cytochrome c oxidase within allopatric populations of a marine copepod. Proc Natl Acad Sci USA 99: 12955–12958. PMID :12271133 doi: 10.1073/pnas.202335899

34. Hartl D, Clark A (2007) Principles of Population Genetics. 4rth Edition. Sinauer Associates.

35. Dykhuizen D, Hartl DL (1980) Selective neutrality of 6GPD allozymes in E. coli and the effects of genetic background. Genetics 96: 801–817. PMID :7021316

36. McDonald JH (2014) Handbook of Biological Statistics (3rd ed) p 145–156. Sparky House Publishing, Baltimore, Maryland.

37. Raynes Y, Gazzara MR, Sniegowski PD (2012) Contrasting dynamics of a mutator allele in asexual populations of differing size. Evolution 66: 2329–2334. doi: 10.1111/j.1558-5646.2011.01577.x. PMID :22759305

38. Antebi A, and Fink GR (1992) The yeast Ca2+-ATPase homologue, PMR1, is required for normal Golgi function and localizes in a novel Golgi-like distribution. Mol Biol Cell 3: 633–654. PMID :1379856 doi: 10.1091/mbc.3.6.633

39. Park SY, Seo SB, Lee SJ, Na JG, Kim YJ (2001). Mutation in PMR1, a Ca(2+)-ATPase in Golgi, confers salt tolerance in Saccharomyces cerevisiae by inducing expression of PMR2, an Na(+)-ATPase in plasma membrane. J Biol Chem 276: 28694–28699. PMID :11387321 doi: 10.1074/jbc.m101185200

40. Zhao J, Lin W, Ma X, Lu Q, Ma X, Bian G, Jiang L (2010) The protein kinase Hal5p is the high-copy suppressor of lithium-sensitive mutations of genes involved in the sporulation and meiosis as well as the ergosterol biosynthesis in Saccharomyces cerevisiae. Genomics 95: 290–298. doi: 10.1016/j.ygeno.2010.02.010. PMID :20206679

41. Cunningham KW, Fink GR (1996) Calcineurin inhibits VCX1-dependent H+/Ca2+ exchange and induces Ca2+ ATPases in Saccharomyces cerevisiae. Mol Cell Biol 16: 2226–2237. PMID :8628289

42. Anderson JB, Funt J, Thompson DA, Prabhu S, Socha A et al. (2010) Determinants of divergent adaptation and Dobzhansky-Muller interaction in experimental yeast populations. Curr Biol 20: 1383–1388. doi: 10.1016/j.cub.2010.06.022. PMID :20637622

43. Lenassi M, Gostinčar C, Jackman S, Turk M, Sadowski I, Nislow C, et al. (2013) Whole genome duplication and enrichment of metal cation transporters revealed by de novo genome sequencing of extremely halotolerant black yeast Hortaea werneckii. PLoS One 8: e71328. doi: 10.1371/journal.pone.0071328. PMID :23977017

44. Zhou M, Schekman R (1999) The engagement of Sec61p in the ER dislocation process. Mol Cell 4: 925–934. PMID :10635318 doi: 10.1016/s1097-2765(00)80222-1

45. Cyert MS and Thorner J (1992) Regulatory subunit (CNB1 gene product) of yeast Ca2+/calmodulin-dependent phosphoprotein phosphatases is required for adaptation to pheromone. Mol Cell Biol 12: 3460–3469. PMID :1321337

46. Kohn LM, Anderson JB (2014) The underlying structure of adaptation under strong selection in 12 experimental yeast populations. Eukaryot Cell 13:1200–1206. doi: 10.1128/EC.00122-14. PMID :25016004

47. Hinnebusch AG and Natarajan K (2002) Gcn4p, a master regulator of gene expression, is controlled at multiple levels by diverse signals of starvation and stress. Eukaryot Cell 1: 22–32. PMID :12455968 doi: 10.1128/ec.01.1.22-32.2002

48. Kakinuma Y, Maruyama T, Nozaki T, Wada Y, Ohsumi Y, Igarashi K (1995) Cloning of the gene encoding a putative serine threonine protein kinase which enhances spermine uptake in Saccharomyces cerevisiae. Biochem Biophys Res Commun 216: 985–992. PMID :7488221 doi: 10.1006/bbrc.1995.2717

49. Sniegowski PD, Gerrish PJ, Lenski RE (1997) Evolution of high mutation rates in experimental populations of E. coli. Nature 387: 703–705. PMID :9192894 doi: 10.1038/42701

50. Funchain P, Yeung A, Stewart JL, Lin R, Slupska MM, Miller JH (2000) The consequences of growth of a mutator strain of Escherichia coli as measured by loss of function among multiple gene targets and loss of fitness. Genetics 154: 959–970. PMID :10757746

51. Woods RJ, Barrick JE, Cooper TF, Shrestha U, Kauth MR, Lenski RE. (2011) Second-order selection for evolvability in a large Escherichia coli population. Science 331: 1433–1436. doi: 10.1126/science.1198914. PMID :21415350

52. Elena SF, Lenski RE (2003) Evolution experiments with microorganisms: the dynamics and genetic bases of adaptation. Nat Rev Genet 4: 457–469. PMID :12776215 doi: 10.1038/nrg1088

53. Sprouffske K, Merlo LM, Gerrish PJ, Maley CC, Sniegowski PD (2012) Cancer in light of experimental evolution. Curr Biol 22: R762–771. doi: 10.1016/j.cub.2012.06.065. PMID :22975007

54. Liti G, Louis EJ (2005) Yeast evolution and comparative genomics. Annu Rev Microbiol 59: 135–153. PMID :15877535 doi: 10.1146/annurev.micro.59.030804.121400

55. Tsai IJ, Bensasson D, Burt A, Koufopanou V (2008) Population genomics of the wild yeast Saccharomyces paradoxus: Quantifying the life cycle. Proc Natl Acad Sci USA 105: 4957–4962. doi: 10.1073/pnas.0707314105. PMID :18344325

56. Magwene PM, Kayıkçı Ö, Granek JA, Reininga JM, Scholl Z, Murray D (2011) Outcrossing, mitotic recombination, and life-history trade-offs shape genome evolution in Saccharomyces cerevisiae. Proc Natl Acad Sci USA 108: 1987–1992. doi: 10.1073/pnas.1012544108. PMID :21245305

57. Ruderfer DM, Pratt SC, Seidel HS, Kruglyak L (2006) Population genomic analysis of outcrossing and recombination in yeast. Nat Genet 38: 1077–1081. PMID :16892060 doi: 10.1038/ng1859

58. Murphy HA, Zeyl CW (2010) Yeast Sex: Surprisingly high rates of outcrossing between asci. PLoS One 5: e10461. doi: 10.1371/journal.pone.0010461. PMID :20463964

59. Reuter M, Bell G, Greig D (2007) Increased outbreeding in yeast in response to dispersal by an insect vector. Curr Biol 17: R81–83. PMID :17276903 doi: 10.1016/j.cub.2006.11.059

60. Lang GI, Botstein D, Desai MM (2011) Genetic variation and the fate of beneficial mutations in asexual populations. Genetics 188: 647–661. doi: 10.1534/genetics.111.128942. PMID :21546542

61. Corbett-Detig RB, Zhou J, Clark AG, Hartl DL, Ayroles JF (2013) Genetic incompatibilities are widespread within species. Nature 504: 135–137. doi: 10.1038/nature12678. PMID :24196712

62. Brem RB, Storey JD, Whittle J, Kruglyak L (2005) Genetic interactions between polymorphisms that affect gene expression in yeast. Nature 436: 701–703. PMID :16079846 doi: 10.1038/nature03865

63. Hunter N, Chambers SR, Louis EJ, Borts RH (1996) The mismatch repair system contributes to meiotic sterility in an interspecific yeast hybrid. EMBO J 15: 1726–1733. PMID :8612597

64. Naumov GI, Naumova ES, Lantto RA, Louis EJ, Korhola M (1992) Genetic homology between Saccharomyces cerevisiae and its sibling species S. paradoxus and S. bayanus: electrophoretic karyotypes. Yeast 8: 599–612. PMID :1441740 doi: 10.1002/yea.320080804

65. Winston F, Dollard C, Ricupero-Hovasse SL (1995) Construction of a set of convenient Saccharomyces cerevisiae strains that are isogenic to S288C. Yeast 11: 53–55. PMID :7762301 doi: 10.1002/yea.320110107

66. Rose MD, Winston F, Hieter P (1990) Methods in yeast genetics: A Laboratory Course Manual. Cold Spring Harbor Laboratory Press, Cold Spring Harbor, NY.

67. Gietz RD, Schiestl RH (2007) Large-scale high-efficiency yeast transformation using the LiAc/SS carrier DNA/PEG method. Nat Protoc 2: 38–41. PMID :17401336 doi: 10.1038/nprot.2007.15

68. Holm C, Meeks-Wagner DW, Fangman WL, Botstein D (1986) A rapid, efficient method for isolating DNA from yeast. Gene 42: 169–173. PMID :3015730 doi: 10.1016/0378-1119(86)90293-3

69. Rosner B, Glynn RJ, Lee M-LT (2006) The Wilcoxon signed rank test for paired comparisons of clustered data. Biometrics 62: 185–192. PMID :16542245 doi: 10.1111/j.1541-0420.2005.00389.x

70. Goldstein AL, McCusker JH (1999) Three new dominant drug resistance cassettes for gene disruption in Saccharomyces cerevisiae. Yeast 15: 1541–1553. PMID :10514571

71. Baganz F, Hayes A, Marren D, Gardner DC, Oliver SG (1997) Suitability of replacement markers for functional analysis studies in Saccharomyces cerevisiae. Yeast 13: 1563–1573. PMID :9509575

72. Tran HT, Keen JD, Kricker M, Resnick MA, Gordenin DA (1997) Hypermutability of homonucleotide runs in mismatch repair and DNA polymerase proofreading yeast mutants. Mol Cell Biol 17: 2859–2865. PMID :9111358

73. Dixon WJ, Massey FJ (1969) Introduction to Statistical Analysis. New York: McGraw-Hill.

74. McKenna A, Hanna M, Banks E, Sivachenko A, Cibulskis K, et al. (2010) The Genome Analysis Toolkit: a MapReduce framework for analyzing next-generation DNA sequencing data. Genome Res 20: 1297–1303. doi: 10.1101/gr.107524.110. PMID :20644199

75. Wanat JJ, Singh N, Alani E (2007) The effect of genetic background on the function of Saccharomyces cerevisiae mlh1 alleles that correspond to HNPCC missense mutations. Hum Mol Genet 16: 445–452. doi: 10.1093/hmg/ddl479. PMID :17210669

CHAPTER 3.

Suppression of a genetic incompatibility in natural yeast strains

* Work in this chapter was a collaborative effort with contributions from Duyen Bui, Anne Friedrich, Jae Joung Choi, Charles Aquadro, and Eric Alani. Contributions were as follows: D.B. performed post adaptation competitions, analyzing for incompatibility and constructing reporters A.F. performed whole genome sequencing of 1011 yeast strains and analyzed variants and singletons. D.B., J.C., C.A. and E.A. contributed to analysis, ideas and interpretation of the research.

ABSTRACT

An elevated mutation rate can be beneficial to an organism because it provides a source of mutations for adaption to a changing environment. However, such benefits are likely to be accompanied by long-term fitness costs due to the accumulation of deleterious mutations. We previously identified a negative-epistatic interaction involving naturally occurring polymorphisms in the *MLH1* and *PMS1* mismatch repair (MMR) genes of baker's yeast. We hypothesize that this interaction was created through mating between divergent yeast strains, creating mutator progeny that can rapidly, but transiently, adapt to an environmental stress. We demonstrated in competition experiments that this MMR incompatibility confers a fitness cost that would likely prevent it from being stably maintained in natural populations. To test this, we analyzed the genomes of 1011 yeast strains and unexpectedly identified a MMR incompatibility genotype in three related clinical isolates. The *MLH1-PMS1* gene combination isolated from these strains conferred a mutator phenotype when expressed in the S288c laboratory background. For two strains this incompatibility was weakened by the presence of a previously characterized intragenic suppressor polymorphism in *MLH1*. Population genetic analysis of genomes of the three clinical isolates indicated that they were unlikely to be mutators. Using a newly created reporter that measures mutation rates in natural strains we confirmed that the two strains bearing the suppressor *MLH1* polymorphism showed lower mutation rates than the strain lacking the polymorphism. However, the overall mutation rate in the three strains was similar to that seen in S288c and SK1 strains containing the compatible *MLH1-PMS1* combination. These observations are consistent with asexual organisms obtaining an adaptive advantage by generating mutator states that provide the raw material for adaptation. In this model incompatible states, which have a long-term fitness cost, are eliminated due to the rapid accumulation of intragenic and extragenic suppressor mutations. These observations highlight an effective strategy for asexual eukaryotes to avoid long-term fitness costs associated with an elevated mutation rate.

INTRODUCTION

Most spontaneous mutations that occur in natural populations are neutral or deleterious [1,2]. However, in changing environments, bacteria and yeast can display mutator phenotypes, often through the loss of DNA mismatch repair (MMR) functions, that provide a competitive advantage by increasing the chance of obtaining the first adaptive mutation(s) [3–11]. Ultimately, such benefits are overshadowed by long-term fitness costs resulting from the accumulation of deleterious mutations. In bacteria, MMR genes are exchanged within populations at higher than average rates through horizontal gene transfer. This exchange is likely to occur at a high frequency due to an elevated rate of genetic recombination seen in MMR-deficient strains [4]. In the case of MMR defective bacteria, once adapted to an environment, adapted cells can recover MMR functions via horizontal gene transfer or suppress the mutator phenotype and thus minimize long-term fitness costs [8,12]. In support of this idea, Taddei et al. (1997) suggested that that it is likely to be common in natural asexual populations for a mutator state to be created and transiently promote adaptive evolution, but then disappear to avoid long-term fitness costs once favorable mutations reach fixation [5].

While it might be common for a eukaryotic organism such as baker's yeast to have lost MMR functions [13, 14], there is little evidence that these functions can be recovered through horizontal gene transfer [15]. One approach that baker's yeast could employ to avoid long-term fitness effects associated with a mutator phenotype is mating to a non-mutator strain, followed by sporulation and segregation of genotypes so that the mutator locus and a beneficial mutation are no longer linked. Such a strategy is considered effective because outcrossing has the potential to generate new genotypes at a much higher frequency than spontaneous mutation [16].

We created a model to explain how a genetic incompatibility involving the DNA mismatch repair genes *MLH1* and *PMS1* could arise in baker's yeast (Fig. 3.1; [10,17,18]). In this model, based on ideas first proposed by Dobzhansky and Muller [19–22], a common ancestral state gives rise to derived strains (S288c, SK1) that acquire neutral or beneficial

mutations in the *MLH1* and *PMS1* MMR genes. Mating between these divergent populations would create a hybrid genotype. In laboratory experiments the hybrid combination was shown to confer a higher mutation rate, and provides a fitness advantage in adaptation to a stress condition [10,17]. These studies also suggested that such an advantage would be transient because the mutator genotype would result in a long-term fitness cost [17]. Consistent with a fitness cost, none of 68 wild, lab, and clinical isolates examined displayed the incompatible genotype despite evidence suggesting that such a genotype could be created by mating. An attractive explanation for this observation is that incompatible strains exist transiently to provide an adaptive advantage, but mechanisms such as outcrossing restore the compatible genotype. Consistent with this idea was a sequencing analysis of a 32 kb genomic region of baker's yeast which provided evidence for recombination between the S288c and SK1 groups (Fig. 3.1; [17]).

A challenge to the above model is that several studies have estimated that the number of clonal generations that two yeast strains would have experienced prior to outcrossing is very high, one outcrossing event per 12,500 to 62,500 generations [16,23]. While such observations suggest that baker's yeast has primarily an asexual lifestyle, random mating between natural strains can be achieved at high rates in the lab and can be elevated in different environments, such as in the gut of the fruit fly [24,25].

Another mechanism for how incompatibility can be eliminated to avoid long-term fitness costs invokes the rapid acquisition and selection of intragenic or extragenic suppressor mutations in the absence of a sexual lifestyle (e.g. [12]). In this scenario incompatible strains containing a beneficial mutation for adaptation continue to rapidly acquire mutations; among these is a suppressor of the mutator phenotype that is selected to reduce the accumulation of deleterious mutations and thus genetic load [12]. Such a scenario has been observed in single cell organisms that have relatively large population sizes [12]. Consistent with this idea, we identified in the 68 strain set mentioned above evidence for polymorphisms in *MLH1* contributing to modify the mutator phenotype due to the *MLH1-PMS1* incompatibility [18].

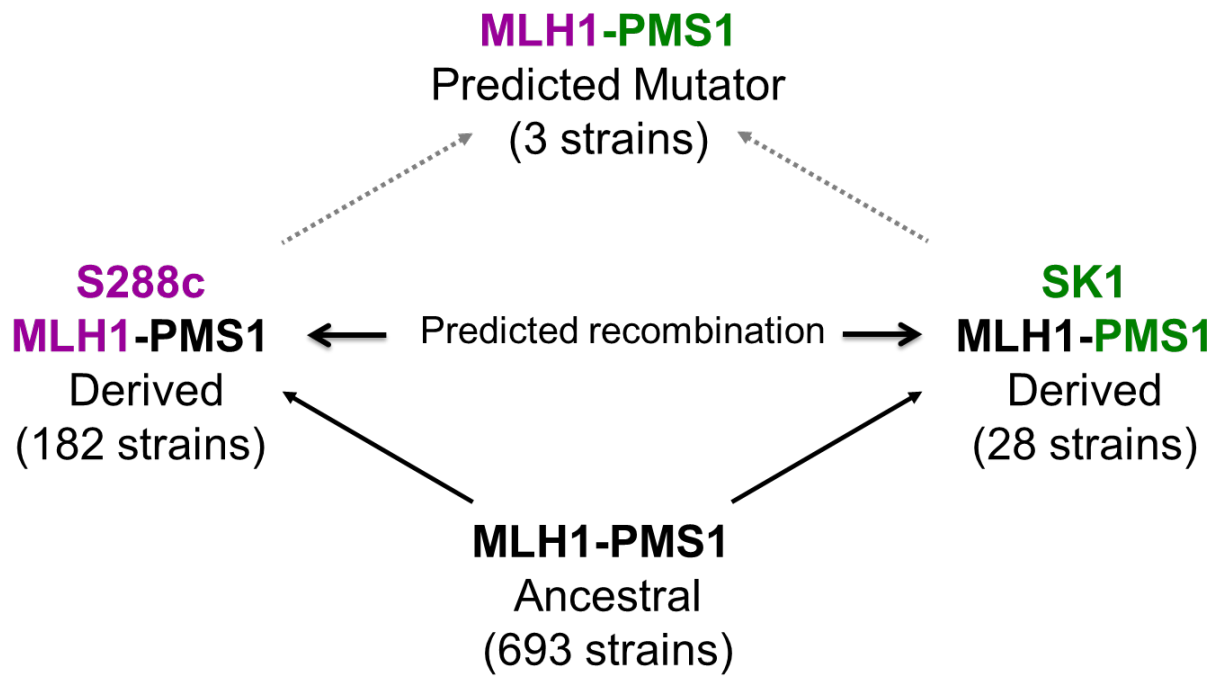

Figure 3.1. A model proposing that an incompatibility involving the MMR genes *MLH1* and *PMS1* drives adaptive evolution. In this model, an ancestral strain bearing MLH1 Gly 761 and PMS1 Arg 818/822 alleles acquire neutral or beneficial mutations that lead to the derived S288c (purple, Asp 761, Arg 818/822) and SK1 (green, Gly 761, Lys 818/822) group strains. Mating between the derived strains can yield an allele combination (MLH1 Asp 761, PMS1 Lys 818/822) that displays negative epistasis and thus a mutator phenotype. Previous work suggested that recombination has occurred between the two derived classes, leading to exchange of genetic information and a hybrid mutator genotype that can also remate to reconstruct derived or ancestral genotypes [17]. As described in the text, sequences of *MLH1* and *PMS1* genes from 1011 *S. cerevisiae* wild, clinical, production, and lab strains from world-wide collections genomes were grouped according to their amino acid residues 761 (G or D) in MLH1 and 818 (R or K) in PMS1. Three strains map to the predicted hybrid mutator category. Of the 1011 strains, 105 are ambiguous for the *MLH1* 761 and *PMS1* 818/822 genotypes, indicating that they are likely heterozygous for the SNPs at these positions (See Results).

Previously, we showed that incompatible strains display a transient fitness advantage [10]. In the present study we examined whether evolved incompatible strains can maintain fitness in non-stress and stress conditions. Our observations showed that incompatible strains rapidly display fitness defects; this encouraged us to survey 1011 *S. cerevisiae* wild, clinical, production, and lab strains from world-wide collections for their *MLH1* and *PMS1* genotypes. We identified and carefully characterized three clinical isolates that displayed the incompatible *MLH1-PMS1* genotype and showed that long-term fitness costs appear to have been avoided in these strains through additional events, both intragenic and extragenic, that suppressed mutation rate. Together these observations suggest that in natural asexual eukaryotic populations, a mutator state can be created to transiently promote adaptive evolution, but can then be suppressed once beneficial mutations go to fixation.

MATERIAL AND METHODS

Strains and media

Saccharomyces cerevisiae spore clones from the S288c strain background (Fig. 3.2; Table 3.1; [26]) were analyzed in competition assays. These strains were grown in YPD (yeast extract, peptone, dextrose) and YPD + 1.2M NaCl ([27]; Table 3.1). Natural and S288c derived strains transformed with pEAA613 (*ARS-CEN NATMX, kanmx::insE-A*$_{14}$; Table 3.2) were maintained in YPD media containing 50 μg/ml clonNAT (Tables 3.5, 3.6). Yeast transformations were performed as described [28].

EAY1365 (*MATa, ura3-52, leu2Δ1, trp1Δ63, his3Δ200, lys2::insE-A14, mlh1Δ::KanMX4, pms1Δ::KanMX4*), an S288c derived strain, was used to measure reversion to Lys$^+$. This strain was transformed with *ARS-CEN, LEU2, MLH1* (pEAA213 and derivatives) and *ARS-CEN, HIS3, PMS1* (pEAA238 and derivatives) plasmids, and were grown in minimal selective media lacking histidine and leucine (Table 3.4; [27]). In this chapter, genes derived from the S288c background are designated with a “c” (e.g. *cMLH1*) and those derived from SK1 with a “k” (e.g. *kMLH1*).

Table 3.1. Strains.

EAY235	*MATa, ura3-52, leu2Δ1, trp1Δ63*
EAY280	*MATa, ura3-52, leu2Δ1, trp1Δ63, msh2Δ::hisG*
EAY1365	*MATa, ura3-52, leu2Δ1, trp1 Δ 63, his3 Δ 200, lys2::insE-A14, mlh1 Δ::KanMX4, pms1 Δ::KanMX4*
EAY1369	*MATalpha*, *ura3-52, leu2Δ1, trp1Δ63, his3Δ200,lys2::insE-A_{14}, cPMS1::HIS3*
EAY1370	*MATalpha*, *ura3-52, leu2Δ1, trp1Δ63, his3Δ200,lys2::insE-A_{14}, kPMS1::HIS3*
EAY1372	*MATa, ura3-52, leu2Δ1, trp1Δ63,, lys2::insE-A14::hisG msh2Δ::hisG*
EAY3191	*MATa, ura3-52, leu2Δ1, trp1Δ63, his3Δ200, kPMS1::HIS3, kMLH1::KANMX*
EAY3236	*MATalpha, ura3-52, leu2Δ1, trp1Δ63, his3Δ200, kPMS1::HIS3, cMLH1::KANMX*
EAY3241	*MATa, ura3-52, leu2Δ1, trp1Δ63, his3Δ200, kPMS1::HIS3, kMLH1::NATMX*
EAY3242	*MATalpha ura3-52, leu2Δ1, trp1Δ63, his3Δ200, kPMS1::HIS3, kMLH1::NATMX*
EAY3688	EAY3236, *pmr1-T412C*
EAY3689	EAY3236*, pmr1-T2G*
EAY3690	EAY3236*, pmr1-T459A*

Table 3.2. Plasmids.

	Relevant genotype
pRS413	*ARS-CEN HIS3*
pRS415	*ARS-CEN, LEU2*
pRS416	*ARS-CEN, URA3*
pLZ259	*ARS-CEN, NATMX*
pEAA611	*ARS-CEN, NATMX,URA3 promoter-KANMX::insE-A*$_{10}$
pEAA612	*ARS-CEN, NATMX,URA3 promoter-kanMX::insE-A*$_{11}$
pEAA613	*ARS-CEN, NATMX,URA3 promoter-kanMX::insE-A*$_{14}$
pEAA614	*ARS-CEN, NATMX,LEU2 promoter-KANMX::insE-A*$_{10}$
pEAA615	*ARS-CEN, NATMX,LEU2 promoter-kanMX::insE-A*$_{11}$
pEAA616	*ARS-CEN, NATMX,LEU2 promoter-kanMX::insE-A*$_{14}$
pEAA608	*ARS-CEN, LEU2, MLH1*-YJM541/YJM554*
pEAA609	*ARS-CEN, LEU2, MLH1*-YJM555
pEAA213	*ARS-CEN, LEU2, MLH1*-S288c
pEAA214	*ARS-CEN, LEU2, MLH1*-SK1
pEAA610	*ARS-CEN, HIS3, PMS1*-YJM541
pEAA238	*ARS-CEN, HIS3, PMS1*-S288c
pEAA239	*ARS-CEN, HIS3, PMS1*-SK1

*The *MLH1* open reading frames in YJM541 and YJM554 are identical in DNA sequence.

Plasmids

pEAA213 (c*MLH1, ARSH4 CEN6, LEU2*) and pEAA214 (k*MLH1, ARSH4 CEN6, LEU2*) were described previously ([17,29]; Table 3.2). *MLH1* expression is driven in both plasmids by the S288c *MLH1* promoter. *MLH1* from YJM541, YJM554, and YJM555 were cloned into pEAA213 by amplifying *MLH1* from genomic DN A [27] using Roche high fidelity polymerase (Roche) and primers AO324 (5'ATAGTGTAGGAGGCGCTG) and AO821 (5'AACTTTGCGGCCGCGGATCCAGCCAAAACGTTTTAAAGTTA). The PCR amplified product containing the entire *MLH1* open reading frame was digested with *Bam*H1-and *Nhe*I and inserted into the corresponding sites of pEAA213. The entire PCR fragment was DNA sequenced. All of the resulting constructs expressed *MLH1* via the S288c *MLH1* promoter.

pEAA238 (c*PMS1, ARSH4, CEN6, HIS3*) and pEAA239 (k*PMS1*, *ARSH4, CEN6, HIS3*) were described previously (Table 3.2; [17,29]. In both plasmids *PMS1* expression is driven by the S288c *PMS1* promoter. *PMS1* from YJM541, YJM554, and YJM555 were cloned into pEAA238 by amplifying *PMS1* from genomic DNA using Roche high fidelity polymerase and primers AO548 (5'CGATTCTAATACAGATTTTAATGACC) and AO481 (5'CCACGTTCATATTCTTAATGGCTAAGC). The PCR amplified product containing the entire *PMS1* open reading frame was digested with *Aat*II-and *Mlu*I and inserted into the corresponding sites of pEAA238. The entire PCR fragment was DNA sequenced. All of the resulting constructs expressed *PMS1* via the S288c *PMS1* promoter.

pEAA613 contains the *URA3 promoter-kanMX::insE-*A_{14} reversion reporter constructed using overlap PCR [30]. Briefly, this reporter is expressed via the *URA3* promoter (-402 to the ATG start site). A 55 bp sequence containing a +1 frameshift in the 14 bp homopolymeric A run (*insE-*A_{14}*;* [31]) was inserted immediately after the *URA3* ATG, followed by codons 18 to 269 of the *KANMX* open reading frame derived from pFA6-KANMX, and 159 bp of *KANMX* downstream sequence that contains a transcription termination sequence (also derived from pFA6-KANMX; [32]). This reporter construct was inserted into pLZ259 (*ARS-CEN, NATMX*, kindly provided by Dr. Lu Zhu, from Dr. Scott Emr laboratory. Derivatives of pEAA613 that

contain homopolymeric tracts of 10 A (in frame, pEAA611) and 11 A (+1 out of frame, pEAA612) residues were also constructed. Finally, a set of reporter constructs (pEAA614-616) were built in which the *kanMX::insE-A*$_{14}$ reporter was expressed via the *LEU2* promoter (-308 to the ATG start site).

Spore clone competitions

Clones derived from incompatible strains (*cMLH1::KANMX, kPMS1::HIS3, pmr1*) evolved in high salt for 70 generations (I10A, I10B, I10C containing *pmr1* mutations T-459A, T412C, T2G, respectively; [10]) were mated with the unevolved and compatible strain EAY3241 (*kPMS1::HIS3, kMLH1::NATMX, PMR1;* Table 3.1). Diploids were selected on YPD plates containing clonNAT (100 µg/ml) and genecitin (200 µg/ml) and then sporulated on 2% agar media containing 1% potassium acetate. The resulting spore clones were genotyped for *PMR1* by isolating chromosomal DNA [33] from individual clones and sequencing the PCR amplified PMR1 locus. These clones were genotyped for *MLH1* by testing for resistance to genecitin and clonNAT, and for the *MAT* locus by mating to tester strains.

Spore clones of the same mating type and of the four possible genotypes (compatible *PMR1*, compatible *pmr1*, incompatible *PMR1*, and incompatible *pmr1*) were grown overnight in YPD and then mixed in equal proportions (Transfer 0). 4, 3, and 3 spore clones of each genotype were competed from the matings involving *pmr1-T459A, pmr1-T412C, pmr1-T2G*, respectively. Ten competitions in total were performed, and different spore clones obtained from different tetrads were pooled to minimize effects of background mutations that might arise in evolved populations. 2 x10^7 cells of the initial mixed culture (Transfer 0) were transferred into 6 ml of YPD or YPD + 1.2M NaCl and then grown for 24 hrs at 30^{o}C (~7 generations of growth). The same amount of cells (to achieve an initial OD_{600} of 0.1, Shimadzu UV-1201 spectrophotometer) was used in subsequent transfers, with cells grown under the same conditions. At transfer numbers indicated in Fig. 3.3, cells in the culture were genotyped for

compatibility (*kPMS1::HIS3, kMLH1::KANMX)* and incompatibility (*kPMS1::HIS3, cMLH1::KANMX)* on YPD plates containing geneticin (200 µg/ml) or clonNAT (100 µg/ml).

Clade analysis

1011 *S. cerevisiae* isolates were investigated in the context of the 1002 yeast genome project (http://1002genomes.u-strasbg.fr/). Illumina reads were mapped against the *S. cerevisiae* 288c reference genome R64-1-1 with bwa 0.7.4-r385 and the sequence of the *MLH1* and *PMS1* genes were inferred for all isolates with GATK (FastaAlternateReferenceMaker). *MLH1* and *PMS1* ORF sequences from these strains were grouped into haplotypes and then analyzed with *S. mikatae* and *S.paradoxus* as outgroups using MEGA7 (http://www.megasoftware.net/). Two neighbor joining trees for *MLH1* and *PMS1* were built using MEGA7 alignment and phylo analysis tools. The evolutionary distances were computed using the Maximum Composite Likelihood Method [34] and are in the units of the number of base substitutions per site. The analysis involved 286 and 323 haplotypes of nucleotide sequences for MLH1 and PMS1 respectively. Codon positions included were 1st+2nd+3rd+Noncoding. All positions containing gaps and missing data were eliminated. Evolutionary analyses using Phylogenetic Analysis tools of MEGA [35].

***lys2-A$_{14}$*reversion assays**

Independent colonies of EAY1365 (relevant genotype *lys2-A$_{14}$*) containing the *ARS-CEN, MLH1* and *ARS-CEN, PMS1* plasmids presented in Table 3.4 were inoculated YPD overnight and then plated onto LYS, HIS, LEU dropout and HIS, LEU dropout synthetic plates. These strains were analyzed for reversion to Lys$^+$ as described previously [10,31]. The 95% confidence intervals were determined as described by Dixon and Massey, 1969 [36]. The Mann-Whitney U test [37] was performed to determine the significance of the differences in median reversion rates.

kanMX::insE-A$_{10-14}$ reversion assays

EAY1369 (*cMLH1-cPMS1*, compatible), EAY1370 (*cMLH1-kPMS1*, incompatible), EAY1372 (*msh2*Δ), and the natural isolates YJM541, YJM554, and YJM555 were transformed with pEAA613 or pEAA616 and grown on YPD media containing clonNAT (100µg/ml). Independent transformants were subsequenty grown overnight in YPD + clonNAT and then plated on to YPD + cloNAT (50 µg/ml) and YPD + clonNAT (50 µg/ml), genecitin (300 µg/ml). These strains were analyzed for reversion to resistance to genecitin using methods described previously [10,31]. The 95% confidence intervals were determined as described by Dixon and Massey, 1969. Pair-wise Kruskal–Wallis tests were performed to determine the significance of the differences in median reversion rates. Mann-Whitney U tests were performed to determine the significance of the differences in median reversion rates [37,38]

RESULTS

Incompatibility confers a fitness cost in evolved strains.

Previously we showed that haploid yeast containing the incompatible S288c *MLH1-SK1 PMS1* genotype (abbreviated as *cMLH1-kPMS1*) displayed a transient growth advantage in high salt that resulted from mutations in the *PMR1* gene. This observation encouraged us to determine the length of time that incompatible strains that display an initial transient adaptive advantage can maintain fitness in non-stress and stress conditions. To answer this question, we mated three different high-salt evolved clones that were constructed to contain the incompatible c*MLH1-kPMS1* combination to the unevolved compatible strain EAY3241. These strains, (EAY3688 *(pmr1-T459A)*, EAY3689*(pmr1-T412C)* and EAY3690*(pmr1-T2G)* were evolved for 70 generations in high salt [10]. The diploids were sporulated and the resulting spores genotyped for incompatibility, mating type, and *PMR1* (Fig. 3.2). We then created mixed

cultures that contained equal proportions of the same mating type spore clones that were *PMR1* compatible, *pmr1* compatible, *PMR1* incompatible, *pmr1* incompatible, and grew them overnight, followed by subsequent transfers, in YPD or YPD + 1.2M NaCl (roughly seven generations of growth per transfer; Materials and Methods). Our goal in these studies was to determine if the incompatible strains would ultimately display a fitness defect in rich media due to the accumulation of recessive mutations, as predicted by [17]. We also tested whether the rapidly evolved incompatible strains would continue to show an adaptive advantage in high salt media.

As shown in Table 3.3 and Fig. 3.3, we measured fitness differences of post-adapted incompatible strains compared to those of compatible strains in rich media. In rich media we observed a gradual decrease in fitness of incompatible compared to compatible cells (Fig. 3.3, Table 3.3). This observation supports the idea that incompatible is not favorable shortly after adaptation, supporting the idea that the adaptive advantage is transient [10]. At the end of the transfer experiment most competitions resulted in a higher proportion of compatible cells and all 28 independent clones (half compatible, half incompatible) isolated from Transfer 24 were *PMR1*, indicating that *pmr1* mutations are deleterious in rich media.

For competitions in YPD +1.2M NaCl, we observed a general decline in the fitness of incompatible strains compared to compatible strains in the first 50 generations of competition. In the next 100 generations some incompatible strains displayed increased fitness while others showed a decrease (Fig. 3.3, Table 3.3). Sequencing of 24 clones (half compatible, half incompatible clones) at Transfer 24 showed that they all retained their initial adaptive *pmr1* mutations. These results showed that the adaptive mutations primarily provide an advantage only in the environment that they arose in, and that further adaptive advantages beyond the initial transient one are likely balanced by fitness effects resulting from the accumulation of deleterious mutations.

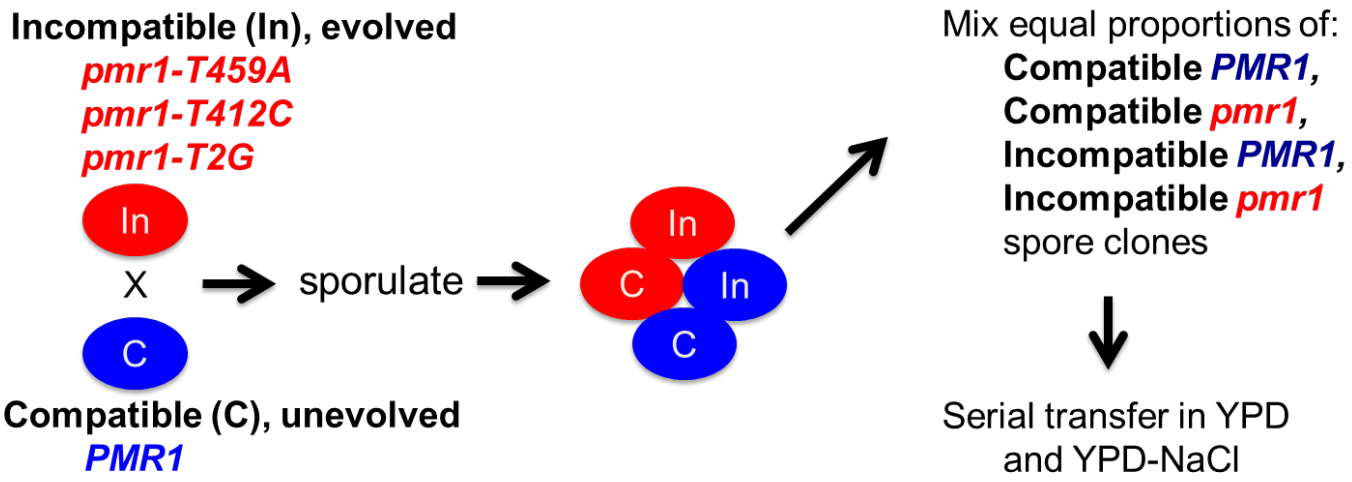

Figure 3.2. Competition experiments of spore clones from post adaptation strains. Clones derived from incompatible strains evolved in high salt for 70 generations (EAY3688 *(pmr1-T459A)*, EAY3689*(pmr1-T412C)* and EAY3690*(pmr1-T2G))* containing *pmr1* mutations T-459A, T412C, T2G, respectively; Bui et al. 2015) were mated with the unevolved and compatible strain EAY3241 (Table 3.1). The resulting diploids were sporulated and genotyped for *PMR1, MLH1, PMS1*, and mating type. Spore clones of the same mating type and of the four possible genotypes (compatible *PMR1*, compatible *pmr1*, incompatible *PMR1*, and incompatible *pmr1*) were grown overnight in YPD and then mixed in equal proportions (Transfer 0). 4, 3, and 3 spore clones of each genotype were competed from the matings involving *pmr1-T459A, pmr1-T412C, pmr1-T2G*, respectively. 2 x10^7 cells of the initial mixed culture (Transfer 0) were transferred into 6 ml of YPD or YPD + 1.2M NaCl and then grown for 24 hrs (~7 generations of growth). The same amount of cells was used in subsequent transfers. At the indicated transfers cells were genotyped for compatibility (*kPMS1::HIS3, kMLH1::KANMX)* and incompatibility (*kPMS1::HIS3, cMLH1::KANMX)* on YPD plates containing geneticin or clonNAT.

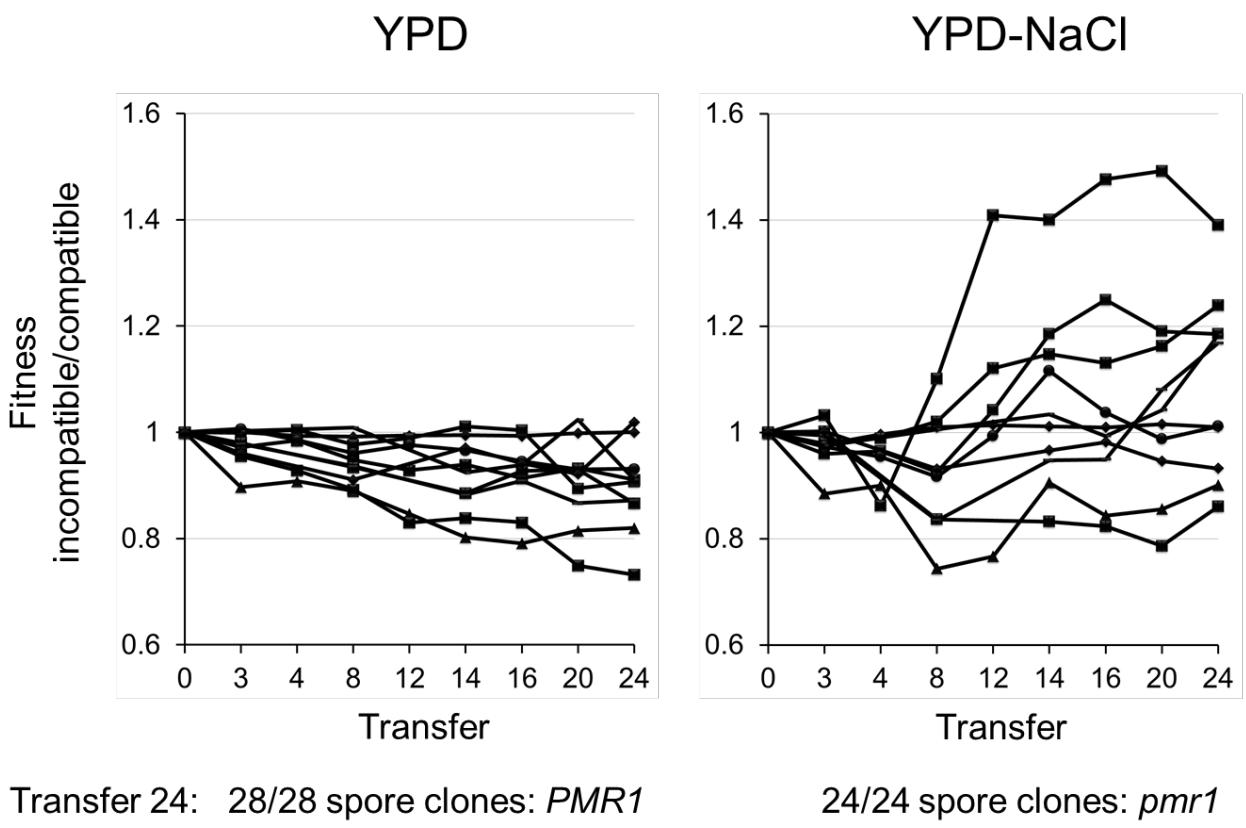

Figure 3.3. Fitness of post-adaptation incompatible and compatible strains in YPD and YPD-1.2M NaCl. Fitness (*w)* was determined in cultures genotyped for *MLH1-PMS1* compatible and incompatible clones in YPD and YPD + 1.2M NaCl as described in the Materials and Methods and Tables 3.3, and Fig. 3.2. A total of 10 same mating-type competitions are shown. For the YPD transfer experiments, 14 incompatible and 14 compatible clones (28 in total) at Transfer 24 (6, 4, 4, each from the *pmr1-T459A*, *pmr1-T412C* and *pmr1-T2G* matings respectively) were genotyped for *PMR1*. For the YPD + 1.2M NaCl transfer experiments, 12 incompatible and 12 compatible clones (24 in total) at Transfer 24 (4 each from the *pmr1-T459A*, *pmr1-T412C* and *pmr1-T2G* matings) were genotyped for *PMR1*.

Table 3.3. Fitness of evolved incompatible and compatible strains as a function of transfer in YPD and YPD + NaCl media.

	Fitness, *w* +/-SEM		
Transfer	YPD	YPD+NaCl	n
3	0.98± 0.01	0.98± 0.01	10
4	0.97± 0.02	0.95± 0.02	6
8	0.95± 0.01	0.93± 0.03	10
12	0.93± 0.03	1.06± 0.09	6
14	0.92± 0.02	1.06± 0.05	10
16	0.92± 0.02	1.05± 0.06	10
20	0.91± 0.02	1.06± 0.06	10
24	0.90± 0.03	1.09± 0.05	10

The proportion of compatible and incompatible genotypes were determined after the indicated number of transfers for spore clone competitions performed in YPD and YPD+ 1.2M NaCl (Figs 3.2, 3.3). Fitness (*w*) values were calculated as $w = ((p_t/q_t)/(p_o/q_o))^{1/t}$, where t equals the number of generations after T transfers (7 generations per transfer; [39]), p_o and q_o are the number of incompatible and compatible cells, respectively at Transfer 0, and p_t and q_t are the number of incompatible and compatible cells, respectively, at the indicated Transfer. n is the number of unique competitions performed for each data set.

Natural strains were identified that contain the incompatible *MLH1-PMS1* genotype.

We took advantage of a recent whole-genome sequencing analysis of 1011 *Saccharomyces cerevisiae* strains to determine if the incompatible combination exists in nature (1002 yeast genome project; http://1002genomes.u-strasbg.fr/). These strains were genotyped for single amino acid polymorphisms in MLH1 (761:G or D) and PMS1 (818:R or K); previously we showed that MLH1-D761-PMS1-K818 conferred a mutator phenotype in *cMLH1-kPMS1* hybrids [17]. As shown in Fig. 3.1, 693 strains (MLH1-G761-PMS1-R818) mapped to the ancestral group, 182 to the S288c group (MLH1-D761-PMS1-R818), 28 in the SK1 group (MLH1-G761-PMS1-K818), and 3 to the incompatible group (MLH1-D761-PMS1-K818). A Fisher's Exact test showed, based on the observed number of strains in each category, that the number of strains in the incompatible group was expected if there were no negative epistatic interactions between this combination of MLH1-PMS1, and no active selection against them ($p = 0.0842$). This result encouraged us to look more closely at the three strains YJM541, YJM554 and YJM555. These strains each displays a homozygous *MLH1* and *PMS1* genotype and are all clinical isolates sampled from the same location (Stanford University Hospital, Stanford, California;[40]; deposited in the Phaff Yeast Culture Collection, University of California, Davis).

Two Neighbor-Joining (NJ) trees were constructed from 1011 yeast genomes based on 285 and 322 haplotypes of Open Reading Frames (ORF) of *MLH1* and *PMS1*, respectively (Fig. 3.4). Phylogenetic relationships of the strains shown by the two NJ trees strongly support our hypothesis. All strains that locate at or near the root of both trees (labeled as CEI, CEG, BAL, BAH, YCR, etc.) possess the *MLH1-PMS1* combinations of the ancestral group (Fig. 3.1). The YJM541, YJM554, and YJM555 *MLH1* and *PMS1* genes were clustered in both trees Fig. 3.4), and genome-wide phylogenetic analysis of 100 *S. cerevisiae* strains also showed that the YJM strains are closely related to each other [40]. We speculate that the three strains are recently derived from the same origin, perhaps created by a single mating event between S288c and SK1 strains (see Discussion).

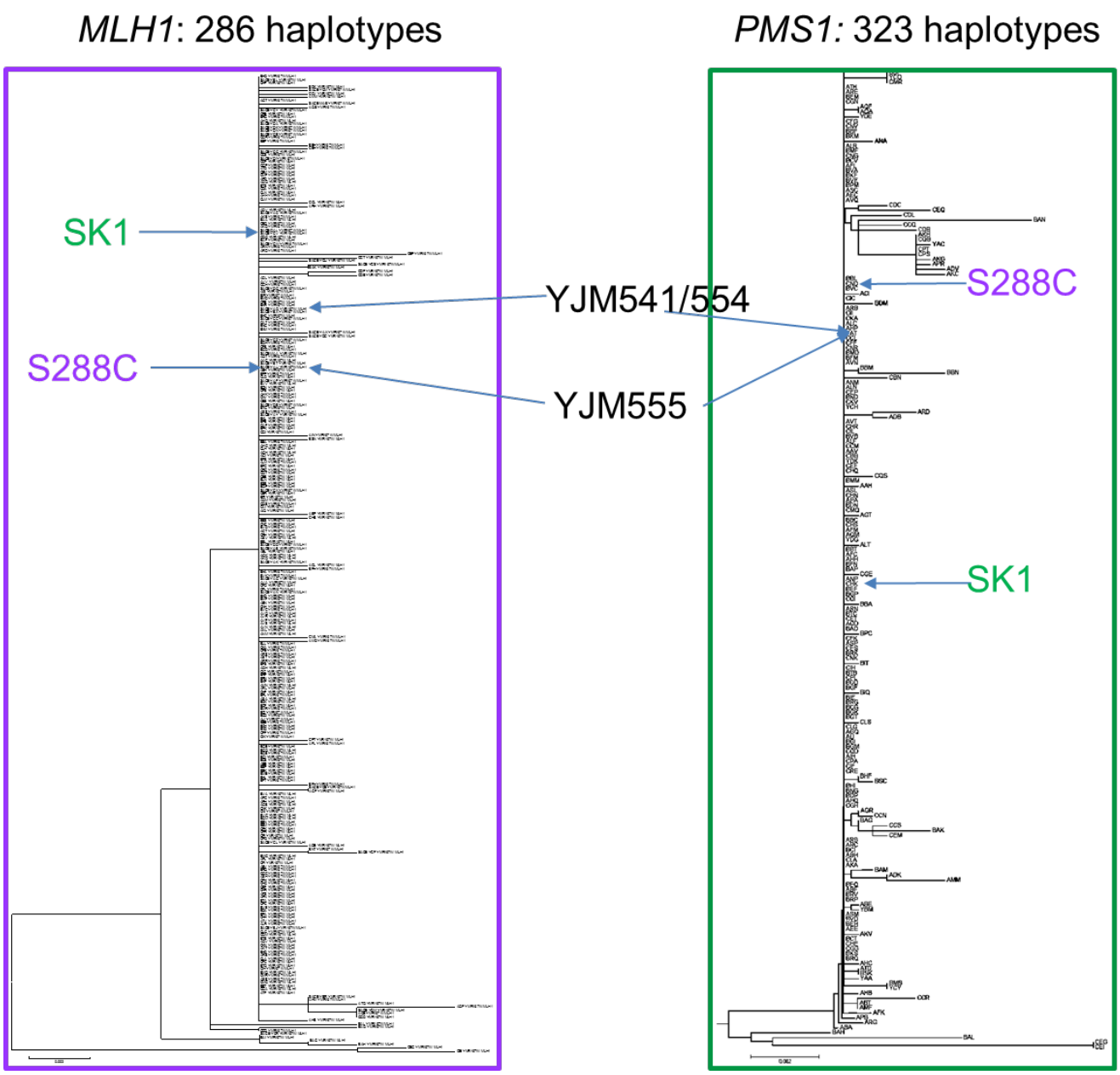

Figure 3.4. Phylogenetic analysis on *MLH1* and *PMS1* sequences. A, Neighbor-Joining trees for 286 haplotypes of *MLH1* ORF sequences and B, Neighbor Joining trees for 323 haplotypes of *PMS1 ORF* sequences. We grouped all 1011 strains into haplotypes for each gene sequence and use phylogenetic tools of MEGA7 to construct the tree. Two Neighbor-Joining trees for *MLH1* and *PMS1* in total scale with *S. mikatae* and *S.paradoxus* as outgroups are presented. The sum of branch lengths, ~ 0.32 for each tree, are shown. The trees are drawn to scale, with branch length in the same units as those of the evolutionary distances used to infer the phylogenetic tree. Subsets of the trees without out-groups are shown. Locations of YJM541, YJM554, YJM555, S288c and SK1 strains are also marked.

Natural strains were identified that show heterozygosity for the incompatible genotype. Analysis of *MLH1* and *PMS1* sequences from the 1011 strains revealed that 105 are heterozygous for the *MLH1* 761 and *PMS1* 818/822 genotypes, indicating that they are likely to be heterozygous for the SNPs at these positions. Previously we showed in experiments where both incompatible and compatible genotypes were present that the incompatible genotype is recessive [29]. Of these 105 strains, 17 have the potential to generate incompatible progeny from meiotic spores, assuming that they are diploids competent to undergo meiosis and form haploid spores. 13 of the 17 strains display a S288c/SK1 *MLH1* (amino acid 761) and S288c/SK1 *PMS1* (amino acid 818/822) genotype, suggesting that could have been created by matings between strains containing S288c and SK1 *MLH*1-*PMS1* genotypes. Sporulation of these strains would yield meiotic progeny in which 25% would be incompatible. One strain displays a S288c *MLH1* and S288c/SK1 *PMS1* genotype, possibly generated through a cross between a compatible and an incompatible strain. If this strain was sporulated, 50% of the meiotic progeny would show incompatibility (Table 3.8).

***MLH1-PMS1* incompatible combinations derived from natural strains confer a mutator phenotype in the S288c strain background.**

We used the *lys2-A*$_{14}$ reversion assay to assess the mutator phenotype of the *MLH1* and *PMS1* gene combinations from YJM541, YJM554 and YJM555. These genes were cloned into *ARS-CEN* vectors and transformed into a *mlh1Δ pms1Δ* S288c strain that was used previously to characterize *MLH1-PMS1* combinations from 65 yeast strains [18]. YJM541 and YJM554 have the same *MLH1* and *PMS1* sequences and were thus grouped together. YJM555 has a different *MLH1* sequence from YJM554 but contains the same *PMS1* sequence as the other two strains (Fig 3.4; Table 3.4).

Table 3.4: Natural strains that contain an incompatible *MLH1-PMS1* combination

Strain code	Strain name	Genotype	
		MLH1	*PMS1*
ADM	CLIB324_2	SK1/S288c	SK1/S288c
ASC	CBS4455	S288c	SK1/S288c
ATV	CECT1462	SK1/S288c	SK1/S288c
BML	NCYC_2780	SK1/S288c	SK1/S288c
BMM	2680	SK1/S288c	SK1/S288c
BTE	YS8(E)	SK1/S288c	SK1/S288c
CBF	SD-15	SK1/S288c	SK1/S288c
CFD	WLP001	SK1/S288c	SK1/S288c
CFI	WLP013	SK1/S288c	SK1
CFN	WLP006	SK1/S288c	SK1
CGC	UCD_06-645	SK1/S288c	SK1/S288c
CHK	Win-8B	SK1/S288c	SK1
CIC	Ponton 11	SK1/S288c	SK1/S288c
CKK	CLI_16	SK1/S288c	SK1/S288c
CKN	CLI_19	SK1/S288c	SK1/S288c
CKS	CLI_23	SK1/S288c	SK1/S288c
CLA	CLI_26	SK1/S288c	SK1/S288c
SACE_YAP	YJM541	S288c	SK1
SACE_YAQ	YJM554	S288c	SK1
SACE_YAR	YJM555	S288c	SK1

SK1/S288c : both S288c and SK1 alleles are present at the indicated loci

Table 3.5. Nonsynonymous changes in *MLH1* and *PMS1* sequences

MLH1 base position

	720	812	997	1393	2032	2108	2282
S288c	C	T	G	G	G	C	A
SK1	A	C*	A	G	A	T	G
YJM541	C	C	G	A	G	C	A
YJM554	C	C	G	A	G	C	A
YJM555	C	T	G	G	G	C	A
aa change	S240R	L271P	E333K	D465N	D678N	P701L	D761G

PMS1

	122	335	1150	1175	1199	1201	1249	1538	1691	2303	2453
S288c	A	T	T	A	C	G		A	C	A	G
SK1	G	C	G	A	G	G	+12**	T	C	A	A
YJM541	A	T	G	T	G	T	+12	A	T	G	A
YJM554	A	T	G	T	G	T	+12	A	T	G	A
YJM555	A	T	G	T	G	T	+12	A	T	G	A
aa change	N41S	I112T	F384V	E392V	T400S	A401S		Y513F	A564V	K768R	R818K

*mutation in *MLH1* that suppresses *cMLH1-kPMS1* incompatibility [18]

**Compared to S288c, SK1 and YJM541, 554 and 555 strains contain a 12 bp (four codon) insertion at amino acid 416 in PMS1.

The YJM541/YJM554 *MLH1-PMS1* combination confers a 22-fold higher mutation rate than the *cMLH1-cPMS1* combination (Table 3.5; note that S288c is denoted as c, SK1 as k). This value was lower than that seen for the *cMLH1-kPMS1* combination (75-fold) and approached levels seen in SK1 strains that are compatible (~4 to 7-fold), but was similar to a laboratory constructed *cMLH1-L271P-kPMS1* combination (24 to 27-fold) containing a polymorphism (*MLH1-L271P*) shown previously to suppress the *cMLH1-kPMS1* mutator phenotype [18]. In fact, YJM541 and YJM554 both contain the L271P polymorphism (Table 3.4). To further confirm the suppression phenotype we examined the YJM541/554 *MLH1-kPMS1* combination and showed that it also conferred a lower mutation rate (19-fold).

The *MLH1* gene in YJM555 does not contain the L271P polymorphism that suppresses the MMR incompatibility; consistent with this result the YJM555 *MLH1*-YJM555 *PMS1* combination confers a 196-fold higher mutation rate than the *cMLH1-cPMS1* combination (Table 3.5). In fact, this mutation rate is higher than that seen for *cMLH1-kPMS1*, indicating that there are polymorphisms present in the two genes that might enhance the incompatibility. Together these data indicate that the *MLH1-PMS1* combination from YJM555 displays a strong incompatibility in the S288c strain background.

Table 3.6. Mutation rates in an S288c strain containing *MLH1* and *PMS1* genes derived from S288c, SK1, YJM541, YJM554, and YJM555 strains.

MLH1-PMS1 genotype	Lys^+ reversion rate (10^{-7}), (95% CI)	Relative rate	(n)
S288c-S288c, compatible	4.1 (1.7-13.8)	1	13
S288c-SK1, incompatible	311 (111-919)**	75	16
YJM541/554-YJM541/554	92 (78.4-690)*	22	29
YJM555-YJM555	808 (566-4,450)**, $^+$	196	39
YJM541/554-SK1	80 (47-182)*	19	15
mlh1Δ, pms1Δ	45,300 (13,170-126,800)**	10,970	10

EAY1365 (relevant genotype *mlh1Δ::KanMX4, pms1Δ::KanMX4)* was transformed with ARS-CEN plasmids containing the *MLH1* and *PMS1* genes obtained from the indicated strains (Table 3.2). Independent cultures (n) were examined for reversion to Lys^+. Median mutation rates are presented with 95% confidence intervals, and relative mutation rates compared to the wild type strain are shown.

*Significantly different from S288c-S288c, compatible ($p < 0.01$, Mann Whitney test)

**Significantly different from S288c-S288c ($p < 0.001$, Mann Whitney test)

$^+$Significantly different from YJM541/554-YJM541/554 ($p < 0.001$, Mann Whitney test).

Development of a reporter plasmid to measure mutation rates in natural strains.

Table 3.6 shows that YJM541, YJM554, and YJM555 *MLH1-PMS1* gene combinations confer mutator phenotypes in the S288c strain background. However, neighbor-tree analysis showed by Strope et al. (2015) show that the branches on trees for the YJM strains are not long, suggesting that the YJM strains could not been mutators for a long evolutionary period. One way to reconcile these observations is that the *MLH1-PMS1* incompatibility formed in the YJM strains facilitated a rapid but transient adaptation that was maintained due to the presence of suppressor mutations that restored MMR functions [40]. Data from *MLH1* sequences of YJM541 and YJM554 support this idea; both strains have a polymorphism in MLH1 (L271P) that we showed previously weakens the *MLH1-PMS1* incompatibility [18]. To test this idea, we constructed a set of vectors (Fig. 3.5; Table 3.7, 3.8; Materials and Methods) that can be transformed into natural yeast strains to serve as a proxy for genome mutation rate. We introduced homopolymeric A sequences into the *KANMX* open reading frame immediately after its methionine 17 codon, with the goal of creating a sensitive mutation detection assay. Previous work showed that homopolymeric runs undergo DNA slippage in a variety of DNA repair mutant backgrounds [31], and such events occur at an especially high frequency in MMR defective strains. For example, msh2Δ strains display a 10,000-fold increase in mutation rate compared to wild-type in strains bearing the *lys2-A*$_{14}$ reporter [31].

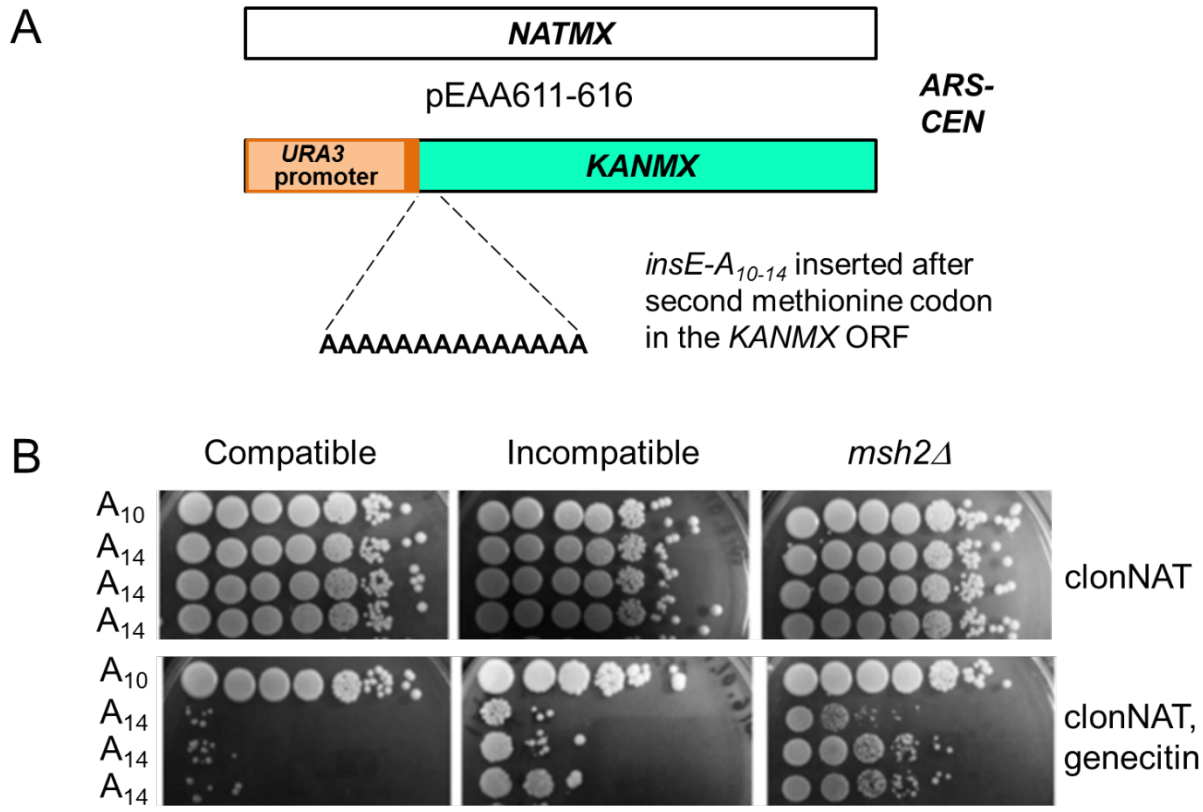

Figure 3.5. Construction of a *URA3 promoter-kanMX::insE-A$_{14}$* plasmid to be used to measure mutation rates in natural yeast strains. A. The *ARS-CEN* vector pEAA613 contains *a NATMX* selectable marker and a frameshift reporter in which the *insE-A$_{14}$* sequence from Tran et al. (1997) was inserted immediately after methionine 17 in the *KANMX* open reading frame. In this reporter the *URA3* gene promoter drives expression of *KANMX*, using the methionine 17 in the *KANMX* open reading frame as the initiation codon. The resulting construct contains a +1 frameshift mutation that disrupts *KANMX* function. A reporter construct that contains the *insE-A$_{10}$* insertion and does not disrupt the *KANMX* open reading frame is shown as an in-frame control. Frameshift mutation events (e.g. a -1 deletion in the homopolymeric A run) are detected on YPD plates containing clonNAT and geneticin.B, Examples of reversion assays performed using the *URA3 promoter-kanMX::insE-A$_{14}$* plasmid. EAY1369 (*cMLH1-cPMS1* compatible), EAY1370 (*cMLH1-kPMS1* incompatible) and EAY1372 (*msh2Δ)* were transformed with pEAA613 and plated in dilutions from 10 μl of a 10X concentrated overnight culture to 10 μl of 10^{0}, 10^{-1}, 10^{-2}, 10^{-3}, 10^{-4}, 10^{-5} dilutions onto YPD clonNAT (50 μg/ml), geneticin (300 μg/ml) plates.

The mutation reporter plasmids contain *ARS-CEN* and *NATMX* markers and a *kanMX::insE-A$_{14}$* construct whose expression is driven by *URA3* or *LEU2* promoters. These promoters replaced the strong *TEF* promoter that drives *KANMX* expression in pFA6-KANMX; we found that the *TEF* promoter prevented the detection of large differences in reversion frequency between in and out of frame *KANMX::insE* constructs, presumably due to high rates of transcriptional slippage (see example in the appendix). In the *URA3* promoter-*kanMX::insE-A$_{14}$* reporter in pEAA613, a 55 bp sequence containing a +1 frameshift in the 14 bp homopolymeric A run (*insE-A$_{14}$;* [31]) was inserted immediately after the *URA3* ATG. This sequence was immediately followed by codons 18 to 269 of the *KANMX* open reading frame. Derivatives were constructed that contained a 10 bp in-frame insertion (pEAA611), or utilized the *LEU2* promoter to drive expression (pEAA616; Table 3.2).

We tested the sensitivity of our reporter assay by transforming pEAA613 and pEAA616 into compatible, incompatible and MMR defective (*msh2Δ*) S288c strains (Table 3.7, 3.8). For strains containing pEAA613 we showed that the *msh2Δ* strain displayed a 2000-fold higher rate of reversion to genecitin resistance compared to the compatible strain and that the incompatible strain showed a ten-fold higher mutation rate compared to the compatible strain (Fig. 3.5, Table 3.7 and Materials and Methods). Importantly, sequencing of the reporter plasmid from geneticin resistant clones showed that a -1 frameshift had occurred in the homopolymeric A sequence in all of the constructs (n=14). While this range is less sensitive than was seen in the *lys2A$_{14}$* reversion assay (~75 fold in an assay with a 10,000 fold range between wild-type and MMR defective; Table 3.5), this reporter construct provides the opportunity to determine mutation rate in natural strains that lack genetic markers.

Table 3.7. Reversion assay using the *URA3 promoter-kanMX::insE-A$_{14}$* plasmid.

strain	genotype	reversion G418^r (10^{-7})	95% CI	relative rate	n
EAY1369	wild-type	6.1	3.1-7.0	1	17
EAY1370	incompatible	59.8 **	25.7-239	9.9	17
EAY1372	*msh2Δ*	13,451**	7,230-46,090	2,142	11
YJM554		1.6*	1.4-1.8	0.26	14
YJM541		2.1	1.8-8.8	0.34	14
YJM555		9.8*, $^+$	6.5 -10.7	1.6	14

The indicated strains (Table 3.1) were transformed with *ARS-CENURA3 promoter-kanMX::insE-A$_{14}$* plasmid pEAA613. Independent cultures (n) were examined for reversion to genecitin resistance as described in the Materials and Methods. Median mutation rates are presented with 95% confidence intervals, and relative mutation rates compared to EAY1369 (S288c compatible) are shown.

*Significantly different from EAY1369 ($p < 0.01$, Mann-Whitney test)

**Significantly different from EAY1369 ($p < 0.001$, Mann-Whitney test)

$^+$Significantly different from YJM554 ($p < 0.001$, Mann Whitney test)

Table 3.8. Reversion assay using the *LEU2 promoter-kanMX::insE-A$_{14}$* plasmid.

strain	genotype	reversion G418^r (10^{-7})	95% CI	relative rate	n
EAY1369	wild-type	6.9	5.3-8.9	1	36
EAY1370	incompatible	32.6***	3.3-38.5	4.7	29
EAY1372	*msh2Δ*	6070***	1,843-7,778	878	29
YJM554		2.1**	1.3-3.4	0.30	35
YJM541		3.4*	1.6-7.3	0.49	35
YJM555		7.2$^+$	4.9-10.4	1.04	35

The indicated strains (Table 3.1) were transformed with *ARS-CENLEU2 promoter-kanMX::insE-A$_{14}$* plasmid pEAA616. Independent cultures (n) were examined for reversion to genecitin resistance as described in the Materials and Methods. Median mutation rates are presented with 95% confidence intervals, and relative mutation rates compared to EAY1369 (S288c compatible) are shown.

*Significantly different from EAY1369 ($p < 0.05$, Mann-Whitney test)

**Significantly different from EAY1369 ($p < 0.01$, Mann-Whitney test)

***Significantly different from EAY1369 ($p < 0.001$, Mann-Whitney test)

$^+$Significantly different from YJM554 ($p < 0.001$, Mann Whitney test)

Natural strains containing the *MLH1-PMS1* incompatible combination display a low mutation rate.

We transformed the *URA3 promoter-kanMX::insE-A$_{14}$* and *LEU2 promoter-kanMX::insE-A$_{14}$* plasmids into YJM541, YJM554 and YJM555 to determine if the strains showed a mutator phenotype consistent with a MMR incompatibility. As shown in Fig. 3.6 and Tables 3.7 and 3.8, YJM541 and YJM554 displayed similarly low mutation rates that were two- to four-fold lower than seen in the S288c compatible strain. The YJM555 strain, which contains *MLH1-PMS1* alleles that display the highest MMR incompatibility when expressed in the S288c strain background, displayed a 3.4- to 6.1-fold higher mutation rate than YJM554 depending which promoter was used. However, even in this case, the overall mutation rate in YJM555 remained similar to that seen in the S288c strain, indicating that the YJM strains apparently compensated for the increased mutation rate conferred by the *MLH1-PMS1* incompatibility. For YJM541 and YJM554 this compensation was partly due to an intragenic suppression polymorphism in *MLH1*.

DISCUSSION

MMR Incompatibility does not appear to be a long-term strategy for adaptation to new environments.

We performed a set of competitions involving populations of yeast that contained different combinations of evolved, unevolved, MMR compatible, and MMR incompatible genotypes (Figs 3.2 and 3.3). In these repetitive transfer experiments we observed long-term fitness costs for MMR incompatibility, suggesting that there is an elevated mutation rate associated with MMR incompatibility that could not be stably maintained in natural populations. We proposed that following a transient adaptive advantage provide by MMR incompatibility, incompatible strains can mate to compatible strains to maintain beneficial mutations, and thus return to MMR compatibility. Such a strategy would avoid the long-term fitness cost of being a mutator [10,12,17,18].

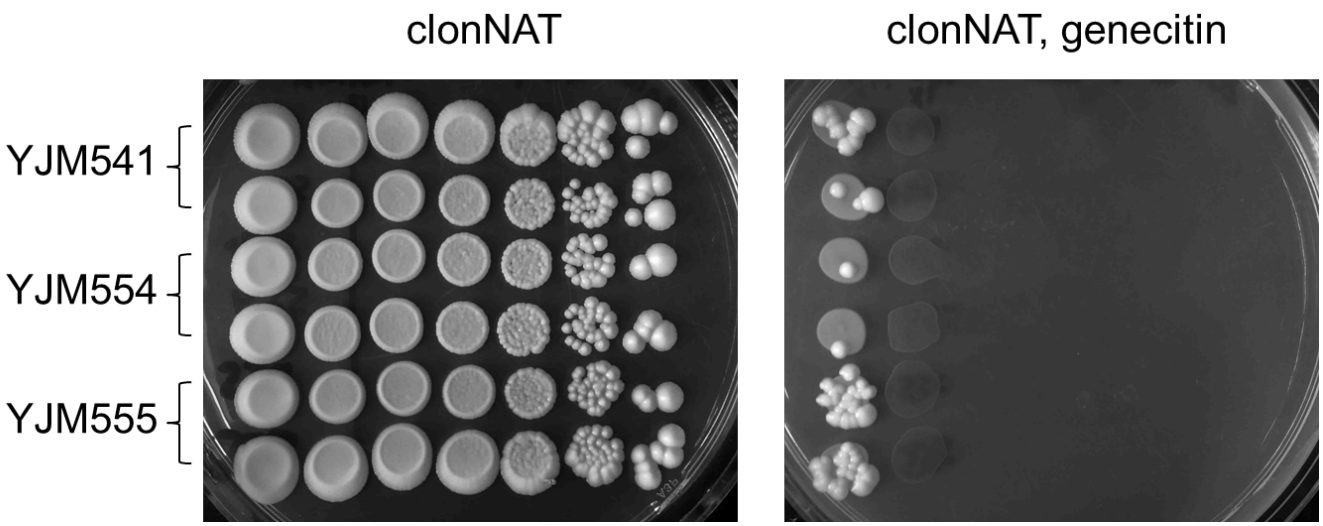

Figure 3.6. Reversion assays performed using the *URA3 promoter-kanMX::insE-A$_{14}$* plasmid pEAA613 transformed into natural yeast strains. Examples of the reversion assay performed for YJM541, YJM554, and YJM555 are shown using plating methods described in Fig. 3.5.

We identified three yeast strains, YJM541, YJM554, YJM555, from among 1011 sampled, that are homozygous for the incompatible genotype. Interestingly, two of these strains contained an intragenic MLH1 polymorphism P271 that suppressed the mutator phenotype associated with incompatibility. The P271 suppressor is common; 813 of 938 strains (73 could not be genotyped due to ambiguity at the 271 position possibly due to heterozygosity) contained this polymorphism. Thus there is an abundant availability of this apparently non-deleterious suppressor polymorphism that can allow strains to minimize mutation rates. Importantly, our data suggest that unknown extragenic mutations in the YJM strains are also present that contribute to suppressing the mutator phenotype associated with incompatibility (see below).

Multiple strategies are used by yeast to take advantage of a MMR incompatibility.

The molecular evolution experiments presented in Fig. 3.3 suggested that once an adaptive mutation reached fixation a mutator state would no longer be favorable. Consistent with this idea are observations made by Taddei et al. (1997), who proposed that a modestly elevated rate in an *E. coli* population would facilitate adaptation, but once adaptive mutations were fixed, the mutation load present in individuals in the population by accumulation of deleterious mutation in the genome that did not revert to a non-mutator state would lead to a decrease their frequency. Both genomic analyses (Fig 3.4 and [40]) and direct mutation rate measurements suggested that the mutation rates in YJM541, YJM554, and YJM555 were lower than observed for the incompatible genotype in the S288c and SK1 backgrounds (Table 3.7, Table 3. 8 and [17,18]). Interestingly, YJM541 and YJM554 each contain the P271 MLH1 polymorphism that we showed previously reduced the strength of the incompatibility. YJM555 does not contain this polymorphism, but still displays an overall mutation rate similar to that seen for S288c compatible strains, and whole genome analysis suggests that YJM555 is not an outlier compared to hundreds of other genomes (Fig 3.4; Tables 3.7 and 3.8; [40]). Because of these findings we hypothesize that the YJM strains acquired extragenic suppressors that lowered the

cellular mutation rate. Thus based on the fact that *MLH1-PMS1* incompatibility was only seen in these three strains, we hypothesize that it formed through mating(s) between S288c and SK1 groups (Fig. 3.1) to create an incompatible precursor of these YJM strains. After beneficial mutations obtained in the incompatible progenitors went to fixation, the P271 intragenic mutator suppressor was then acquired in YJM541 and YJM554 that suppressed the incompatibility [5,8,12].

An alternative to the above possibility is that the YJM strains never encountered situations where they had entered a mutator state in response to a changing environment and instead had inherently low mutation rates that could tolerate an incompatible genotype. We do not favor this hypothesis because genomic mutation rates tend to vary by less than an order of magnitude in organisms such as *E. coli, Neurospora crassa, and S. cerevisiae* [41,42], indicating that deviations from a typical rate would be selected against.

How were the MLH1-PMS1 incompatible genotypes generated that are found in YJM541, YJM554 and YJM555 strains?

Our data are consistent with YJM541, YJM554, and YJM555 strains arising through matings between S288c and SK1 strains. However, how they acquired mutation suppressor variants is less clear. The YJM541 and YJM554 strains are very closely related (Strope et al 2015), and also share the intragenic mutator suppressor variant MLH1-P271. YJM555 is slightly more distantly related to the other two strains, and like YJM541 and YJM554 carries the incompatible *MLH1-PMS1* genotype. However, YJM555 does not contain the MLH1-P271 variant. Like YJM541 and YJM554, YJM555 appears to also have unmapped mutator suppressor(s) elsewhere in its genome. We make the argument for extragenic suppressors because the *MLH1* and *PMS1* genes from all three strains confer a higher mutation rate in the S288c background compared to their native backgrounds (compare Table 3.5 to Table

3.7). Since all three strains are clinical isolates from the same hospital, it is possible that they all derive from a single common ancestor strain that carried the *MLH1-PMS1* incompatible genotype that arose once by mating between S288c and SK1-like strains. In this model the ancestor could have experienced an elevated mutation rate that was subsequently suppressed by extragenic suppressor(s). YJM555 would then have diverged off first from the ancestor strain common to both YJM541 and YJM554.

The above scenario is consistent with the presence of common PMS1 variants in YJM541, YJM554, and YJM555. The amino acid sequence of *PMS1* is identical in all three strains and in YJM320. There are four amino acid polymorphisms in these four strains that were not found in any of the other 1007 yeast strains. YJM320 is on the same branch as the other three strains [40]. This pattern suggests that the incompatible *MLH1-PMS1* genotype was generated first, followed by the acquisition of the intragenic mutation suppressor variant MLH1-P271 in the YJM 541/554 lineage. With our available data we are not able to distinguish whether acquisition of mutator suppressors occurred by de novo mutation or by recombination with a strain carrying a suppressor variant.

Development of a reporter construct to sensitively detect mutation rates in natural yeast strains.

The *ARS-CEN kanMX::insE-A*$_{10-14}$ reporter construct described in the paper provides a new approach to measure mutation rates in a large number of natural strains that lack markers that are typically used for genetic manipulation and whose chromosome content can vary with respect to ploidy and chromosome copy number [40,43]. In these constructs the *NATMX* antibiotic resistance marker is used to select for the plasmid, and the *KANMX* marker is used to identify frameshift reversion events (Fig. 3.5). The pEAA613 construct displayed a 2000-fold difference in mutation rate between wild-type and MMR null. This difference is only five-fold

lower than that seen using an integrated *lys2-A$_{14}$* reporter, which to our knowledge is the most sensitive assay developed to measure differences in frameshift reversion frequency between wild-type and MMR mutants (Table 3.5; [31]). Importantly, our reporter plasmid assay was capable of distinguishing between mutation rates in wild-type and MMR incompatible strains. In the *lys2-A$_{14}$* assay this difference was 75 to 100-fold in a 10,000-fold range; in the *kanMX::insE-A$_{10-14}$* assay it was 10-fold in a 2000 fold range (Table 3.5). We believe that this sensitive plasmid-based assay, in conjunction with whole-genome sequencing data and classical mutation accumulation analyses [44–46] will allow groups to accurately measure variation in mutation rate in natural strains and determine if this rate varies under different environmental conditions. Furthermore, one can modify the sequences present in the *insE* part of the reporter to examine reversion to genecitin resistance due to base substitution and other types of frameshift events. pEAA613 and derivatives can also be easily modified to integrate the *kanMX::insE-A$_{10-14}$* reporter at a specific chromosomal location.

ACKNOWLEDGEMENTS

We thank members of the Alani lab, and Jae Choi for helpful comments and technical advice.

REFERENCES

1. Kimura M (1967) On the evolutionary adjustment of spontaneous mutation rates. Genetical Research 9: 23-34.

2. Eyre-Walker A, Keightley PD (2007) The distribution of fitness effects of new mutations. Nat Rev Genet 8: 610-618. doi:10.1038/nrg2146.

3. LeClerc JE, Li B, Payne WL, Cebula TA (1996) High mutation frequencies among *Escherichia coli* and *Salmonella* pathogens. Science 274: 1208-1211. doi:10.1126/science.274.5290.1208.

4. Denamur E., Lecointre G, Darlu P, Tenaillon O, Acquaviva C et al. (2000) Evolutionary implications of the frequent horizontal transfer of mismatch repair genes. Cell 103: 711-721. doi:10.1016/S0092-8674(00)00175-6.

5. Taddei F, Radman M, Maynard-Smith J, Toupance B, Gouyon PH, et al. (1997) Role of mutator alleles in adaptive evolution. Nature 387: 700–702.

6. Tanaka MM, Bergstrom CT, Levin BR (2003) The evolution of mutator genes in bacterial populations: the roles of environmental change and timing. Genetics 164: 843–854.

7. Townsend JP, Nielsen KM, Fisher DS, Hartl DL (2003) Horizontal acquisition of divergent chromosomal DNA in bacteria: effects of mutator phenotypes. Genetics 164: 13–21.

8. Giraud A, Matic I, Tenaillon O, Clara A, Radman M, et al. (2001) Costs and benefits of high mutation rates: adaptive evolution of bacteria in the mouse gut. Science 291: 2606-2608. doi:10.1126/science.1056421.

9. Chao L, Cox, EC (1983) Competition between high and low mutating strains of *Escherichia coli*. Evolution 37: 125-134.

10. Bui DT, Dine E, Anderson JB, Aquadro CF, Alani EE (2015). A Genetic Incompatibility Accelerates Adaptation in Yeast. PLoS Genetics, 11(7), e1005407. http://doi.org/10.1371/journal.pgen.1005407.

11. Boe L, Danielsen M, Knudsen S, Petersen JB, Maymann J, et al. (2000) The frequency of mutators in populations of *Escherichia coli*. Mutat Res 448: 47–55. doi:10.1016/S0027-5107(99)00239-0.

12. Wielgoss S, Barrick JE, Tenaillon O, Wiser MJ, Dittmar WJ, Cruveiller S, Chane-Woon-Ming B, Médigue C, Lenski RE, Schneider D (2013) Mutation rate dynamics in a bacterial population reflect tension between adaptation and genetic load. Proc Natl Acad Sci USA 110: 222-227. doi: 10.1073/pnas.1219574110.

13. Thompson DA, Desai MM, Murray AW. (2006) Ploidy controls the success of mutators and nature of mutations during budding yeast evolution. Curr Biol 16: 1581-1590. doi:10.1016/j.cub.2006.06.070.

14. Raynes Y, Gazzara MR, Sniegowski PD (2012) Contrasting dynamics of a mutator allele in asexual populations of differing size. Evolution 66: 2329-2334. doi:10.1111/j.1558-5646.2011.01577.x

15. Liti G, Louis EJ (2005) Yeast evolution and comparative genomics. Annu Rev Microbiol 59: 135-153. doi:10.1146/annurev.micro.59.030804.121400.

16. Ruderfer DM, Pratt SC, Seidel HS, Kruglyak L (2006) Population genomic analysis of outcrossing and recombination in yeast. Nat Genet 38: 1077-1081. doi:10.1038/ng1859 .

17. Heck JA, Argueso JL, Gemici Z, Reeves RG, Bernard A, et al. (2006) Negative epistasis between natural variants of the *Saccharomyces cerevisiae MLH1* and *PMS1* genes results in a defect in mismatch repair. Proc Natl Acad Sci USA 103: 3256–3261. doi:10.1073/pnas.0510998103.

18. Demogines A, Wong A, Aquadro C, Alani E (2008) Incompatibilities involving yeast mismatch repair genes: a role for genetic modifiers and implications for disease penetrance and variation in genomic mutation rates. PLoS Genetics 4: e1000103. doi:10.1371/journal.pgen.1000103.

19. Muller HJ, Pontecorvo G (1940) Recombinants between Drosophila Species the F1 Hybrids of which are sterile. Nature 146: 199–200.

20. Muller HJ (1939) Reversibility in evolution considered from the standpoint of genetics. Biol Rev Camb Philos Soc 14: 261–280.

21. Dobzhansky T (1936) Studies on Hybrid Sterility. II. Localization of Sterility Factors in Drosophila Pseudoobscura Hybrids. Genetics 21: 113–135. PMID: 17246786.

22. Orr HA (1995) The population genetics of speciation: the evolution of hybrid incompatibilities. Genetics 139: 1805–1813. PMID: 7789779.

23. Magwene PM, Kayıkçı Ö, Granek JA, Reininga JM, Scholl Z, Murray D (2011) Outcrossing, mitotic recombination, and life-history trade-offs shape genome evolution in *Saccharomyces cerevisiae*. Proc Natl Acad Sci USA 108: 1987-1992. doi:10.1073/pnas.1012544108.

24. Murphy HA, Zeyl CW (2010) Yeast Sex: Surprisingly high rates of outcrossing between asci. PLoS One 5: e10461. doi:10.1371/journal.pone.0010461.

25. Reuter M, Bell G, Greig D (2007) Increased outbreeding in yeast in response to dispersal by an insect vector. Curr Biol 17: R81-83. doi:10.1016/j.cub.2006.11.059.

26. Winston F, Dollard C, Ricupero-Hovasse SL (1995) Construction of a set of convenient *Saccharomyces cerevisiae* strains that are isogenic to S288C. Yeast 11: 53-55. doi:10.1002/yea.320110107.

27. Rose MD, Winston F, Hieter P (1990) Methods in yeast genetics: A Laboratory Course Manual. Cold Spring Harbor Laboratory Press, Cold Spring Harbor, NY. doi:10.1016/0307-4412(91)90039-B.

28. Gietz RD, Schiestl RH (2007) Large-scale high-efficiency yeast transformation using the LiAc/SS carrier DNA/PEG method. Nat Protoc 2: 38-41. doi:10.1038/nprot.2007.15

29. Argueso JL, Kijas AW, Sarin S, Heck J, Waase M, Alani E (2003) Systematic mutagenesis of the Saccharomyces cerevisiae MLH1 gene reveals distinct roles for Mlh1p in meiotic crossing over and in vegetative and meiotic mismatch repair. Mol Cell Biol 23: 873-886.

30. Ho SN, Hunt HD, Horton RM, Pullen JK, Pease LR (1989) Site-directed mutagenesis by overlap extension using the polymerase chain reaction. Gene 77: 51-59.

31. Tran HT, Keen JD, Kricker M, Resnick MA, Gordenin DA (1997) Hypermutability of homonucleotide runs in mismatch repair and DNA polymerase proofreading yeast mutants. Mol Cell Biol 17: 2859-2865.

32. Goldstein AL, McCusker JH (1999) Three new dominant drug resistance cassettes for gene disruption in *Saccharomyces cerevisiae*. Yeast 15: 1541-1553. doi:10.1002/(SICI)1097-0061(199910)15:14<1541::AID-YEA476>3.0.CO;2-K

33. Holm C, Meeks-Wagner DW, Fangman WL, Botstein D (1986) A rapid, efficient method for isolating DNA from yeast. Gene 42: 169-173.

34. Tamura K, Nei M, Kumar S (2004) Prospects for inferring very large phylogenies by using the neighbor-joining method. Proc Natl Acad Sci USA 101: 11030-11035.

35. Tamura K, Stecher G, Peterson D, Filipski A, Kumar S (2013) MEGA6: Molecular Evolutionary Genetics Analysis version 6.0. Mol Biol Evol 30: 2725-2729. doi: 10.1093/molbev/mst197

36. Dixon WJ, Massey FJ (1969) Introduction to Statistical Analysis. New York: McGraw-Hill.

37. Mann HB, Whitney DR (1947) On a test of whether one of two random variables is stochastically larger than the other. Annals of Mathematical Statistics, 18: 50–60.

38. Wilcoxon F (1945) Individual comparisons by ranking methods. Biometrics Bulletin, 1: 80–83.

39. Hartl D, Clark A (2007) Principles of Population Genetics. 4rth Edition. Sinauer Associates. doi:10.1002/ajpa.1330800314.

40. Strope PK, Skelly DA, Kozmin SG, Mahadevan G, Stone EA, Magwene PM, Dietrich FS, McCusker JH (2015) The 100-genomes strains, an S. cerevisiae resource that illuminates its natural phenotypic and genotypic variation and emergence as an opportunistic pathogen. Genome Res 25: 762-74.

41. Zeyl C, DeVisser JA (2001) Estimates of the rate and distribution of fitness effects of spontaneous mutation in Saccharomyces cerevisiae. Genetics 157: 53-61.

42. Drake JW, Charlesworth B, Charlesworth D, Crow JF (1998) Rates of spontaneous mutation. Genetics 148: 1667-1686.

43. Storchova Z (2014) Ploidy changes and genome stability in yeast. Yeast 31: 421-430. doi:10.1002/yea.3037.

44. Nishant KT, Singh ND, Alani E. (2009) Genomic mutation rates: what high-throughput method can tell us. Bioessays 31: 912-920. doi:10.1002/bies.200900017.

45. Lujan SA, Clausen AR, Clark AB, MacAlpine HK, MacAlpine DM, Malc EP, Mieczkowski PA, Burkholder AB, Fargo DC, Gordenin DA, Kunkel TA (2014) Heterogeneous polymerase fidelity and mismatch repair bias genome variation and composition. Genome Res 24: 1751-1764. doi:10.1101/gr.178335.114.

46. Nishant KT, Wei W, Mancera E, Argueso JL, Schlattl A, Delhomme N, Ma X, Bustamante CD, Korbel JO, Gu Z, Steinmetz LM, Alani E (2010) The baker's yeast diploid genome is remarkably stable in vegetative growth and meiosis. PLoS Genet 6: e1001109. doi:10.1371/journal.pgen.1001109.

CHAPTER 4

CONCLUSIONS AND PERSPECTIVES

In my thesis, I investigated how *S. cerevisiae* populations bearing incompatible *MLH1-PMS1* combinations behave in different environments. I showed that such strains display an adaptive advantage when grown in high salt (Chapter 2). The fitness advantage, as measured in independent and competitive growth experiments, was due to a greater mutation supply in mutator, incompatible populations (Fig. 2.5). This advantage was rapid, but transient, because I observed that isogenic wild type populations that were not mutators eventually caught up to the mutator, incompatible populations (Fig. 2.4, Table 2.3). Using whole genome sequencing and analyses of evolved strains and of bulk segregants, I found that non-mutator populations also reached the same level of adaptation by acquiring mutations at the same locus as incompatible populations (Table 2.5, Fig. 2.7). Based on these results, I hypothesize that hybrid incompatibility plays an important role in adaptive evolution.

I was able to identify incompatible genotypes in natural yeast strains (Chapter 3). Characterizing these strains for mutation rate suggested a mechanism for how incompatible genotypes can be maintained in nature; I obtained evidence for intragenic and extragenic suppressors that lowered the mutator phenotype resulting from incompatibility (Table 3.2). I then proposed a model to explain how this MMR incompatibility was created. It has been an exciting journey because, piece by piece, I found experimental evidence and natural examples that fulfill the model's predictions. Subsequently, these observations have created a new set of interesting questions to answer.

A reversion assay that could sensitively detect strains with mild mutation rates among natural yeast strains.

In this study, I constructed and standardized reporters that can sensitively detect mild mutators in natural yeast strains; a 2000-fold difference in rate can be detected between wild type and MMR defective strains and a ten-fold difference can be detected between compatible and incompatible genotypes (Table 3.2). In addition, these reporters were built so that they can be transformed into natural yeast strains lacking genetic markers for selection. Therefore, these reporters could serve as very useful tools to compare mutation rates between natural strains isolated from around the world. I would like to test analogous constructs in other model organisms and cell cultures, especially in systems that do not have easily selectable markers.

These reporters were used to compare mutation rates based on the efficiency of the MMR machinery to detect and correct insertion/deletion loops. Therefore, other types of mutagenesis independent of the slippage mechanism might not be detected through this assay. For example, gene duplication mechanisms occurring via retrotransposition, aneuploidy or polyploidy are likely to not be captured by my reporter. However, DNA slippage reporters have been used extensively to measure defects in DNA repair and replication. For example, these reporters have been used to measure defects in DNA polymerases like α, δ, ε as well as MMR and recombination proteins such as Rad27, PCNA, Exo1, and polymerase ε [58]. Defects in recombinational repair proteins such as Rad50 and Rad52 also lead to higher slippage between distant short direct repeats [59]. In short, I believe that my reporter is likely to be a good proxy for general defects in DNA replication and recombination.

Identifying other natural polymorphisms that could display high mutation rates linked to variants in MMR genes.

In the future I would assess mutation rates of natural strains that possess *MLH1* and *PMS1* sequences suggesting that they are mutators. Previous studies using the *lys2-A$_{14}$* assay showed that the *SK1 MLH1-SK1 PMS1* genotype in the S288c isogenic background conferred a 4 to 7-fold higher mutation rate than the endogenous *S288c MLH1-S288c PMS1* genotype in the same background [23,35,42]. In addition, the *MLH1* sequence in SK1 or SK1-like strains show that they contain the L271 suppressor (Table 3.4). Therefore, it is intriguing to investigate strains that possess *SK1 MLH1-SK1 PMS1* combinations but lack the suppressor in their *MLH1* sequence.

Similarly, I would like to determine whether the *PMS1* sequence from the YJM555 yeast strain possesses a mutator-enhancer phenotype. The *MLH1* and *PMS1* gene combination from YJM555 confers a 200-fold increase in mutation rates when expressed in the wild type s288c background. However, in this same background, even incompatible combinations of *S288c MLH1- SK1 PMS1* only show 75-fold increase in the mutation rate compared to the wild type (Table 3.2). There was one polymorphism in the *PMS1* gene described to be a mutator enhancer, but YJM555 does not have this polymorphism ([42] and Table 3.6). Moreover, all four mutations found in YJM555 *PMS1* have not been characterized; thus, it would be interesting to see whether they can alter PMS1 function and whether they are positively selected for during the course of evolution.

After analyzing MMR gene sequences and narrowing down the number of strains that have a potential to be mutators, I would like to further characterize all strains that show a mutator phenotype. In addition, I would be interested in mapping loci that contributed to the mutator phenotype, though such mapping approach might be difficult due to the combination of many unlinked loci [6].

Understanding relationships between mutator phenotypes, adaptation and selection.

In *E. coli*, many theoretical and experimental approaches have been used to understand relationships between mutator phenotype, adaptation and natural selection [7-9]. Some studies have proposed that selection is more important than mutator phenotype for obtaining a selective advantage [10]. Can we develop models for eukaryote populations such as yeast? A reporter to identify mutators in natural yeast strains would be a first step to understand of the dynamics of adaptive evolution in natural yeast populations. Therefore, I hope the reporters that I built for the reversion assays described in Chapter 3 would serve such a purpose. Upon detection of natural mutators in their own habitats, researchers should be able to create models of how these mutator could be maintained based upon what kind of selection that the strains have adapted to, their natural habitat, and how their environment might determine whether a mutator genotype would be maintained. This work in turn could result in new models that would then fuel further experimental studies.

Implications for naturally engineered strains that possess commercial characteristics.

Many wine and beer manufacturing processes require yeast strains that are tolerant to extreme living environments (i.e. high ethanol, high salt or high temperature). The work I presented indicates that being a mutator enlarges the pool of beneficial mutations. When subjected to strong selection, beneficial mutations would sweep through the population, quickly becoming dominant, and thus could be identified easily. Once a target for adaptation has been fixed, I would need to restore the strains back to non-mutators to maintain them in the long term.

With this strategy, I could modify yeast strains that are used in industry so that they could become mutators. Such strains would then more rapidly acquire mutations that can better tolerate a high percentage of alcohol/salt or high temperature etc.. Identifying the beneficial mutations from such adaptation might then result in novel commercial yeast strains, as well as provide candidate loci for the genetic engineering of other eukaryotic organisms. This is only

one example of the many industrial applications that could result once strains with various backgrounds can be assessed for mutator phenotypes.

REFERENCES

1. Gary R, Park MS, Nolan JP, Cornelius HL, Kozyreva OG, Tran HT, et al. A novel role in DNA metabolism for the binding of Fen1/Rad27 to PCNA and implications for genetic risk. Mol Cell Biol. 1999;19: 5373–82.

2. Tran HT, Degtyareva NP, Koloteva NN, Sugino A, Masumoto H, Gordenin DA, et al. Replication slippage between distant short repeats in Saccharomyces cerevisiae depends on the direction of replication and the RAD50 and RAD52 genes. Mol Cell Biol. 1995;15: 5607–17.

3. Heck JA, Argueso JL, Gemici Z, Reeves RG, Bernard A, Aquadro CF, et al. Negative epistasis between natural variants of the Saccharomyces cerevisiae MLH1 and PMS1 genes results in a defect in mismatch repair. Proc Natl Acad Sci U S A. 2006;103: 3256–61. doi:10.1073/pnas.0510998103

4. Demogines A, Wong A, Aquadro C, Alani E. Incompatibilities involving yeast mismatch repair genes: a role for genetic modifiers and implications for disease penetrance and variation in genomic mutation rates. PLoS Genet. 2008;4: e1000103. doi:10.1371/journal.pgen.1000103

5. Bui DT, Dine E, Anderson JB, Aquadro CF, Alani EE. A Genetic Incompatibility Accelerates Adaptation in Yeast. PLoS Genet. 2015;11: e1005407. doi:10.1371/journal.pgen.1005407

6. Demogines A, Smith E, Kruglyak L, Alani E. Identification and dissection of a complex DNA repair sensitivity phenotype in Baker's yeast. PLoS Genet. 2008;4: e1000123. doi:10.1371/journal.pgen.1000123

7. Taddei F, Radman M, Maynard-Smith J, Toupance B, Gouyon PH, Godelle B. Role of mutator alleles in adaptive evolution. Nature. 1997;387: 700–702. doi:10.1038/42696

8. Chao L, Cox EC. Competition Between High and Low Mutating Strains of Escherichia coli. Soc study Evol. 1983;37: 125–134.

9. Sniegowski PD, Gerrish PJ, Lenski RE. Evolution of high mutation rates in experimental populations of E. coli. 1997;387: 703–705.

10. Tomlinson IP, Novelli MR, Bodmer WF. The mutation rate and cancer. Proc Natl Acad Sci U S A. National Academy of Sciences; 1996;93: 14800–3.

APPENDIX I

An outline of the cloning steps used to construct reporters to measure mutation rates in natural strains.

Step 1: Overlap PCR was performed to construct promoters that drive expression of an open reading frame that contains the Insert E sequence bearing 10-14 homopolymeric A sequences joined to the KANMX or NATMX open reading frames.

PCR 1: URA3 primers, LEU2 primers (see each maps for specific primer number)

PCR 2: HP-ORF amplification primers (see each maps for specific primer number)

PCR 3: Overlap PCR primers

Phusion High Fidelity DNA Pol (Thermo Sci) was used.

PCR 1: promoter amplification:

pRS416 (for *URA3* promoter) or pRS415 (for *LEU2* promoter) were used as DNA templates

Phusion PCR1 conditions

step		temperature	time
initial denaturation		98 ºC	30 s
	denature	98 ºC	10 s
15 cycles	anneal	52 ºC	20 s
	extend	72 ºC	9s (20 s/kb)
final extension		72 ºC	5 min
hold		4 ºC	forever

PCR 2: HP-ORF amplification

pEAO150 (for KANMX ORF) or pEAO155 (for NATMX ORF) were used as DNA templates

Phusion PCR2 conditions

Step		temperature	time
initial denaturation		98 ºC	30 s
	denature	98 ºC	10 s
15 cycles	anneal	55 ºC	20 s
	extend	72 ºC	31 s (20 s/kb)
final extension		72 ºC	5 min
Hold		4 ºC	forever

PCR 3: promoter-HP-ORF amplification; purified products of PCR 1 and 2 were used as templates

Phusion PCR3 conditions

step		Temperature	time	for NATMX
initial denaturation		98 ºC	30 s	
	denature	98 ºC	10 s	
15 cycles	anneal	55 ºC	20 s	
	extend	72 ºC	35 s (20 s/kb)	28s
(Continued previous page) final extension		72 ºC	5 min	
hold		4 ºC	forever	

Step 2: Digest PCR 3 products and pLZ259 with *Bam*H1 and *Eco*R1 and ligate

Step 3: DNA sequencing was performed to make sure that the cloned sequences are correct. The primers below allow for sequencing of the entire PCR 3 product.

Primer #1: AO816: 5'GTAATACGACTCACTATAGGGC

Primer #2: AO817 5'AATTAACCCTCACTAAAGGG

Step 4: Transform the reporter into yeast and measure reversion to antibiotic resistance

Step 5: Revertants to antibiotic resistance were confirmed my isolating reporter plasmids from Chromosomal preps and resequencing to confirm that the KANMX/NATMX ORF is correct.

For constructs including TEF promoter transcriptional slippage was likely to have occurred because DNA sequencing did not show any evidence of frameshift mutations that restored the open reading frame of the +1 frameshift mutations inserted into the KANMX and NATMX ORFs.

Step 6: Choose optimal reporter by compare *msh2*Δ/WT reversion rates:

		Ratio cells reverting to Geneticin^r /total #of cells			
		11A HP		14A HP	
TEFpromoter–HP NATMX – PRS416 (URA3 backbone)	WT	highly reversible/ transcriptional slipage		highly reversible/ transcriptional slipage	
	*msh2*Δ				
	*msh2*Δ/WT				
LEU2promoter–HP NATMX –PRS416 (URA3 backbone)	WT	1.8	*10^-6	30	*10^-6
	*msh2*Δ	12500	*10^-6	85714	*10^-6
	*msh2*Δ/WT	6944		2857.1	
URA3promoter–HP NATMX –PRS415 (LEU2 backbone)	WT	3.1	*10^-6	N/A	
	*msh2*Δ	15000	*10^-6	N/A	
	*msh2*Δ/WT	4839			
TEFpromoter–HP at2nd ATG of KANMX – pLZ259(NATMX backbone)	WT	highly reversible/ transcriptional slipage		highly reversible/ transcriptional slipage	
	*msh2*Δ				
	*msh2*Δ/WT				
LEU2promoter–HP at2nd ATG of KANMX – pLZ259(NATMX backbone)	WT	1.58	*10^-6	0.95	*10^-6
	*msh2*Δ	4760	*10^-6	9950	*10^-6
	*msh2*Δ/WT	2584.3		10431.4	
URA3 promoter –HP at2nd ATG of KANMX – pLZ259(NATMX backbone)	WT	0.87	*10^-6	1.68	*10^-6
	*msh2*Δ	4710	*10^-6	10900	*10^-6
	*msh2*Δ/WT	5404.5		6498.7	

Maps of the plasmids used in this assay:

pEAA611 Plasmid Name and Map

Plasmid Markers

ARS-CEN, NATMX,URA3 promoter-KANMX::insE-A_{10}

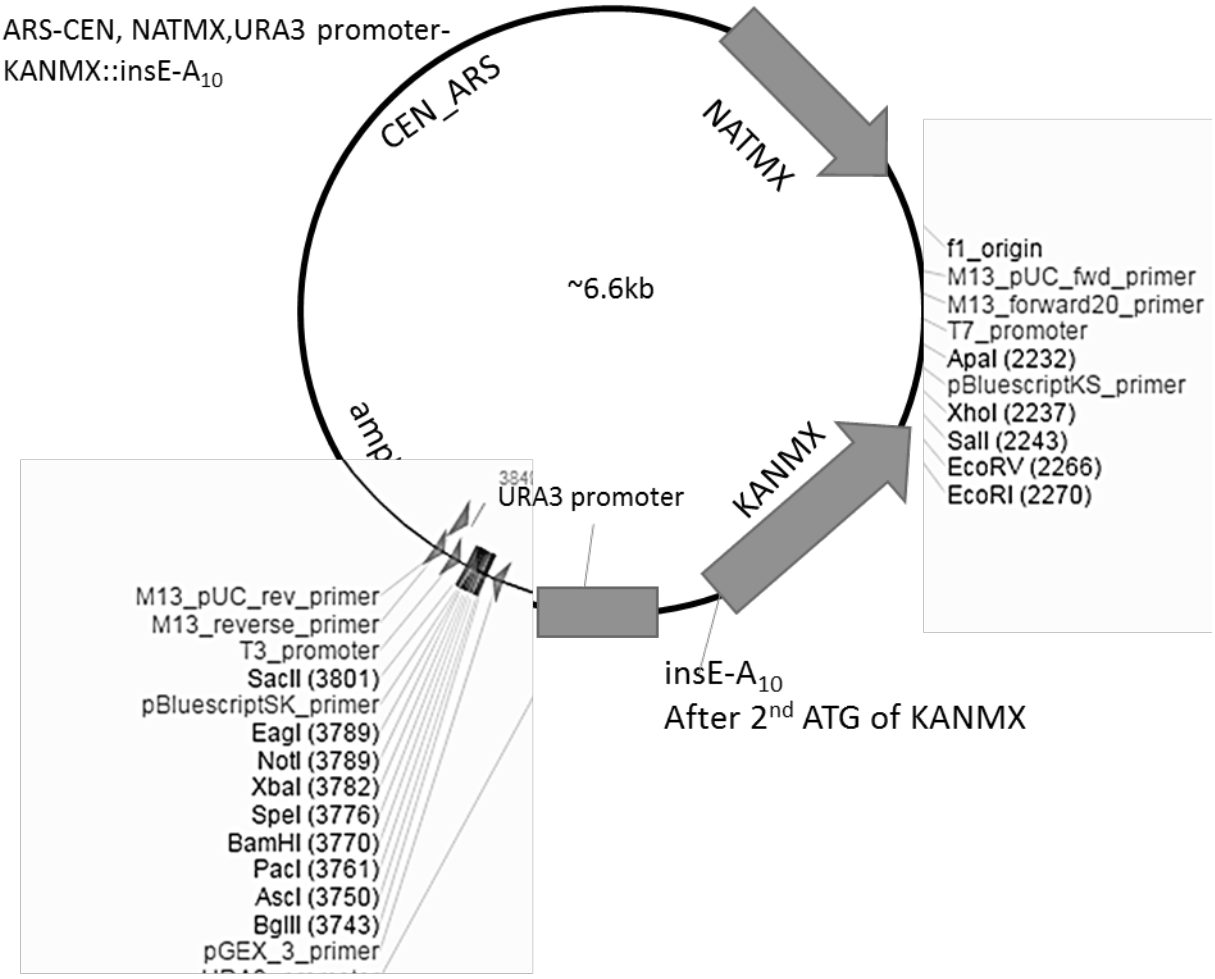

Derivation:
URA3 promoter was amplify from PRS416 using PCR: AO3527 and 3529 (PCR1)
InsE-KANMX was amplify from pEAO150 using AO3457 and AO3442 (PCR2)
Overlap PCR using AO3527 and 3442 using products of PCR1 and 2 (PCR3)
pEAO454 and PCR3 product was digested w/ BamH1 and EcoR1 and ligate

Sources: pEAO 454: pLZ259 (ARS-CEN, NATMX, provided by Dr. Lu Zhu, Emr lab

pEAA612

Plasmid Markers

ARS-CEN, NATMX,URA3 promoter-KANMX::insE-A_{11}

Derivation:
URA3 promoter was amplify from PRS416 using PCR: AO3527 and 3528 (PCR1)
InsE-KANMX was amplify from pEAO150 using AO3457 and AO3442 (PCR2)
Overlap PCR using AO3527 and 3442 using products of PCR1 and 2 (PCR3)
pEAO454 and PCR3 product was digested w/ BamH1 and EcoR1 and ligate

Sources: See pEAA611

Plasmid Name and Map

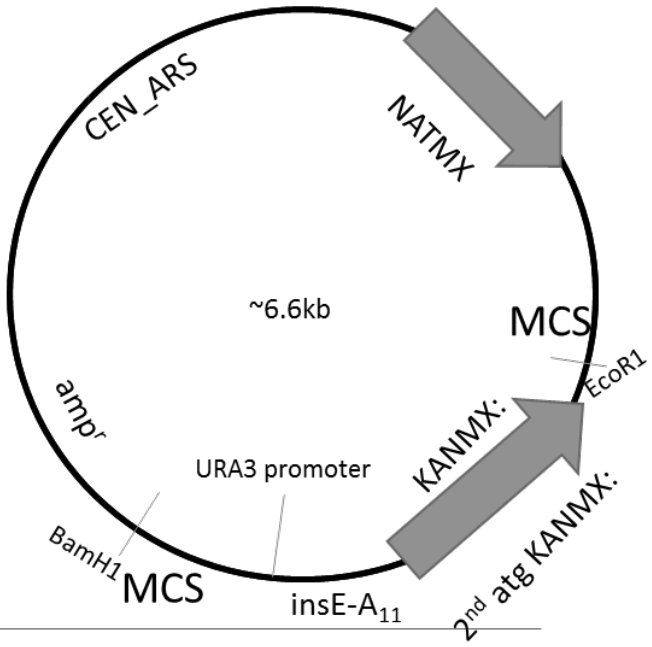

pEAA613

Plasmid Markers
ARS-CEN, NATMX,URA3 promoter-KANMX::insE-A_{14}

Derivation:
URA3 promoter was amplify from PRS416 using PCR: AO3527 and 3531 (PCR1)
InsE-KANMX was amplify from pEAO150 using AO3457 and AO3442 (PCR2)
Overlap PCR using AO3527 and 3442 using products of PCR1 and 2 (PCR3)
pEAO454 and PCR3 product was digested w/ BamH1 and EcoR1 and ligate

Sources: See pEAA611

Plasmid Name and Map

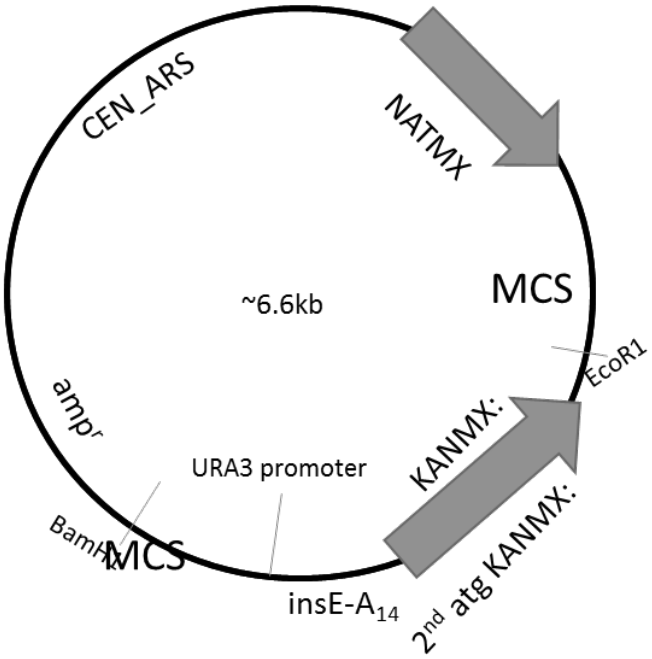

pEAA614

Plasmid Markers

ARS-CEN, NATMX,LEU2 promoter-KANMX::insE-A_{10}

Derivation:
LEU2 promoter was amplify from PRS415 using PCR: AO3505 and 3509 (PCR1)
InsE-KANMX was amplify from pEAO150 using AO3457 and AO3442 (PCR2)
Overlap PCR using AO3505 and 3442 using products of PCR1 and 2 (PCR3)
pEAO454 and PCR3 product was digested w/ BamH1 and EcoR1 and ligate

Sources: See pEAA611

Plasmid Name and Map

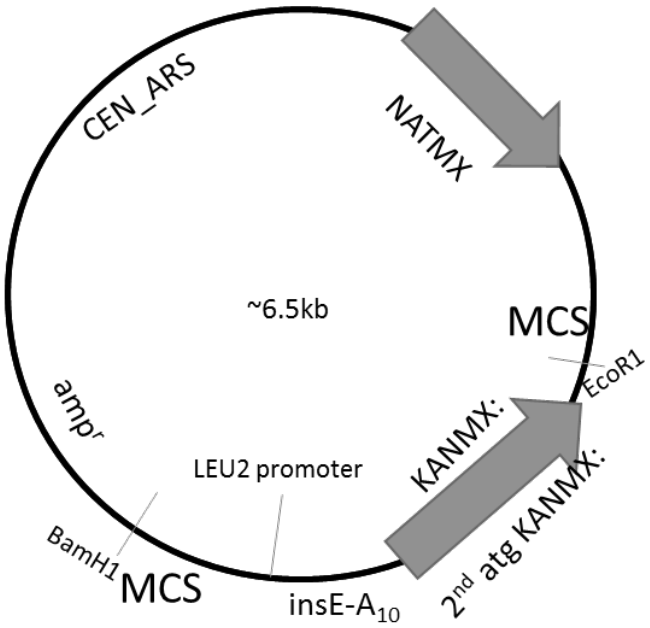

pEAA615

Plasmid Markers
ARS-CEN, NATMX,LEU2 promoter-KANMX::insE-A_{11}

Derivation:
LEU2 promoter was amplify from PRS415 using PCR: AO3505 and 3509 (PCR1)
InsE-KANMX was amplify from pEAO150 using AO3457 and AO3442 (PCR2)
Overlap PCR using AO3505 and 3442 using products of PCR1 and 2 (PCR3)
pEAO454 and PCR3 product was digested w/ BamH1 and EcoR1 and ligate

Sources: See pEAA611

Plasmid Name and Map

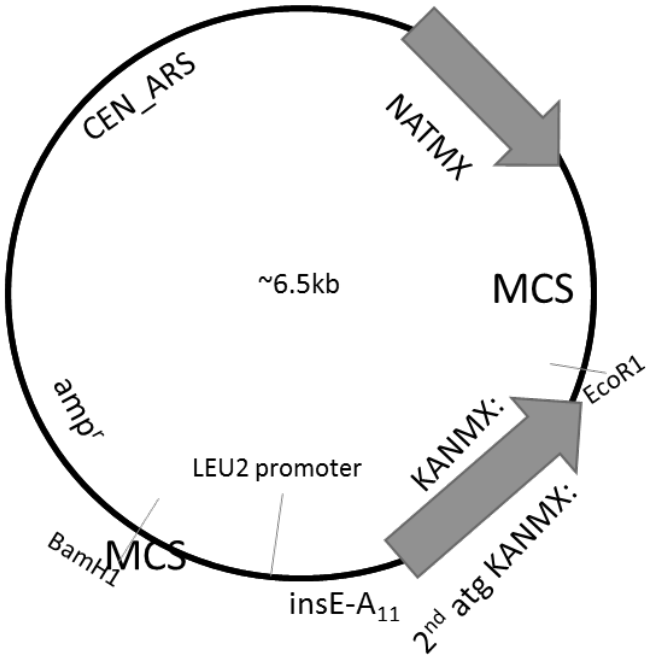

pEAA616

Plasmid Markers

ARS-CEN, NATMX,LEU2 promoter-KANMX::insE-A_{14}

Derivation:
LEU2 promoter was amplify from PRS415 using PCR: AO3505 and 3511 (PCR1)
InsE-KANMX was amplify from pEAO150 using AO3457 and AO3442 (PCR2)
Overlap PCR using AO3505 and 3442 using products of PCR1 and 2 (PCR3)
pEAO454 and PCR3 product was digested w/ BamH1 and EcoR1 and ligate

Sources: See pEAA611

Plasmid Name and Map

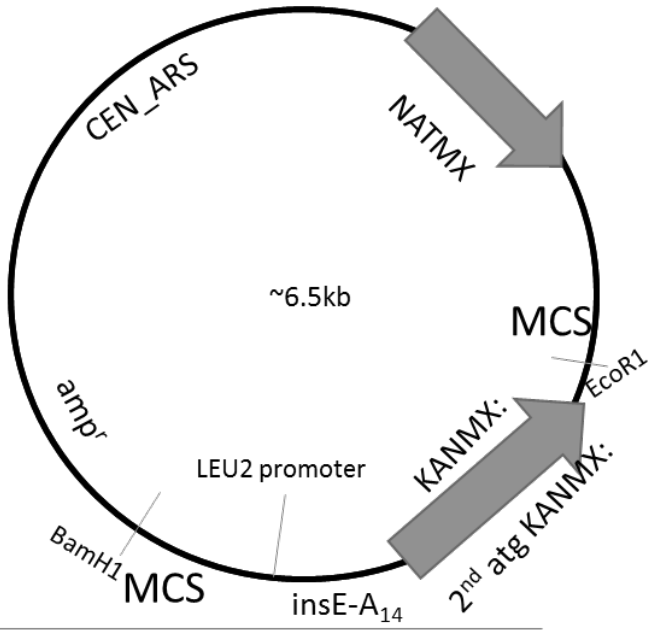

pEAA617

Plasmid Markers
ARS-CEN, URA3,LEU2 promoter-kanMX::insE-A11
Derivation:
LEU2 promoter was amplify from PRS415 using PCR: AO3505 and 3509 (PCR1)
InsE-KANMX was amplify from pEAO150 using AO3405 and AO3442 (PCR2)
Overlap PCR using AO3505 and 3442 using products of PCR1 and 2 (PCR3)
pRS416 and PCR3 product was digested w/ BamH1 and EcoR1 and ligate

Sources:

Plasmid Name and Map

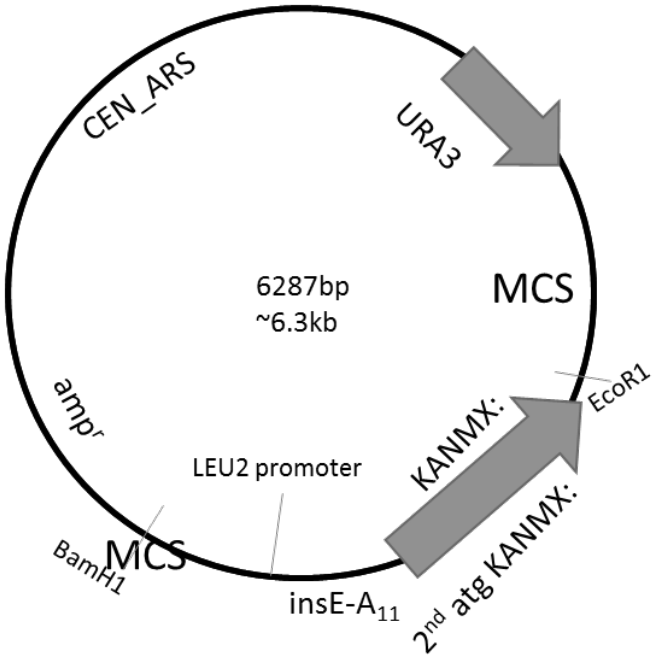

pEAA618

Plasmid Markers

ARS-CEN, NATMX,URA3 promoter-KANMX::insE-A_{13}

Derivation:
URA3 promoter was amplify from PRS416 using PCR: AO3527 and 3530 (PCR1)
InsE-KANMX was amplify from pEAO150 using AO3457 and AO3442 (PCR2)
Overlap PCR using AO3527 and 3442 using products of PCR1 and 2 (PCR3)
pEAO454 and PCR3 product was digested w/ BamH1 and EcoR1 and ligate

Sources: See pEAA611

Plasmid Name and Map

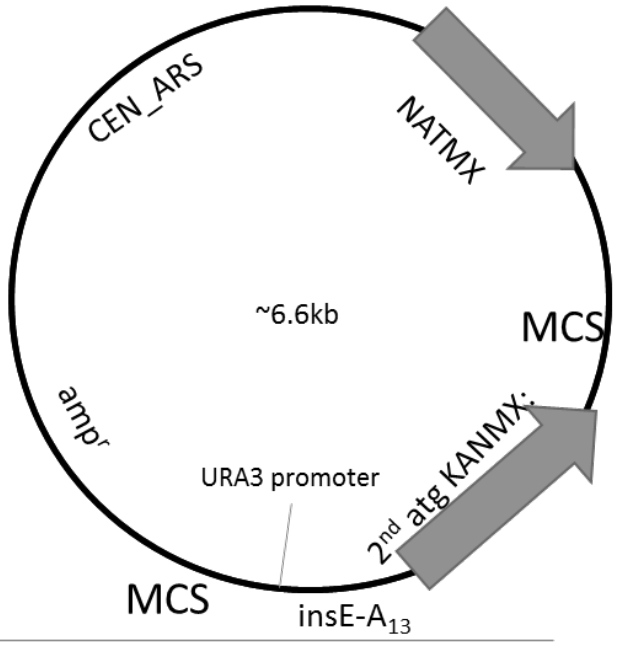

pEAA619

Plasmid Markers
ARS-CEN, NATMX,LEU2 promoter-KANMX::insE-A_{13}

Derivation:
LEU2 promoter was amplify from PRS415 using PCR: AO3505 and 3513 (PCR1)
InsE-KANMX was amplify from pEAO150 using AO3457 and AO3442 (PCR2)
Overlap PCR using AO3505 and 3442 using products of PCR1 and 2 (PCR3)
pEAO454 and PCR3 product was digested w/ BamH1 and EcoR1 and ligate

Sources: See pEAA611

Plasmid Name and Map

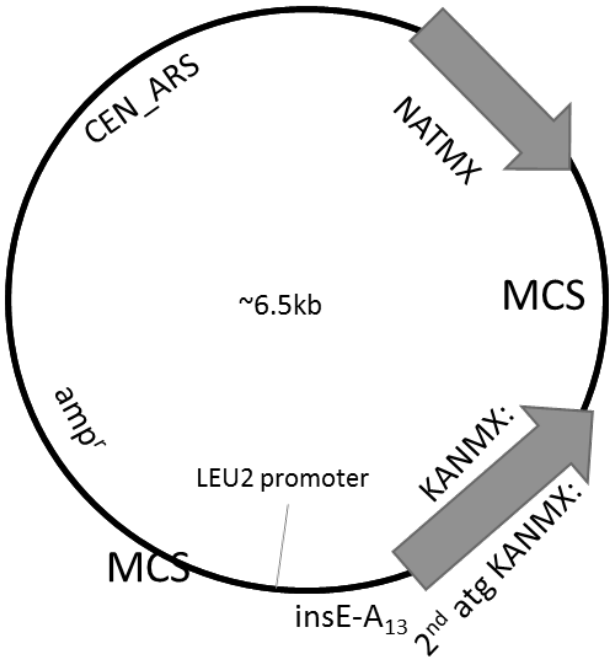

pEAA629

Plasmid Markers
ARS-CEN, LEU2, URA3 promoter-natMX::insE-A11
Derivation:
URA3 promoter was amplify from PRS416 using PCR: AO3527 and 3528 (PCR1)
NATMX sequence with insE-A_{11} was amplified from pEAO155 using AO3444 and AO3442 (PCR2)
Then, overlap PCR using AO3527 and AO3442 (PCR3)
-Disgest pRS415 and product PCR3 using BamHI and SacI and ligate

Sources:

Plasmid Name and Map

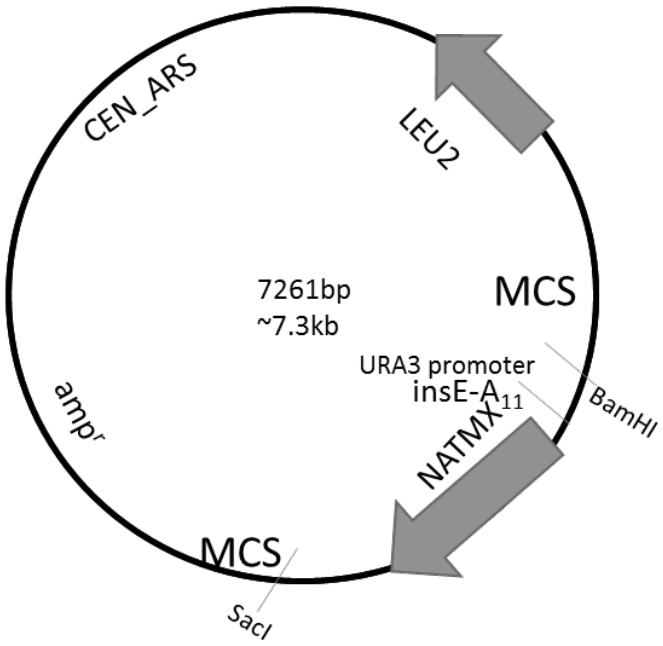

---

pEAA630

Plasmid Markers
ARS-CEN, LEU2, URA3 promoter-NATMX::insE-A13
Derivation:
URA3 promoter was amplify from PRS416 using PCR: AO3527 and 3530 (PCR1)
NATMX sequence with insE-A_{13} was amplified from pEAO155 using AO3444 and AO3442 (PCR2)
Then, overlap PCR using AO3527 and AO3442 (PCR3)
-Disgest pRS415 and product PCR3 using BamHI and SacI and ligate

Sources:

Plasmid Name and Map

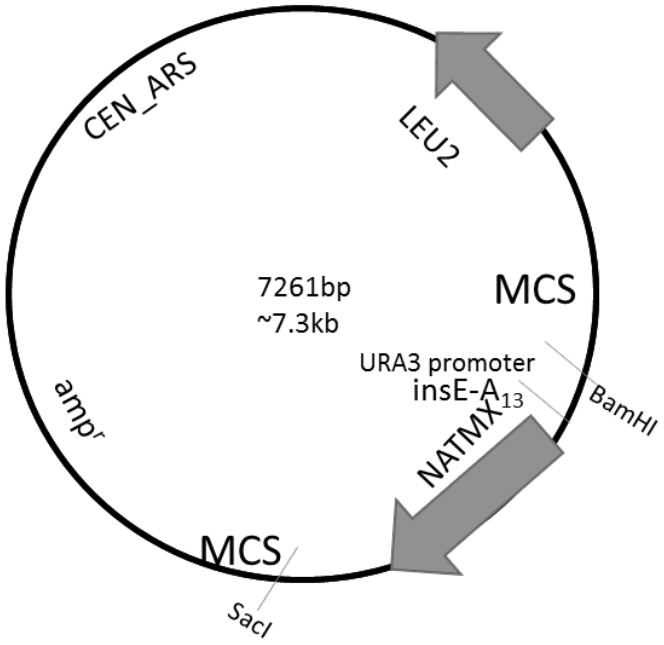

pEAA631

Plasmid Markers

ARS-CEN, LEU2, URA3 promoter-natMX::insE-A14

Derivation:

URA3 promoter was amplify from PRS416 using PCR: AO3527 and 3531 (PCR1)

NATMX sequence with insE-A_{14} was amplified from pEAO155 using AO3444 and AO3442 (PCR2)

Then, overlap PCR using AO3527 and AO3442 (PCR3)

-Disgest pRS415 and product PCR3 using BamHI and SacI and ligate

Sources:

Plasmid Name and Map

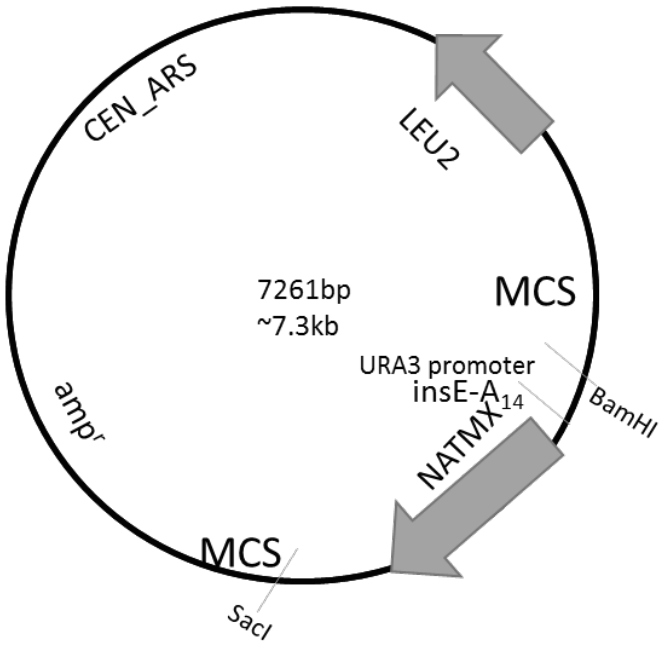

---

pEAA632

Plasmid Markers

ARS-CEN, URA3, LEU2 promoter-NATMX::insE-A_{10}

Derivation:

LEU2 promoter was amplify from PRS415 using PCR: AO3505 and 3509 (PCR1)

NATMX sequence with insE-A_{10} was amplified from pEAO155 using AO3444 and AO3442 (PCR2)

Then, overlap PCR using AO3505 and AO3442 (PCR3)

pRS416 and PCR3 product was digested w/ BamH1 and EcoR1 and ligate

Sources:

Plasmid Name and Map

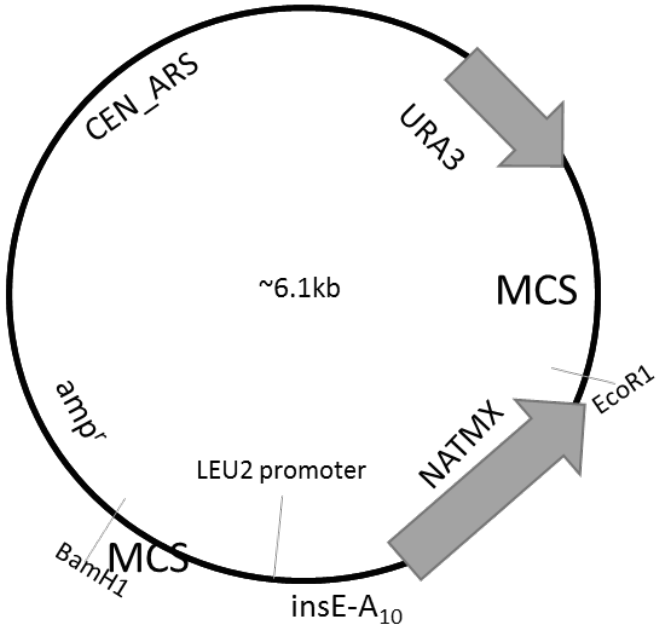

pEAA633

Plasmid Markers
ARS-CEN, URA3, LEU2 promoter-natMX::insE-A$_{11}$
Derivation:
LEU2 promoter was amplify from PRS415 using PCR: AO3505 and 3507 (PCR1)
NATMX sequence with insE-A$_{11}$ was amplified from pEAO155 using AO3444 and AO3442 (PCR2)
Then, overlap PCR using AO3505 and AO3442 (PCR3)
pRS416 and PCR3 product was digested w/ BamH1 and EcoR1 and ligate

Sources:

Plasmid Name and Map

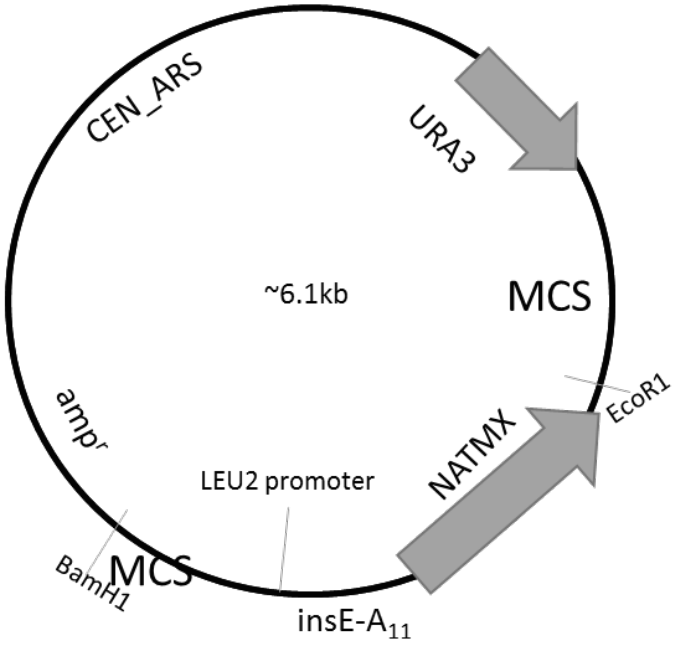

---

pEAA634

Plasmid Markers
ARS-CEN, URA3, LEU2 promoter-NATMX::insE-A$_{13}$
Derivation:
LEU2 promoter was amplify from PRS415 using PCR: AO3505 and 3513 (PCR1)
NATMX sequence with insE-A$_{14}$ was amplified from pEAO155 using AO3444 and AO3442 (PCR2)
Then, overlap PCR using AO3505 and AO3442 (PCR3)
pRS416 and PCR3 product was digested w/ BamH1 and EcoR1 and ligate

Sources:

Plasmid Name and Map

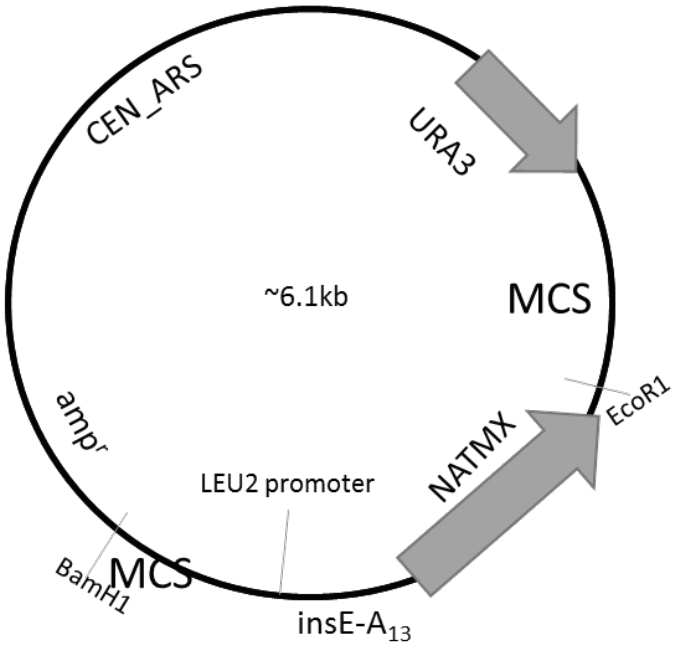

pEAA635

Plasmid Markers
ARS-CEN, URA3, LEU2 promoter-natMX::insE-A$_{14}$
Derivation:
LEU2 promoter was amplify from PRS415 using PCR: AO3505 and 3511 (PCR1)
NATMX sequence with insE-A$_{14}$ was amplified from pEAO155 using AO3444 and AO3442 (PCR2)
Then, overlap PCR using AO3505 and AO3442 (PCR3)
pRS416 and PCR3 product was digested w/ BamH1 and EcoR1 and ligate

Sources:

Plasmid Name and Map

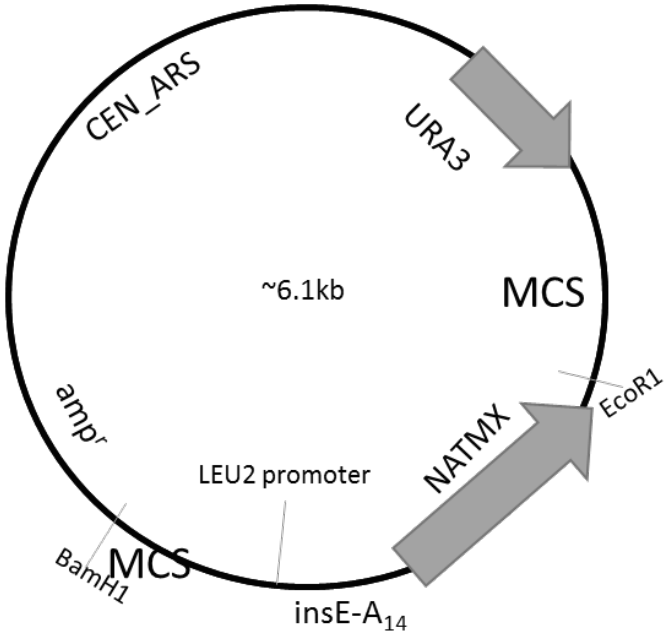

---

pEAA628

Plasmid Markers
ARS-CEN, LEU2, URA3 promoter-NATMX::insE-A10
Derivation:
URA3 promoter was amplify from PRS416 using PCR: AO3527 and 3529 (PCR1)
NATMX sequence with insE-A$_{10}$ was amplified from pEAO155 using AO3444 and AO3442 (PCR2)
Then, overlap PCR using AO3527 and AO3442 (PCR3)
-Disgest pRS415 and product PCR3 using BamHI and SacI and ligate

Sources:

Plasmid Name and Map